THE INFLUENCE OF GLACIER CHANGE ON SEDIMENT YIELD, PEYTO BASIN, ALBERTA, CANADA

by

Theodore John Mlynowski

B.Sc., University of Northern British Columbia, 2008

THESIS SUBMITTED IN PARTIAL FULFILLMENT OF
THE REQUIREMENTS FOR THE DEGREE OF
MASTER OF SCIENCE
IN
NATURAL RESOURCES AND ENVIRONMENTAL STUDIES
(GEOGRAPHY)

UNIVERSITY OF NORTHERN BRITISH COLUMBIA

September 2013

Abstract

The relation between sediment yield and glacier fluctuations at timescales less than a century remains uncertain. The primary goal of this study was to assess the influence of glacier activity on sediment yield within the Peyto Lake watershed. The research focused on a small alpine watershed in the Rocky Mountains of Alberta containing Peyto Glacier and the proglacial Peyto Lake. Using photogrammetric methods I determined changes in length, area, and volume of Peyto Glacier from a topographic survey map (1917) and 18 sets of aerial photographs (1947 - 2005). I also collected 18 sediment cores from Peyto Lake that consists of laminated, silt-clay couplets which can be shown through ^{137}Cs activity to be clastic varves. Varve thickness and sediment properties were combined to produce an annual record (1917 - 2010) of specific sediment yield (SSY) for the watershed. I then compared the SSY record to dimensional changes of Peyto Glacier as well as available mass balance records, hydrometric records, and climate records over the study period (1917 - 2010). Over the period 1917 - 2005, Peyto Glacier retreated 2198 ± 18 m, shrank 4.0 ± 0.9 km^2, thinned 44 ± 31 m, and lost 581 ± 404 × 10^6 m^3 water equivalent (w.e.). I measured an additional 85 ± 4 × 10^6 m^3 w.e. of ice loss from thinning ice-cored moraines adjacent to the glacier. Over the period 1917 - 2005 SSY averaged 446 ± 176 Mg km^2 yr^{-1}, which is among the highest measured yields in the Canadian Cordillera; however, this value is relatively low for glaciated basins worldwide. The SSY record has a poor relation to short-term dimensional changes of Peyto Glacier, likely due to the complexity of sediment transfers in proglacial environments. Long-term trends in SSY are hypothesized to arise from increasing (1870 - 1940) and decreasing (1970 - 2010) glacier contribution to streamflow over the past century.

Table of contents

List of tables

List of figures

List of appendices

Acknowledgements

The completion of this thesis could not have been possible without a number of caring people who have supported me and believed in me throughout this challenging and rewarding process. I would first like to thank my supervisor, Dr. Brian Menounos, for providing a diverse project and the opportunity to be his student. It is obvious that you are passionate about science, but your dedication was shown with sweat, blood, and tears when you dragged my sediment cores up Heartbreak Hill. I am grateful for your mentorship whenever I needed it, your high expectations, and your encouragement.

For the past three years my wife, Caroline Mlynowski, has made great sacrifices so that I could pursue my Masters. I am forever indebt to you for your unquestionable support, encouragement, and devotion.

The three field work expeditions at Peyto Lake were the hardest and most rewarding part of my Masters. I am appreciative of all my field helpers, Caroline, Brian, Rob Vogt, Mary Samolczyk, and Dr. Joel Cubley who endured long, cold days on the ice, before dragging heavy sediment cores back to the truck. I am particularly thankful to Caroline and Rob for their willingness to even get out of the truck when it was -31 °C.

There were many facets of my Masters that required additional help, knowledge, and services. The guidance and help from Teresa Brewis and Christina Tennant saved me many hours of technical difficulties with Vr Mapping software. I also express gratitude to Cardinal Systems, LLC for providing a license and support for their Vr Mapping software. I thank Bill Holmes from the Alberta Air Photo Distribution and Daniel Brown from National Air Photo Library for providing additional air photographs of Peyto Glacier. I am also grateful to Lyssa Maurer for showing me the required methodology and techniques to play with mud. I appreciate Matt Beedle's quick and in-depth replies to my questions about glacier mass balance. Finally, I would like to acknowledge the generosity of Flett Research Ltd. for processing additional sediment samples free of charge.

This project was made possible through funding obtained from the University of Northern British Columbia (UNBC), Geological Society of America (GSA), and the National Sciences and Engineering Research Council of Canada (NSERC).

1. Introduction

1.1 Research motivation

Annually laminated (varved) lake sediments provide a detailed record of environmental change. These lake sediment records are particularly important in many regions of western Canada where instrumental records are short or absent. In alpine environments, for example, varved lake sediments have been used as proxies for glacier fluctuations (referred hereafter as glacier activity) which have then been used to infer paleoclimatic conditions (Denton and Karlén, 1973; Leonard, 1997).

Although past climate conditions have been inferred from lake sediment records, such inferences must be approached with caution. The climate-glacier-lake sediment system is complex and strong connections among climate, glaciers, and lakes are difficult to demonstrate (Jansson et al., 2005; Hodder et al., 2007). Identifying a relation between just two variables such as glacier activity and lake sedimentation is challenging enough (Leonard, 1997; Loso et al., 2004). Such difficulties may arise from glacier records being temporally limited (e.g., Loso et al., 2004) or incomplete (e.g., Leonard, 1997).

Previous studies have considered how glacier activity influences sediment production (e.g., Leonard, 1997), but exactly how this relationship changes through time is not clear. At the centennial to millennial timescales, it is hypothesized that glacial erosion is proportional to ice-cover, so long-term changes in glacier extent should be evident in the clastic sediment record (Hallet et al., 1996; Leonard, 1997). At the annual to decadal timescales, the relation of ice cover and sedimentation has been examined (e.g., Loso et al., 2004). What has yet to be understood, however, is the degree to which glacier fluctuations control sediment fluxes at decadal timescales.

The proposed research will specifically investigate the relation between changes in glacier dimensions and sediment yield at the decadal to centennial timescales. Geodetic data for Peyto Glacier will be compared to annually laminated (varved) lake sediments from a downstream proglacial lake. The results of the proposed research will aim to clarify the relation between sediment yield and mountain glaciers. Insight into landscape evolution, flood control, aquatic ecosystem health, and transport of environmental pollutants all require insight into the production, distribution, and delivery of fine sediments in montane catchments.

1.2 Thesis objectives

The goal of this study is to assess the influence of glacier change on sediment yield within the Peyto Lake watershed. The objectives of this study are to:

(1) use photogrammetry and geographic information systems (GIS) to determine the dimensional (length, area, and volume) changes of Peyto glacier from 1917 to 2005;

(2) measure varved sediments and calculate sediment yield for the Peyto Lake watershed for the period 1917 - 2010; and

(3) assess whether sediment yield is fundamental related to the dimensional changes of Peyto Glacier.

I will specifically be able to assess the degree to which long term glacier fluctuations influence proglacial lake sedimentation. To my knowledge, this will be the one of the few studies that directly compares a detailed record of sediment yield to a long record of glacier mass balance.

1.3 Thesis outline

I wrote and organized this thesis in a traditional format. Following this introductory chapter, Chapter 2 reviews literature relevant to sediment yield, the relation of glaciers and sediment production, Peyto Glacier, and sedimentology within the Peyto Lake watershed. In Chapter 3, I describe the methods used to determine the historical glacier dimensions of Peyto Glacier and calculate sediment yield from lake sediment core samples. Chapter 4 summarizes the dimensional changes of Peyto Glacier, measured sediment yield and how they covary. In Chapter 5, I discuss the study's major findings and describe sources of error and uncertainty. Finally, Chapter 6 summarizes the major findings and provides suggestions for future research.

2. Literature review

2.1 Sediment yield

Of the sediments entrained in a river system, some of the sediments are deposited within sediment stores and the remaining sediments are transported by the river system as dissolved, suspended, and bed-load fractions. Collectively the suspended and bed-loads fractions are known as sediment yield which is described by Vanoni (2006) as the total sediment outflow from a watershed that can be measured at a cross section of reference over a specified period of time (expressed as mass per unit area per unit time).

Sediment yields depend on rates of primary erosion, changes in sediment storage, and transportation capacity of the medium (e.g., river or glacier) within the watershed. Some controlling factors on sediment production and sediment storage include local topography, soil properties, climate, vegetation cover, catchment morphology, drainage network characteristics and land use among others (Walling, 1994; Hovius, 1998). The relative importance of each factor varies for each watersheds. For example, Restrepo et al. (2006) found mean annual runoff explained 51% of the variance in sediment yield for the Magdalena watershed, Columbia. Hovius (1998), however, examined 97 watersheds from around the world and found five environmental variables (specific runoff, drainage area, maximum height, mean annual temperature, and annual temperature range) accounted for 49 % of the variance in 86 of the watersheds.

Quantifying the changes in sediment storage through time and space are also difficult to determine. One method uses the sediment delivery ratio (SDR), defined as the proportion of sediment exported from a watershed relative to the proportion of upland erosion (Walling, 1983). The SDR varies between 0 and 1 and is influenced by a range of environmental factors that include: the nature, extent and location of sediment sources; relief and slope characteristics; the drainage pattern and channel conditions; vegetation cover; land use; and soil texture (Walling, 1983). Specific sediment stores in the basin might include the base of the slope, in swales, on the flood plain, or within the channel (Walling, 1983). A common view suggests that specific sediment yield declines as basin area increases (i.e., SDR decreases) due to increased sediment storage on lower slopes and increased erosion in non-vegetated areas at higher elevations (Walling, 1983; Ballantyne, 2002). Contrary to this view, Dedkov and Moszherin (1992) demonstrate that a river system can have an inverse relationship (i.e., SDR increases) when channel erosion is dominant. For example in British Columbia, Church and Slaymaker (1989) found that secondary remobilization of Quaternary sediments increased at all spatial scales up to 3×10^4 km^2.

Sediment yield can be determined by a variety of methods depending on the research focus, time limits, and study area. Sediment yield is typically derived from measurements of sediment load within a river; however, this method can be labour intensive, especially for obtaining a dataset that spans a decade or more. Another method to calculate sediment yield is to measure the mass of sediment deposited on the lake bottom for a given period of time. Although it is possible to obtain long records of sediment yield through time (Menounos, 2006), the sediment entering and leaving the lake must be accounted for (Foster et al., 1990). For instance, Owens and Slaymaker (1993) studied four lakes in the southern Coast Mountains of British Columbia and found 55 - 99 % of the sediment accumulation over the last 2350 years originated from four external sources (aquatic production of (1) organic matter and (2) biogenic silica; (3) lake bank erosion; and (4) atmospheric dust derived from outside the catchments) that do not contribute to denudation rates within the basin.

Additional variables such as sediment trap efficiency, re-suspension processes, sediment density changes, and mixing processes of the lake must also be determined (Foster et al., 1990). Alternatively, sediment yield can be estimated by generalized equations (Slaymaker, 1977). Such equations tend to simplify the watersheds' characteristics and do not account for variability and stochastic processes (e.g., heavy rainfall). Therefore, Slaymaker (1977) suggested equations that estimate sediment yield should not be used beyond the basin from which the data were derived. Sediment yield models, however, allow the user to specify variables that characterize a specific basin through space and time. The benefits of using equations and models are that they do not entail data collection in the field (unless for validation); however, the validity and precision of each model can substantially vary for a given watershed. The precision and predictive ability of sediment yield models thus depends on the knowledge of basin's characteristics and environmental controls.

2.2 Sediment yield and glaciers

Generally when glacierized catchments are compared to alpine catchments free of contemporary ice cover, glacierized catchments usually have a higher sediment yield (Leonard, 1986; Hallet et al., 1996). This view is generally true in glacierized watersheds because effective erosion rates and the mobilization of sediments are dominated by glaciers. Conversely, Hicks et al. (1990) found that precipitation rates influenced sediment yield to a greater degree than percent glacier cover. The difficulties of comparing erosion rates for glacial and non-glacial processes are summarized by Harbor and Warburton (1993); they highlight the reasons why erosion rates for glacierized and unglacierized basins are nearly impossible to compare.

For glacierized watersheds, sediment yield is commonly related to percent glacier cover. Globally, the relation between sediment yield and glacier cover has been shown to be poor (Hallet et al., 1996; Hodder et al., 2007). There are a variety of factors that contribute to this scatter including regional climate and environmental differences (e.g., geology, slope, aspect), as well as, localized changes to sediment storage. Mass wasting (e.g., Johnson and Power, 1985) and fluvial erosion in the glacier's forefield (e.g., Orwin and Smart, 2004), for example, can elevate sediment yields, particularly during heavy rainfall events.

Alternatively, sediment yield may depend on the dynamic state of glaciers (i.e., advancing, retreating, and downwasting) rather than percent glacier cover. For the Tyndall Glacier in southeast Alaska, for example, Koppes and Hallett (2006) found a strong, positive correlation between glacier retreat rates and glacial sediment yields. The highest rates of sedimentation in Hector Lake, Alberta coincided with periods of glacier retreat or rapid glacial advance rather than during times of maximum ice extent (Leonard, 1997). Additionally, the thinning of a glacier could further influence sediment production without exhibiting significant retreats or advances.

Compounded with glacier dynamics, sediment yield may further be affected by the rate at which sediment can be produced and evacuated from the sub-glacial environment (Riihimaki et al., 2005). The rate that sediments can be produced through processes of plucking, abrasion, and crushing can be variable through time and space in the sub-glacial environment. How sediments are evacuated from beneath the glacier is influenced by sub-glacial water flow (Jansson et al., 2005; Bartholomaus et al., 2008). There is a non-linear relationship between the rate at which sediments are evacuated and water availability. Specifically, the increase of water availability to the sub-glacial environment can increase water pressure beneath the glacier which effectively separates the glacier from its bed. Once this separation has occurred, the flushing of sediments can commence. However, as the conduits enlarge, it takes increasingly larger amounts of water to maintain the same water pressure needed to evacuate sediments. This non-linear relationship is evident at seasonal, inter-seasonal, and sub-daily timescales (Jansson et al., 2005; Riihimaki et al., 2005).

2.3 History of Peyto Glacier

Detailed evidence of glacier activity is widespread in the Peyto Lake watershed and as a result, Peyto Glacier is the focus of many research studies (Luckman, 2006). Average aggregation of the Peyto Creek delta suggests that Peyto Glacier retreated from Peyto Lake about 13,000 calendar years before present (cal yr BP; Smith and Jol, 1997). Peyto Glacier likely continued to retreat until 3000 cal yr BP to an elevation around 2125 m above sea level (asl). *In situ* wood fragments found in a paleosol beneath till indicates Peyto Glacier overrode a forest 3000 - 2800 ^{14}C yr BP (formally known as the Peyto advance). It is unknown whether the glacier continued to advance until 2500 ^{14}C yr BP or whether a second advance occurred shortly thereafter. Two additional advances occurred at 1550 yr ^{14}C BP and 820 ^{14}C yr BP, and Peyto Glacier respectively reached positions at least 1 km and 1.4 km downvalley from the 1990 terminus extent (Luckman et al., 1993). The glacier attained its Holocene maximum downvalley extent during the latter half of the Little Ice Age (LIA), or about 150 - 300 years ago (Luckman, 2006).

Heusser (1956) constrained the timing of the LIA advance to sometime between AD 1711 - 1863 by dating trees growing on trimlines on the lateral moraines on the east side of the valley. Luckman (1996) investigated the area and confirmed the nineteenth century minimum dates for the main moraine crest, but did not find evidence for an earlier trimline described by Heusser (1956). Along the lower western lateral moraine, Luckman (1996) found 11 standing and sheared tree snags along a sharply defined trimline in the forest. His results indicate that Peyto Glacier achieved its maximum Holocene extent between AD 1837 and 1841. Just beyond the LIA limit, Luckman and Osborn (1979) identified a tephra layer from the Mazama volcanic eruption suggesting Peyto Glacier has not been more extensive than its LIA limit since *ca.* 7700 cal yr. BP.

Research on post LIA activity of Peyto Glacier used dendrochronology and photogrammetry to demarcate the position of the glacier. Luckman (1996) collected an extensive dendrochronological dataset for the Peyto watershed spanning *ca.* AD 1700 - 1990. Watson and Luckman (2004) used dendroclimatology to reconstruct the summer, winter and net mass balance record for Peyto glacier for the period AD 1673 - 1994. Generally, reconstructed positive mass balance characterized the period AD 1673 - 1883 (+70 mm water equivalent (w.e.) yr^{-1}) followed by a period dominated by negative mass balance (-317 mm w.e. yr^{-1}). Notably, the periods AD 1695 - 1720, 1810 - 1825, and 1845 - 1880 reflect intervals of pronounced positive mass balance. By using photographs, tree-ring data, and measurements of ice wastage, Bunger et al. (1967) mapped glacier retreat positions from AD 1897 to 1965. Wallace (1995) estimated the volumetric change for nearly the same period (AD 1896 to 1966) as 108.9×10^7 m^3. Holdsworth et al. (2006) calculated the loss of ice from AD 1966 to 1995 as 139×10^6 m^3. Data from by Wallace (1995), Holdsworth et al. (2006), and additional mass balance values in Demuth and Keller (2006) indicate that Peyto Glacier has lost roughly 70% of its volume over the period AD 1896 - 1995. In terms of aerial coverage, Peyto Glacier covered an estimated area of 17.15 km^2 in AD 1897, 13.35 km^2 in AD 1966, and 11.81 km^2 in AD 1993 (Wallace, 1995; Demuth and Keller, 2006).

2.4 Sedimentology within the Peyto Lake watershed

Many studies within the watershed have focused on the dynamics of sediment laden, glacier discharge flowing into Peyto Lake. Vendl (1978) examined controls of sedimentation in Peyto Lake and found large pulses of sediment travelled along the bottom topography of the lake before settling. Approximately 33 times more sediment is deposited in the proximal basin (161 mg cm^{-2} d^{-1}) than in the distal basin (4.9 mg cm^{-2} d^{-1}) of the lake. Smith et al. (1982) compared the sedimentation regime of Peyto Lake to three other glacier-fed lakes within close proximity to each other. Of these four lakes, Peyto Lake receives the highest and most variable inflowing suspended sediment concentrations (SSC; mean: 720 mg l^{-1}, range: 138 - 2156 mg l^{-1}). Binda (1984) investigated the suspended sediment and hydro-chemical dynamics of discharge from Peyto Glacier by measuring discharge, electrical conductivity, temperature, and suspended sediment concentrations from Peyto Creek. From his results, he hypothesized that the re-organization of sub-glacial channels under changing hydrostatic pressures and sediment availability was a major factor that influenced the output of suspended sediment from Peyto Glacier. The complex sediment dynamics of Peyto Lake are further documented by Chikita (1993). He found the sediment laden undercurrent pooled in the proximal basin and would only 'spill' over the central sill into the distal basin when SSC exceeded 80 mg l^{-1} at 6.5 °C. Chikita (1993) believed that most suspended sediment originates from beneath the glacier because the sediment in and around the Peyto Creek channel is dominated by gravel and sand.

Previous work has also considered sediments contained in Peyto Lake. Smith et al. (1982) recovered 26 short, sediment cores from the lake. They found the sediment cores contained horizontal laminations with a wide range of thicknesses (< 1 mm to > 1 cm). They thought the sediments were varved, but detailed analyses and independent dating were never performed.

3. Study area and methods

3.1 Study area

The Peyto Lake watershed (48.9 km^2; 51°72' N, 116°52' W) is located 45 km north-northwest of Lake Louise in Banff National Park, Alberta, Canada (Figure 3.1). Peyto Glacier flows northeast and is one of the outlets of the Wapta Icefield. Peyto Glacier (~ 11.2 km^2 in 2005) and five other small cirque glaciers (1.5 km^2) cover approximately 26% (12.7 km^2) of the watershed. Peyto Glacier lies between 2100 - 3200 m above sea level (asl), has a mean equilibrium line altitude of 2665 m asl, and a mean accumulation area ratio of 0.40. Several moraines adjacent to Peyto Glacier are ice-cored and cover an area of roughly 1.2 km^2 (Ommanney, 1972).

Peyto Lake, the larger of two lakes in the watershed, covers an area of 1.5 km^2 at an elevation of 1876 m asl and is situated 3 km downvalley from Peyto Glacier. Caldron Lake (0.4 km^2) is situated in a cirque 524 m (2400 m asl) above Peyto Lake and does not receive glacier meltwater from Peyto Glacier. Peyto Lake consists of two deeper basins connected by a relatively shallow sill (See Figure 3.5 for Peyto Lake bathymetry). The proximal basin to Peyto Creek has a maximum depth of 43 m, whereas the deepest point in the distal basin is 49 m (Chikita et al., 1996). Peyto Lake receives an annual inflow of approximately 45.3×10^6 m^3; the lake has an approximate capacity of 40.3×10^6 m^3 which equates to a residence time of roughly 11 months (Schuster and Young, 2006). Peyto Creek is dominated by glacier and nival runoff where approximately 82% of the runoff into Peyto Lake occurs from June to August. The lake is nearly isothermal, varying from 5 °C to 7.5 °C in the summer, but the distal basin may develop weak thermal stratification on warmer days. The isothermal lake conditions, coupled with high SSC of Peyto Creek cause underflow currents (i.e., hyperpycnal inflow) to dominate (Smith et al., 1982). Sediment-laden underflows account for 61% of the lake's sedimentation compared to 32% and 7% for delta progradation and overflows/interflows, respectively (Chikita, 1992).

Steep and mountainous alpine terrain (bedrock, talus, thin soils) represents about 53% of the watershed while forests cover about 17 % of the catchment. Peyto and Cauldron lakes represent the remaining 4% of the watershed. The underlying geology of the basin is primarily Precambrian and Cambrian argillite, limestone, and dolomite (Chikita, 1993).

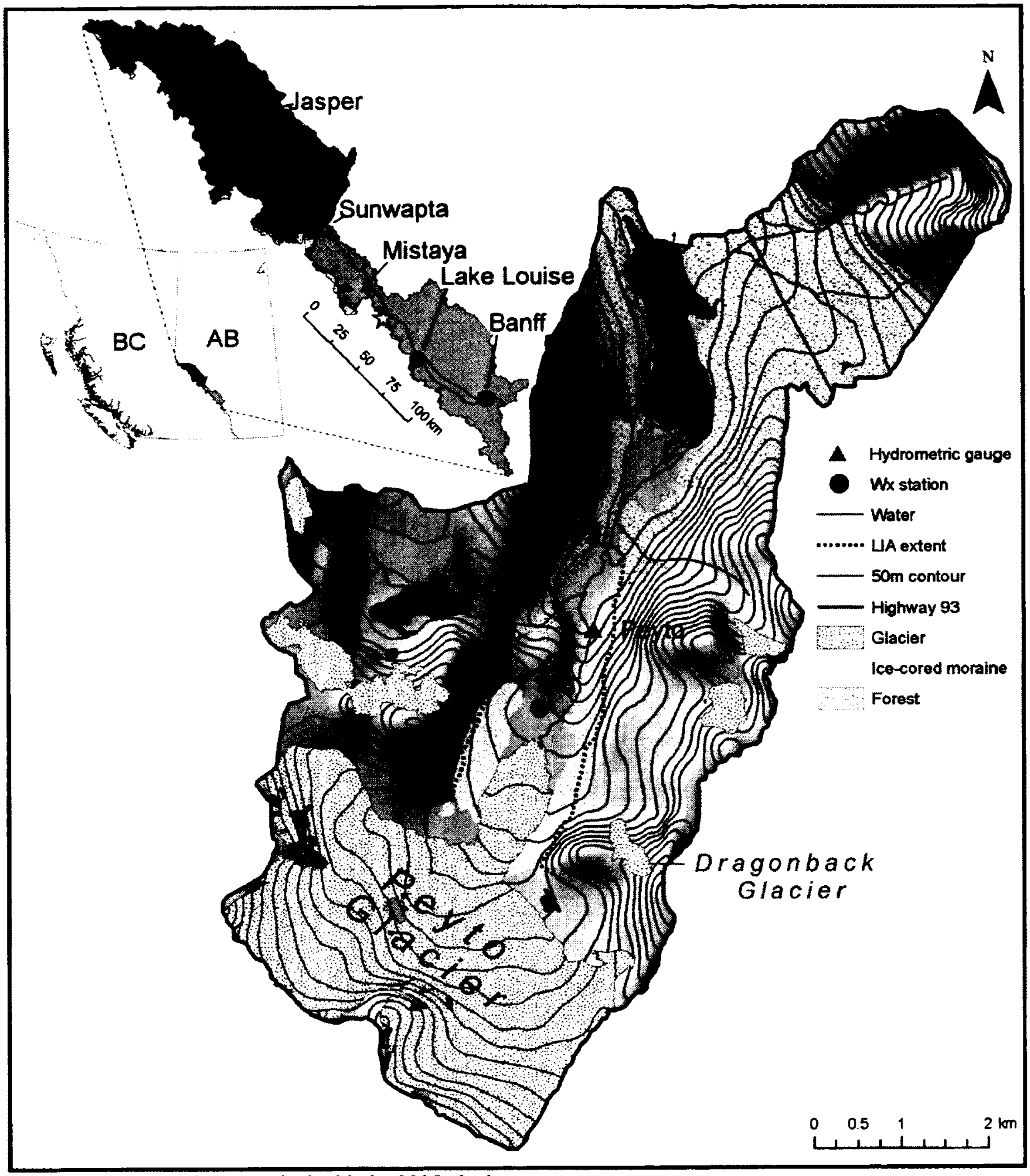

Figure 3.1 Peyto Lake watershed with the 2005 glacier extents.

3.2 Methods for estimation of glacier dimensions

Length, area, and volumetric changes to Peyto Glacier were measured and calculated from a historical map (1917) and 18 sets of available air photos (1947 - 2005) using standard photogrammetric methods (McGlone, 2004).

3.2.1 Data sources and preparation

3.2.1.1 Interprovincial Boundary Commission Survey map

Some of the earliest maps in the Rocky Mountains were produced during the Interprovincial Boundary Commission Survey (IBCS) of the Alberta-British Columbia border between 1903 and 1924. Surveyors took oblique, terrestrial photographs from mountain ridges and peaks then applied photo-topographic methods to produce topographic maps. Although the main objective of the survey was to define the crest of the Rocky Mountains separating the provinces of Alberta and British Columbia, the survey concurrently documented early extents of many glaciers in the Rocky Mountains (Interprovincial Boundary Commission, 1917; Wheeler, 1920). A digital copy of IBCS map #17, which contains Peyto Glacier, was obtained from Library and Archives Canada (LAC). Map #17 was surveyed in 1917 and has a scale of 1:62,500 with a 100 ft (30.48 m) contour interval. Thirty-three mountain peaks and ridges on map #17 were used as ground control points (GCPs) and referenced to previously orthorectified Landsat Thematic Mapper (TM) imagery, and a shaded relief model derived from BC Terrain Resource Information Management (TRIM) digital elevation model (Tennant and Menounos, 2013). The IBCS map was geo-rectified with PCI Geomatica OrthoEngine v.10.3 using the polynomial transformation model. The total root mean square error (RMSE) for the Easting (x) and Northing (y) coordinates is ± 15.18 m. The geo-rectified IBCS map had a significant ridgeline discrepancy that did not align with the actual terrain resulting in erroneous glacier morphology (Figure 3.2). To fix the terrain discrepancy, an additional 21 GCPs were collected and used in a thin plate spline (TPS) transformation model. The TPS transformation model linearly stretched the terrain between the GCPs yielding no RMSE values.

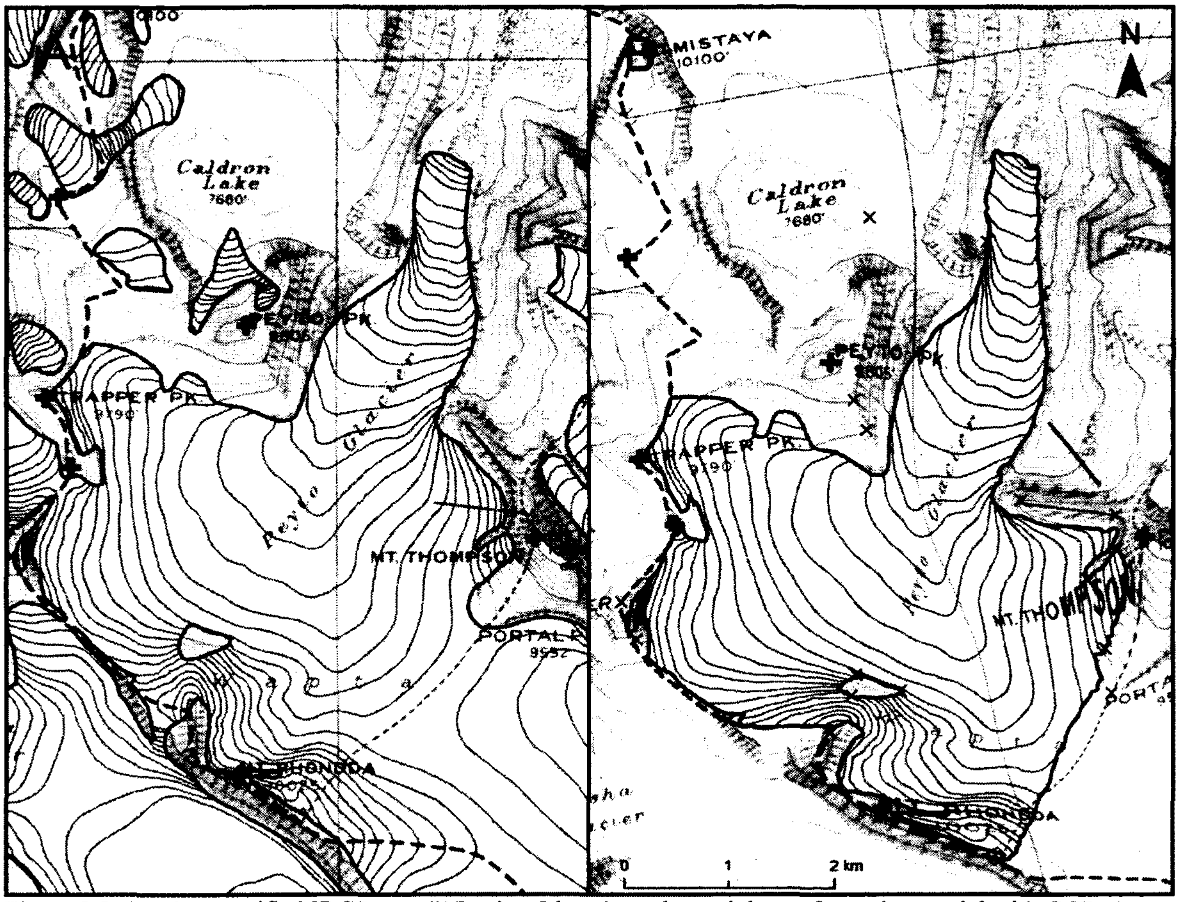

Figure 3.2 (A) Geo-rectified IBCS map #17 using 5th order polynomial transformation model with GCPs (+ symbols). (B) Additional adjustment to map using a thin plate spline (TPS) transformation model with additional GCPs (× symbols). Maps show the transformation of the ridgeline discrepancy before the TPS transformation (red line) and after the TPS transformation (green line).

3.2.1.2 *Aerial photographs*

For this study there are 18 sets of air photographs available from 1947 to 2005. Sequential air photographs were acquired 1 - 11 years apart; however, they were also acquired at different times during the melt season which varied from 2 to 61 days apart. Aerial photographs used in this study were scanned to a digital format at various resolutions from the Canadian National Air Photo Library (NAPL; 12 - 14 μm), GeoBC within the British Columbia government (10 - 16 μm), and the Air Photo Distribution within the Alberta government (20 μm; Table 3.1). The scale of the air photographs ranged from 1:15,000 - 1:90,000. The 2001 and 2005 air photos exist as aerial triangulation (AT) scans rather than 'regular' air photos scans (1947 - 1997). The small area covered by Peyto Glacier enabled the entire region to be captured in stereo in as few as two photographs for some years, but as many as 13 for large-scale photographs.

Depending on the year, only a portion of the accumulation zone was captured in the photographs, but the terminus was captured for all years (Table 3.1). Poor contrast exists in many of the photographs, particularly in the uppermost elevations, which affected my ability to make surface elevation models. Only the 1952, 1977, and 2005 air photographs had excellent contrast in the accumulation zone and 100 % photographic coverage of the glacier.

Table 3.1 Aerial photographs and metadata used in glacier analyses.

Year	Acquisition date	Days before last day of melt¥	TSL (m asl)	Government Source	Flight line	No. of photos	Scale	Glacier cover in photos (%)	Contrast in accumulation area
2005*	3-Aug-05	52	2600	BC	15BCC05017	8	1:30,000	100	excellent
2001*	14-Sep-01	20	-	BC	15BCB01035	3	1:35,000	94	fair
1997	5-Aug-97	50	2540	BC	30BCB97052	13	1:15,000	99	poor
1993	18-Sep-93	6	-	Federal	A27991	6	1:50,000	100	poor
1991	4-Sep-91	20	2625	Federal	A27790	2	1:50,000	100	fair
1986	15-Aug-86	40	2490	BC	15BC86085	2	1:60,000	100	fair - good
1982	30-Jul-12	56	2475	BC	15BC82021	2	1:60,000	87	fair - good
1977	1-Aug-77	54	2500	Federal	A24776	5	1:70,000	100	excellent
1973	24-Jul-73	62	2450	Federal	A23408	7	1:40,000	97	poor
1971	23-Sep-71	1	-	Federal	A22443	2	1:90,000	100	good
1967	25-Jul-67	61	2625	Federal	A20145	9	1:30,000	72	excellent
1966	20-Aug-66	35	2530	Federal	A19434	6	1:40,000	99.5	fair
1955	24-Sep-55	0	-	Federal	A15085	3	1:35,000	49	poor
1952	31-Jul-52	55	2525	Alberta	AS0162	5	1:40,000	100	excellent
1951	6-Sep-51	18	2550	Federal	A13321	5	1:35,000	100	poor
1950	5-Aug-50	50	2470	Federal	A12816	12	1:35,000	98	fair
1949	31-Aug-49	24	2625	Federal	A12313	5	1:40,000	92	excellent
1947	22-Sep-47	2	2640	Federal	A11120	2	1:40,000	56	good

*Aerial triangulations scans

¥ The last air photo was acquired September 24th and approximates the last day of melt.

TSL = Transient Snow Line

3.2.1.3 Supplemental data (mass balance, discharge, climate)

Glacier mass balance refers to the difference between winter accumulation (snowfall) and summer ablation (melting) integrated over the glacier area for a balance year, usually expressed as an average depth in water equivalent (mm w.e.; Cogley et al., 2011). In 1965 the Canadian government selected Peyto Glacier as a representative glacier basin to be monitored in the Rocky Mountains (Ommanney, 2002). The annual mass balance record for Peyto Glacier is the longest and most complete in western Canada (1965 - 1990 and 1993 - 2010; Demuth and Keller, 2006). Unfortunately, both winter and summer mass balances were only measured for the periods 1966 - 1990 and 1993 - 1995. The standard error for the mass balance measurements were estimated by Demuth and Keller (2006) as 150 - 200 mm w.e. In addition to glacier mass balance records, equilibrium line altitude (ELA) and accumulation area ratio (AAR) measurements were provided. ELA is the elevation at which snow accumulation equals snow ablation at the end of summer; it is approximated by the transient snow line (Cogley et al., 2011). AAR is the ratio of the area of the accumulation zone to the area of the glacier, usually expressed as a percentage (Cogley et al., 2011). Net, winter, and summer mass balances, ELA, and AAR records were obtained from World Glacier Monitoring Service (http://www.wgms.ch/index.html), Young (1981), and Demuth et al. (2009).

Hydrometric records for the Peyto Lake watershed are limited. Environment Canada had a seasonal hydrometric gauge (Gauge ID: 05DA008) on Peyto Creek from 1967 to 1977, but these data are neither complete nor long enough to compare to annual sediment yield. Instead, I used records from nearby hydrometric gauges on the Mistaya River (Gauged ID: 05DA007) and the Sunwapta River (Gauged ID: 07AA007). Peyto Creek is a tributary of the

Mistaya River which covers an area of 248 km^2. The Mistaya and Sunwapta stations are approximately 53 km apart and more than 23 km from Peyto Glacier (See Figure 3.1). The Mistaya gauge has seasonal and continuous hydrometric data for the periods 1950 - 1966 and 1967 - 2013, respectively. I created one contiguous record for the entire period (1950 - 2013) by only using daily data between May and October. The Sunwapta River is an outlet of the Columbia Icefields and is in the neighbouring basin north of Mistaya River watershed. The Sunwapta gauge has seasonal hydrometric data for 1949 - 1996 and 2005 - 2011. I used to use the Sunwapta gauge to determine whether changes to the Mistaya River streamflow occur at regional and/or local scales.

Representative climate records for the Peyto watershed are either temporally limited or located too far away to be representative of the watershed's climate. The short, unpublished climate record (1967 - 1977) near Peyto Glacier did not have as strong of a relation to the mass balance record as the climate recorded at other stations in the Canadian Rocky Mountains (Letreguilly, 1988). Munro (2006) suggests the climate station was too close to Peyto Glacier where local cooling from snow and ice reduced the variance in temperature and relation to mass balance. The Improved Processes and Parameterization for Prediction in Cold Regions (IP3) research network erected a climate station near Peyto Glacier from 2002 to 2007, but the climate record is not of sufficient length for a long-term comparison; however, I use these data in a temperature index model to estimate ice melt for years of aerial photography acquired early in the melt season (see section 3.2.3.6). Although Lake Louise has the nearest climate station to Peyto Glacier, the meteorological tower was moved numerous times and the data were deemed unreliable (Letreguilly, 1988). Even though Jasper and Banff have more distant climate stations, their climate records have good correlations with the mass balance records of Peyto Glacier (e.g., Letreguilly, 1988; Watson and Luckman, 2004; Munro, 2006). I use the homogenized surface air temperature data (Vincent et al., 2012) and adjusted precipitation data (Mekis and Vicent, 2011) from Banff and Jasper climate stations. Selected monthly climate averages from Banff and Jasper, unlike data from ClimateWNA (Wang et al., 2012), have the strongest relation to the mass balance record.

3.2.2 Measuring glacier surface and extents

In the next four sections, I describe how I created stereo models from 18 years of aerial photographs, digitized glacier extents and surfaces, conducted quality control, and calculated changes to glacier length, area and volume.

3.2.2.1 Stereo model development

I digitized extents and surfaces of Peyto Glacier using the Vr Mapping Software suite courtesy of Cardinal Systems, LLC. I specifically used the Vr AirTrig, Vr Two Orientation, and the Vr Two software for the specific steps mentioned below. A slightly different approach was undertaken depending whether the digital air photographs were 'regular' or aerial trangulation (AT) scans. AT scans include aero-triangulation data, also known as the exterior orientation file, which allows the user to create a three-dimensional (3-D) surface. Regular air photographs, on the other hand, do not have aero-triangulation data associated with their collection.

I followed a series of steps to create stereo models from the 2005 AT scans. In Vr AirTrig, the photometry was provided by government issued camera calibration reports, then the photograph fiducial marks were identified on the AT scans. Neighbouring photographs were linked to each other with six common 'tie points' and adjacent flight lines were linked with three common 'pass points'. The aforementioned process is referred to as Inner Orientation. In Vr Two Orientation, the exterior orientation file (i.e., aero-triangulation data) was used to create 3-D stereo models of the 2005 AT scans. Once the quality of the 2005 stereo models was assured, 31 GCPs were measured on sparsely vegetated, stable surfaces surrounding Peyto Glacier. GCPs were on stable bedrock features, free of snow/ice, vegetation and loose debris, that are not expected to change from year to year (Kääb and Vollmer, 2000; Schiefer and Gilbert, 2007). Locations of GCPs were evenly distributed, in terms of elevation and plane, on the terrain surrounding Peyto Glacier. The known 3-D coordinates (i.e., Easting, Northing, and elevation) of the GCPs were then used as reference points in the creation of stereo models for regular air photos.

Like the 2005 AT scans, each year of regular aerial photographs were imported into Vr AirTrig for Interior Orientation. The same GCPs collected from the 2005 AT scans were identified in the regular air photos and given the same coordinate (i.e., Easting, Northing, and elevation). The collected GCPs were used to create an exterior orientation file and determine the root means square error (RMSE) in the tie points, pass points, and GCPs. The lowest RMSE value was always desired, but a RMSE < 1 m was considered suitable for this study. With the newly created exterior orientation files, stereo models were built in Vr Two Orientation. Once stereo models were created from sets of AT scans and regular air photographs, I used Vr Two to digitize and measure the extent and surface of Peyto Glacier for the 18 sets of aerial photographs.

3.2.2.2 *Data collection from stereo models*

From the developed stereo models, I digitized and measured 3-D coordinates of the glacier's surfaces and extents using Vr Two software. Unfortunately, measurements were hindered by environmental variables. Late-lying snow in the accumulation zone, for example, obscured the identification of bare earth or ice. Visibility of the glacier, along the eastern edge of Peyto's terminus, was frequently obscured by shadows and steep terrain. The western region in the accumulation zone and a medial moraine were also frequently obscured by debris cover. These problematic features were compared in subsequent years to ensure continuity and consistency in measurements. The extents of the ice-cored moraines were not easily identified, so I delineated their extents by the observed deflation through subsequent years.

Glacier and moraine surfaces were digitized by measuring elevation points (mass points) on a 100 × 100 m grid yielding roughly 1,400 possible points for a given year of photography. I measured mass points within the 1917 IBCS glacier boundary for each year. For all years, mass points were collected on the terminus; however, fresh snow, poor photographic contrast, or missing glacier coverage in the air photos prevented mass points to be collected in the accumulation zone (Figure 3.3; VanLooy and Forster, 2011). If a mass point could not be digitized and measured with confidence, its elevation was estimated by two different methods. First, if a missing mass point for a given year occurred between two adjacent years with measured mass point data, the missing elevation values would be interpolated (based on time) by the difference between the adjacent years. By using this approach, I was able to constrain a likely elevation from known data which is not possible with the second method. Many points were infilled by this sandwiching method, but if they were not, the second method was employed. For this second method, instead of estimating the elevation of an unknown mass point, the average elevation change between two sequential years would be estimated from surrounding known mass points for a designated elevation band. Average elevation changes of mass points on Peyto Glacier were calculated by 100 m elevation bands (e.g., 3100 - 3200 m asl).

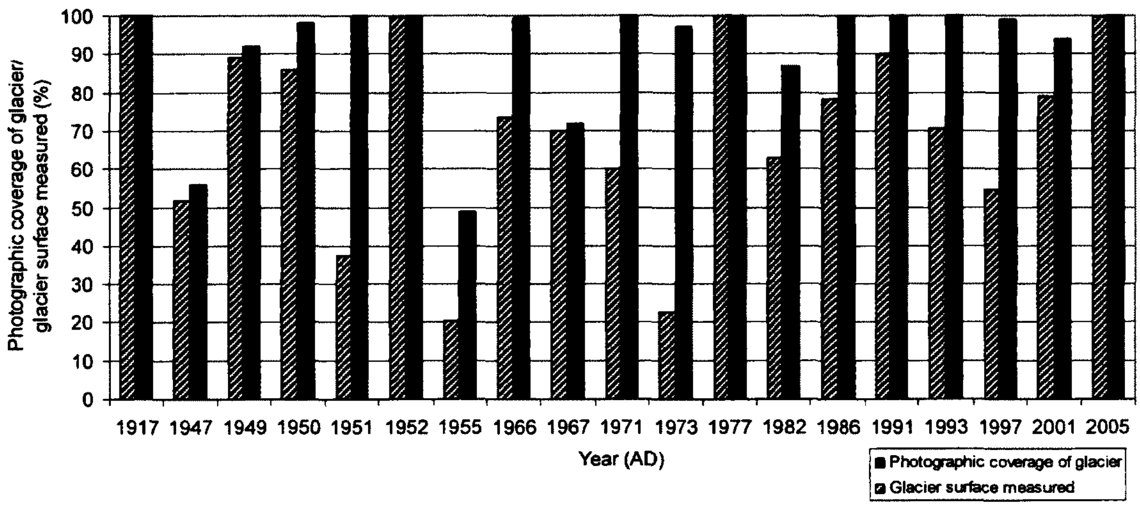

Figure 3.3 The amount of glacier surface that could be measured each year based on photographic coverage of the glacier (solid black bars) and the amount of glacier surface that was measured (stripped bars).

3.2.2.3 Stereo model quality control

I assessed the precision of stereo models by comparing stable surfaces of a given year to the 2005 stereo models (i.e., reference year). I measured a series of points (checkpoints) for a year, then I compared these to the same checkpoints measured from the 2005 photographs. The elevation difference between checkpoints indicates a topographic bias between the two stereo models. Checkpoints were measured on a 5 × 5 grid and spaced 10 m apart which I collectively refer to as a 'checkpatch'. Similar to GCPs, checkpatches were located on stable bedrock features free of snow/ice, vegetation and loose debris. Ten checkpatches were measured at a range of elevations distributed around Peyto Glacier. The Wapta Icefield and steep terrain surrounding Peyto Glacier limited the location and number of checkpatches measured. Depending on photography coverage for that year, 5 - 10 checkpatches were used.

I assessed spatial bias in the stereo models by plotting checkpoint residuals against their respective Easting, Northing, and elevation coordinates (Figure 3.4). The linear model with the highest, significant correlation indicated the strongest bias present in the stereo model (Table 3.2). I used the linear model coefficient to remove the bias (Figure 3.4) from the stereo models of each year (Tennant and Menounos, 2013). Only one bias was removed from the models as a method to prevent over-manipulation of the measured data.

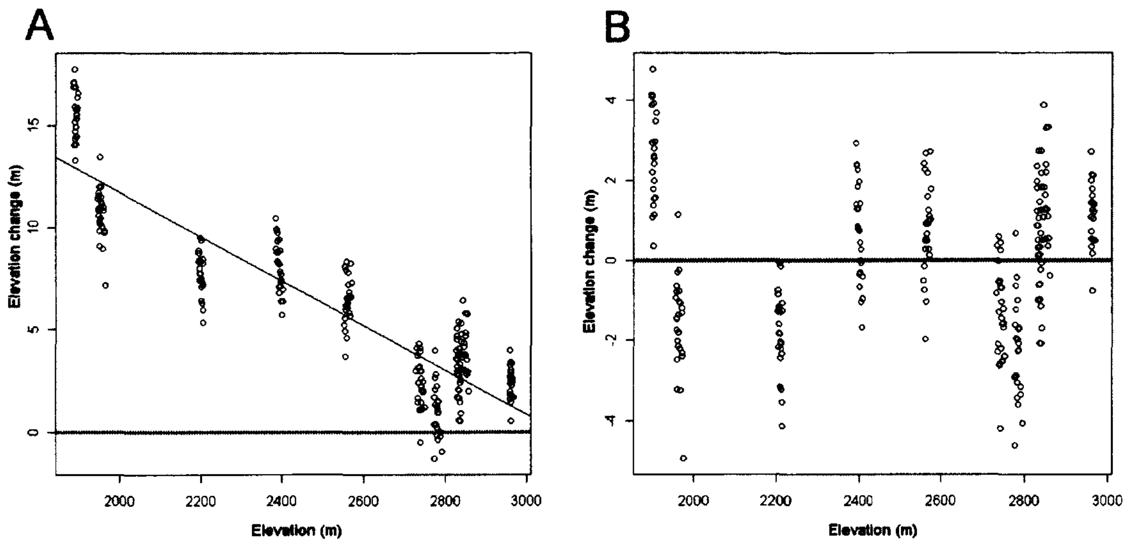

Figure 3.4 Example of checkpoints measured in the 1991 air photos (A) before bias removal and (B) after bias removal.

Table 3.2 Pearson correlation coefficient (r) and significance (p) for checkpoint residuals versus topographic predictors (Elevation, Easting, and Northing). The largest correlations are **bolded** and the respective topographic biases were removed from the models.

Year	Elevation		Easting		Northing	
	(r)	(p)	(r)	(p)	(r)	(p)
2001	-0.644	$2.20E^{-16}$	**0.709**	**$2.20E^{-16}$**	0.313	$9.97E^{-05}$
1997	**-0.555**	**$1.53E^{-15}$**	0.143	$5.99E^{-02}$	0.498	$2.45E^{-12}$
1993	**-0.374**	**$9.99E^{-10}$**	-0.229	$2.65E^{-04}$	0.255	$4.64E^{-05}$
1991	**-0.904**	**$2.20E^{-16}$**	0.248	$7.47E^{-05}$	0.851	$2.20E^{-16}$
1986	0.496	$2.82E^{-12}$	**-0.610**	**$2.20E^{-16}$**	-0.447	$5.37E^{-10}$
1982	**-0.502**	**$9.13E^{-19}$**	-0.075	$2.62E^{-01}$	0.445	$2.54E^{-12}$
1977	0.018	$7.83E^{-01}$	**-0.173**	**$9.46E^{-03}$**	-0.017	$8.05E^{-01}$
1973	-0.034	$6.17E^{-01}$	**0.454**	**$7.27E^{-13}$**	-0.169	$1.09E^{-02}$
1971	0.331	$3.69E^{-07}$	-0.097	$1.44E^{-01}$	**-0.362**	**$2.27E^{-08}$**
1967	0.569	$6.22E^{-13}$	0.302	$4.99E^{-05}$	**-0.717**	**$2.20E^{-16}$**
1966	**-0.749**	**$2.20E^{-16}$**	0.390	$7.72E^{-07}$	0.611	$2.20E^{-16}$
1955	**-0.330**	**$3.81E^{-05}$**	0.173	$3.42E^{-02}$	0.072	$3.84E^{-01}$
1952	**0.662**	**$2.20E^{-16}$**	0.217	$1.04E^{-03}$	-0.580	$2.20E^{-16}$
1951	0.349	$7.54E^{-08}$	**0.483**	**$1.40E^{-14}$**	-0.400	$4.55E^{-10}$
1950	**0.689**	**$2.20E^{-16}$**	-0.050	$4.58E^{-01}$	-0.578	$2.20E^{-16}$
1949	-0.542	$2.20E^{-16}$	**0.611**	**$2.20E^{-16}$**	0.238	$3.09E^{-04}$
1947	**-0.628**	**$4.64E^{-15}$**	-0.494	$4.79E^{-09}$	0.534	$1.37E^{-10}$
1917	-0.216	$2.12E^{-03}$	-0.191	$6.67E^{-03}$	**0.347**	**$4.82E^{-07}$**

3.2.2.4 Glacier change analysis

I imported glacier extents and mass points datasets into ESRI ArcMap 10.1 where changes in glacier length, area, and volume were calculated, and their respective errors assessed. Prior to calculations, the identified model bias for each year was removed from the measured glacier extents and mass point datasets. The entire extent of Peyto Glacier was visible in the aerial photographs for nine years, so the remaining years with incomplete glacier extents had the missing boundaries replaced from the nearest year. Missing boundaries were always in the accumulation zone where areal changes were negligible. The hydrological divide between Peyto Glacier and the rest of the Wapta Icefield was demarcated with the hydrologic analysis tool available in ArcMap.

Changes in glacier length, and area were calculated by differencing the sequential year of data (e.g., 1997 minus 2001) where a receding glacier is denoted as negative and an advancing glacier is denoted as positive. The lengths of Peyto Glacier were measured perpendicular to the glacier terminus and parallel to the glacier's flow line (Andreassen et al., 2002). The length error term is the sum of the mean horizontal RMSE*xy* (Easting (x) and Northing (y) positional errors calculated in Vr Two for stereo model batch adjustments) and one-half of the digital pixel resolution of each year of data (Table 3.3). From 1991 to 1997 there was a large, thin region of 'dead ice' that detached from Peyto Glacier, so the glacier polygons were summed together accordingly. The area error term is equal to a buffer surrounding the inside and outside of the glacier extent (Granshaw and Fountain, 2006; Bolch et al., 2010). The buffer width is equal to the length error term. Error change (E_Δ) for length or area between two consecutive years is thus:

$$E_\Delta = \sqrt{(E_1^2 + E_2^2)}, \tag{3.1}$$

where E_1 and E_2 denote the error terms for length or area for two consecutive years.

Changes between glacier volumes were calculated by differencing the sequential year of mass point data and multiplying the difference of each mass point by its representative area (10000 m^2; VanLooy and Forster, 2011). Elevation changes for points greater than three standard deviations ($\pm$ 3 σ) of the mean were considered outliers and removed from the analysis. The volume change error ($VE\Delta$) for a period is thus a function of elevation and area change:

$$VE_\Delta = \sqrt{({Z_\Delta}^2 E_A^2 + A^2 {\sigma_{\Delta Z}}^2)}, \tag{3.2}$$

where □$_{\Delta Z}$ is the standard deviation ($\pm$ 1 σ) of the elevation change for a period calculated by the checkpoints after bias removal; Z_Δ is the mean elevation change for a period calculated by the checkpoints after bias removal; A is the area of the largest extent used to calculated volume change; and E_A is the area error term of the largest extent.

Table 3.3 Information used to create stereo models and assess their accuracy and error.

Year	Pixel size (m)	No. of GCPs	No. of checkpatches	RMSE *x* (m)	RMSE *y* (m)	RMSE *xy* (m)	RMSE *z* (m)
2005	0.371	-	10	-	-	-	-
2001	0.440	18	6	0.207	0.214	0.298	0.041
1997	0.152	23	10	0.294	0.339	0.449	0.130
1993	0.637	22	10	0.193	0.169	0.257	0.045
1991	0.124	28	10	0.264	0.225	0.347	0.022
1986	0.757	10	7	0.197	0.276	0.339	0.028
1982	0.741	24	7	0.244	0.253	0.351	0.037
1977	0.640	27	10	0.255	0.250	0.357	0.045
1973	0.156	18	7	0.221	0.310	0.381	0.155
1971	0.611	26	7	0.294	0.302	0.421	0.033
1967	0.088	20	7	0.525	0.357	0.635	0.304
1966	0.159	19	7	0.284	0.237	0.370	0.152
1955	0.662	20	6	0.231	0.256	0.345	0.044
1952	0.401	25	9	0.577	0.635	0.858	0.404
1951	0.675	24	9	0.409	0.448	0.607	0.266
1950	0.108	18	9	0.611	0.999	1.171	0.903
1949	0.271	23	9	0.581	0.450	0.735	0.414
1947	0.399	17	5	0.246	0.246	0.348	0.059
			Mean RMSE	0.330	0.350	0.490	0.180
1917	-	33*	8	9.62	11.74	15.18	-

GCPs = Ground Control Points, RMSExyz = Root Mean Square Error on the Easting (x), Northing (y) and elevation (z) axes. * Mountain peaks were used as GCPs in the 1917 map, but not used in aerial photographs.

3.2.2.5 Glacier volume change conversion

I converted the measured changes of glacier volume to snow water equivalent (w.e.), so that I could compensate for seasonal melt differences that resulted from the date aerial photographs were acquired. The measured changes to glacier volume were converted to snow water equivalent using an average density of 760 kg m^{-3}. I calculated average density using the mean accumulation area ratio for Peyto glacier of 0.40 where ice density in the ablation zone was assumed 900 kg m^{-3} and ice density in the accumulation zone was assumed 550 kg m^{-3} (Schiefer et al., 2007).

To adjust volumetric changes of Peyto Glacier attributed to when aerial photographs where acquired, I used a basic temperature index model given by Hock (2003):

$$\sum_{i=1}^{n} M = DDF \sum_{i=1}^{n} T^{+} \Delta t \,, \tag{3.3}$$

where M is the total amount of ice or snow melt, T^{+} is the positive air temperatures, Δt is the day for the period (n), and DDF is the degree-day factors (expressed as mm $°C^{-1}$ d^{-1}). For melt factors (or DDF), I used the values 2.32 mm $°C^{-1}$ d^{-1} for snow and 5.57 mm $°C^{-1}$ d^{-1} for ice that were derived from the glacier mass balance records of Peyto Glacier (Shea et al. 2009). I distinguished different DDF surfaces (snow and ice) by the transient snow line apparent in the aerial photographs. For the unknown mean daily temperature values, I compared mean daily temperatures for August and September from Banff (1396 m asl) to values recorded at the IP3 station (2240 m asl) near Peyto Glacier from 2002 to 2007 and calculated a linear lapse rate of 5.51°C km^{-1}. From the Banff climate data, mean daily temperatures were adjusted on the mass point grid (100 m × 100 m) across the surface of Peyto Glacier. For the study period, aerial photographs were acquired from as early as July 24th to as late as September 24th. Therefore, daily differential adjustments to glacier volume were calculated and summed from the date aerial photographs were acquired until the end-date of the melt season approximated as September 24th.

3.3 Methods to estimate sediment yield

3.3.1 Field sampling

I retrieved core samples of lake sediments taken from the bottom of Peyto Lake throughout March 2010, February 2011, and April 2011. A 250 m sampling grid was selected to capture the diversity of the lake's topography (i.e., basins and sills), and provide a large enough sample size to conduct spatial analysis and statistics (Schiefer, 2004). In total, 20 percussion, two Ekman box, and five gravity cores were collected. With coring instruments I collected 0.2 - 3.0 m long sediment cores along specified grid locations on the frozen lake surface (Reasoner, 1993; Glew et al., 2001). Generally, the longer cores were collected in the deeper basins or in close proximity to the Peyto Creek delta. I used Ekman box and gravity corers to collect undisturbed sediments at the water-sediment interface (i.e. the upper 10 - 15 cm of the sediment surface; Hodder et al. 2006), which can be disturbed by the use of a percussion corer. The recovered sediment cores were transported to UNBC and stored in a refrigerator at 4 °C until further laboratory analyses were conducted (Appendix A).

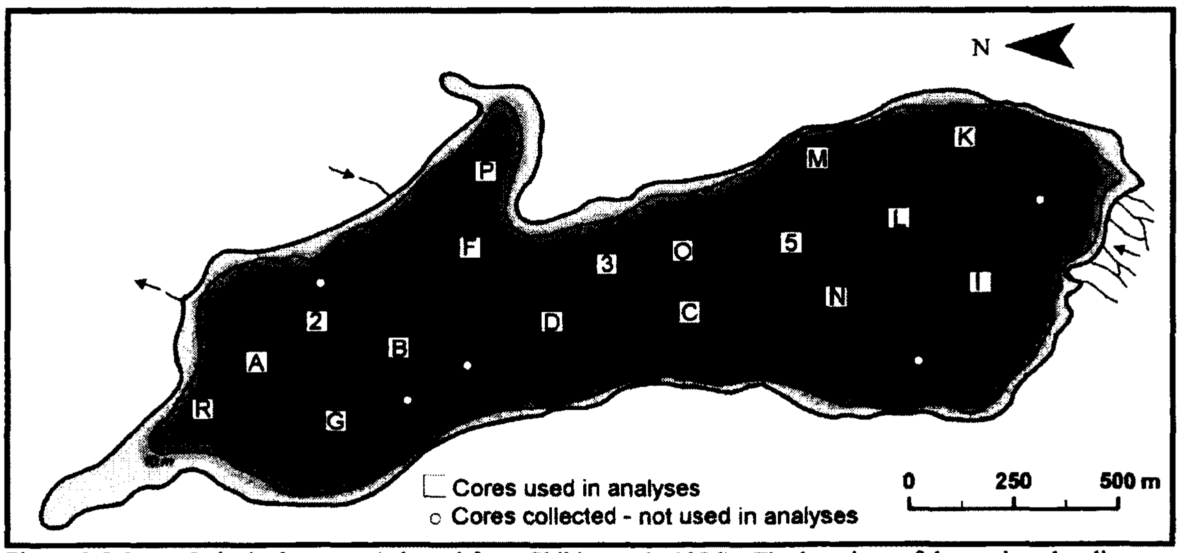

Figure 3.5 Peyto Lake bathymetry (adapted from Chikita et al., 1996). The locations of the retrieved sediment core samples are shown. Note: core 10-Peyto(01) was taken from the same location as core 10-Peyto(02). The small arrows indicate the primary inflow and outflow of Peyto Creek.

3.3.2 Laboratory analysis

3.3.2.1 Photography

I split all cores lengthwise where the working halves were sub-sampled for bulk-physical properties (see section 3.3.2.2) and the archive halves were photographed. I used a Nikon D90 SLR camera with an 18 - 105 mm zoom lens to capture digital images that contained a resolution of 12 megapixels. To capture maximum depth of field and reduce radial lens distortion, images were taken at the maximum aperture of F-32 with a focal length of 50 mm. Each image referenced core direction, sediment depth, date, times photographed, and a scale bar. From the clearest images, I measured the length of cores and silt-clay couplets with a precision of 0.2 mm using a script program written to operate with UTHSCSA Image Tool software V. 2.01 (Wilcox et al., 2002). The visible detail, color, and texture of the core samples changed considerably as they dried at room temperature, so cores were photographed multiple times as they dried. Often the laminated sediments were not clearly discernable until the sediments were allowed to dry out completely; unfortunately the drying processes also caused cracks throughout the sediments (Figure 3.6). Both wet and dry cores were measured as a method to quantify the size of cracks and sediment shrinkage when the photographs were taken.

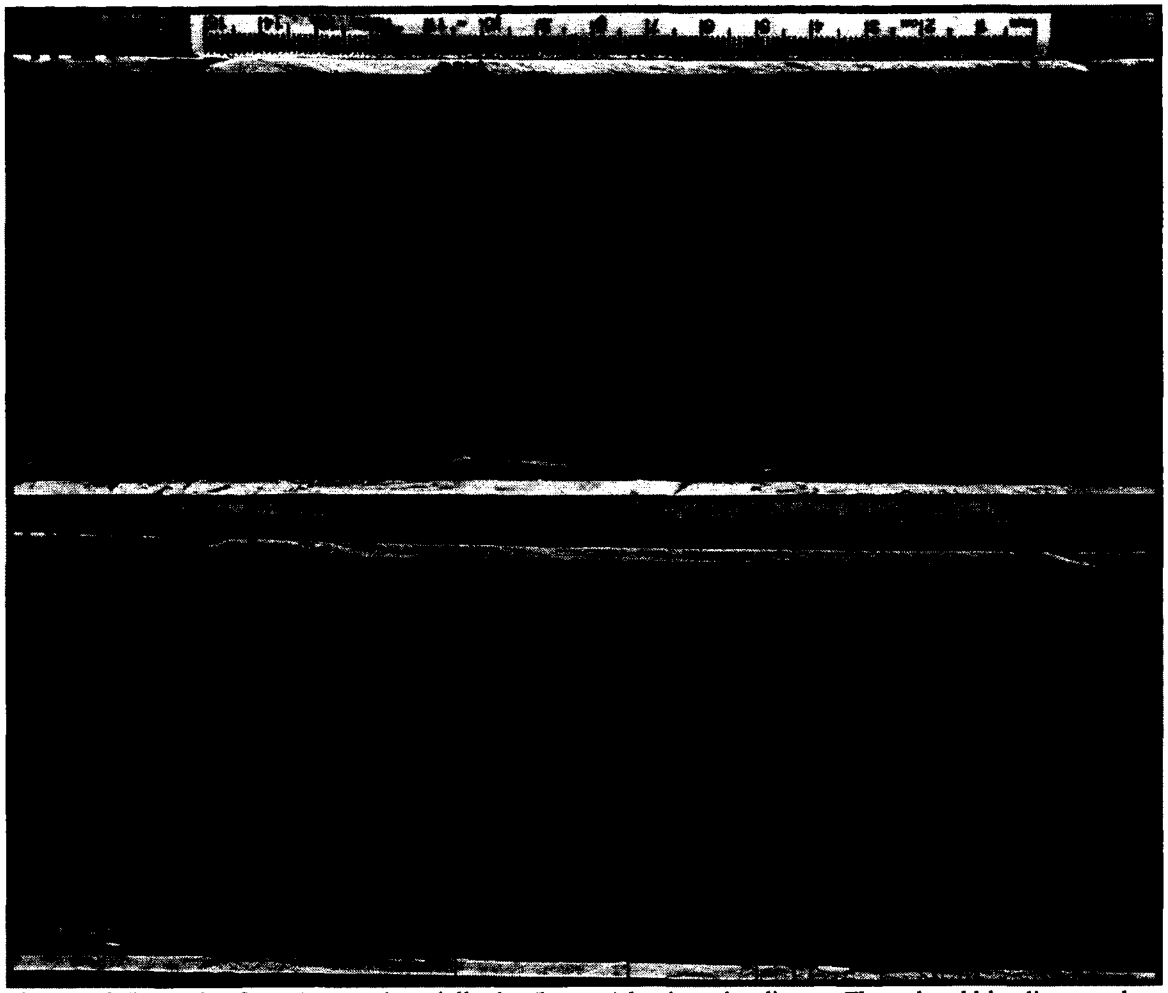

Figure 3.6 Example of wet (top) and partially dry (bottom) laminated sediment. The red and blue lines on the dry sediments are measurements from the UTHSCSA Image Tool software. The water-sediment interface is towards the right.

3.3.2.2 Bulk-physical properties

I sub-sampled bulk-physical properties by standard methods outlined by Håkanson and Jansson (2002). The sub-sampling interval varied by non-master and master core types. Non-master cores were sub-sampled at 10 cm intervals for the primary purpose of interpolating spatial variation (areal and depth) of sediment distribution within Peyto Lake. The master core sites align with the longitudinal axis of the lake and were sub-sampled at 2 cm intervals as a way to determine the variation of bulk physical properties at a higher resolution. Sub-samples (2.0 ml) were taken with a 14 mm syringe along the longitudinal axis of the core where minimal disturbance occurred. Sub-samples were weighed, oven-dried at 105 °C for 12 to 24 hours, and then reweighed again at room temperature (Heiri et al., 2001). Water content and dry bulk density were calculated as follows:

$$Percent\ water\ content = \frac{Wet\ mass\ (g) - Dry\ mass_{105}\ (g)}{Wet\ mass\ (g)} \times 100 \tag{3.4}$$

$$Dry\ bulk\ density = \frac{Dry\ mass_{105}\ (g)}{Wet\ Volume\ (cm^3)}, \tag{3.5}$$

where the subscription denotes the oven treatment temperature. Variations in water content variation reflect the quality and character of the deposits, sedimentation rates, degree of compaction, organic content, and degree of bioturbation (Menounos, 1997; Håkanson and Jansson, 2002). The following loss-on-ignition (LOI) technique is a commonly used method to estimate organic content of sediments (Heiri, 2001; Håkanson and Jansson, 2002). To determine organic matter (OM) content, samples were heated in an oven to 550 °C for four hours where the organic matter oxidized to carbon dioxide and ash. Once samples cooled to room temperature, they were reweighed, so that OM content could be calculated:

$$OM\ LOI_{550} = \left(\frac{Dry\ mass_{105}(g) - Dry\ mass_{550}\ (g)}{Dry\ mass_{105}\ (g)} \right) \times 100 \tag{3.6}$$

High-levels of OM content may reflect periods of flooding, mass movement events, or changes in primary productivity levels within the lake (Håkanson, 1995; Lacourse and Gajewski, 2000; Heiri et al., 2001).

3.3.3 Core chronology

3.3.3.1 Cesium-137 analysis

An annual chronology of sediment yield requires independent confirmation that silt-clay couplets in the cores are varves. The isotope Cesium-137 (^{137}Cs) is an artificial fallout radionuclide that has two primary sources: (1) atmospheric nuclear weapons tests for the period 1953 - 1963, and (2) the Chernobyl reactor fire of 1986 (Appleby, 2001). The presence of ^{137}Cs sediments allows researchers to verify the annual nature of sediment records (Lamoureux, 2001). From the North America ^{137}Cs fallout record, peak nuclide activity corresponds to 1963. ^{137}Cs activity associated with the peak levels of the 1986 Chernobyl reactor fire has not been detected in western Canada. Sub-samples were taken at 10 cm intervals down the entire length of core 10-Peyto(02). To constrain the dating of 1963, additional sub-samples were taken at assumed varve locations on both sides of where I counted the 1963 varve should be located (a total of 21 sub-samples). Sub-samples yielding >5 grams dry weight were taken with a 14 mm diameter syringe and freeze-dried for 24 hours before being sent to Flett Research Ltd., Winnipeg, Canada, for ^{137}Cs activity measurements by gamma spectrometry using 19% and 25% efficient HPGe detectors.

3.3.3.2 Master chronology

I produced a master varve chronology by merging individual varve records obtained from the sediment cores. A varve chronology enables incorrectly identified varves and missing sediment layers in cores to be identified (Lamoureux, 2001). A complete chronology is needed for all cores for an accurate sediment yield to be calculated. From the ^{137}Cs radionuclide dating results described in section 4.2.3, I was able to create a chronology for core 10-Peyto(02) and convert it to calendar years (AD). I produced a varve chronology for the remaining cores by matching unique sediment layers (marker beds) among cores. Although the high sedimentation rate of Peyto Lake resulted in large varves that could easily be linked among multiple cores, there were only three key marker beds identified among all cores: two light coloured beds deposited in 1834 and 1846; and an unusually thick layer deposited in 1983. In July of 1983, a rainfall-triggered flood destroyed the hydrometric monitoring station on Peyto Creek (Schuster and Young, 2006). Although, small flood and mudflows had previously been observed, nothing approached the magnitude of the 1983 event described by Johnson and Power (1985). According to their study, large amounts of precipitation eroded an ice-cored moraine and the subsequent gravel (6000 m^3) was deposited down valley.

Once varve chronologies were created for all cores, I created a master chronology following the methods in Desloges (1994) which standardizes varve thickness:

$$VS_i = \frac{V_i - \overline{V}}{\sigma_v}, \tag{3.7}$$

where VS_i is the standardized thickness for year i, V_i is the measured varve thickness, $\overline{V}$ is the mean varve thickness for the core, and σ_v is the standard deviation. The standardized values for each core were averaged for that year which resulted in a master chronology of varve thickness variation. This chronology, in particular, is important for highlighting a common signal among cores and identifying rates when varve thicknesses were above or below average.

3.3.4 Sediment yield calculations

3.3.4.1 Spatial sediment interpolations

In most cores, the sediment laminations near the water-sediment interface were disturbed, unidentifiable, or missing. The unknown sediment thickness for a single core was estimated by a ratio determined by a neighbouring core with the highest correlation of varve thickness variation. For instance, if core X has 75 % of the sedimentation as core Z and they have a significant correlation with each other, the missing sediment thickness for core X is equal to 75% of core Z for the same region.

For Peyto Lake, annual variation in sediment thickness could not be explained by environmental variables (e.g., distance to the delta and lake depth) like that found by Schiefer (2004) for Green Lake, BC. Instead of using a multiple linear regression to interpolate sediment thickness, I used two methods of interpolation: Thiessen polygons and regularized spline. These two methods of interpolation provide a range of possible sediment yield values that cannot be independently confirmed by a simple technique. The first method uses Thiessen polygons as representative areas around each core sample (e.g., Figure 4.16; Evans 1997). This method assumes that sedimentation occurs at all lake depths equally within each polygon. In reality, however, a lake environment dominated by underflow and influenced by environmental variables, such as lake depth and wind, limits sedimentation above a certain depth (Smith and Ashley, 1985). Therefore, I also conducted a first-order sensitivity analysis to estimate the limits of where sedimentation could have occurred in Peyto Lake when lake depths were deeper than 0 m, 10 m, and 20 m (covering 100 %, 86 %, and 73 % of the lake area, respectively). The second method of interpolation uses a regularized spline which estimates values using a mathematical function to minimize overall surface curvature (e.g.,

Figure 4.16). Even though the regularized spline method does not encompass bathymetry, it produces a smoothed surface that is similar to the expected sedimentation pattern. For both methods, the interpolated surface passes exactly through the sample points.

3.3.4.2 Lake trap efficiency

Verstraeten and Poesen (2000) reviewed methodologies to estimate the percent of sediment remaining in a lake after flowing into it, also known as the lake's trap efficiency (TE). They provide a modification of the Brune (1953) TE curve that has a focus on lakes dominated by different sediment textures. Specific to fine-grained sediments (silt and clay), TE is defined as:

$$TE = 94 - (3.38 \left| \ln\left(\frac{C}{I}\right) \right|^{1.92}), \tag{3.8}$$

(formula originally cited in Harbor et al., 1997)

where C is volumetric capacity of the lake and I is the annual inflow to the lake.

3.3.4.3 Sediment yield

Calculation of sediment yield (SY) from multiple cores follows a similar equation to that used by Evans (1997):

$$SY = \sum_{i=1}^{n} \left[Z_i A_i D_i \left(1 - \left(\frac{L_i}{100} \right) \right) \right] \times \left[\frac{100}{TE} \right], \tag{3.9}$$

where Z_i is sediment thickness (measured or interpolated) of a unit in core i; A_i is the representative area (Thiessen polygon or raster pixel); D_i is the mean dry weight/wet volume; L_i is the mean percentage LOI value; and TE is the estimated trap efficiency of the lake (see section 3.3.4.2.).

Mean diatom and authigenic carbonate concentrations are two additional variables that can affect SY values, but they are not easily measured. The diatom concentration in Peyto Lake was not measured; however, the concentration is expected to be negligible as shown in nearby lakes (Hickman and Reasoner, 1998; Hobbs et al., 2011). For watersheds dominated by carbonate bedrock, like Peyto basin, authigenic carbonate content determined by LOI methods is not possible (Evans, 1997).

To compare sediment yield among different sized watersheds, sediment yield is divided by watershed area which is then defined as specific sediment yield (SSY):

$$SSY = \frac{SY(Mg\ yr^{-1})}{Watershed\ area\ (km^2)} \tag{3.10}$$

4. Results

The results are categorized into three sections regarding glacier dimensions, sediment analyses, and environmental controls on sediment yield.

4.1 Glacier dimensions

In the following three sections, I assessed the quality of the stereo models and determined environmental biases (i.e., Easting, Northing, or elevation); I quantified data availability by photographic coverage and measurable glacier surface; and I determined changes to glacier length, area and volume.

4.1.1 Stereo model verification and bias removal

Identified biases from the photographic based stereo models and 1917 IBCS map were quantified and removed. The mean horizontal (*xy*) and vertical (z) RMSE calculated for the 18 years of aerial photography were respectively 0.49 m and 0.18 m (Table 3.3). Mean checkpatch elevation difference before bias removal was 2.67 ± 2.95 m. There were significant linear biases in all stereo models. Elevation biases were present in majority of models, but Easting biases were present in 1949, 1951, 1973, 1977, 1986, and 2001; Northing biases were present in 1967 and 1971 (Table 3.3). The linear model coefficients (Table 3.2) were used to adjust the stereo models, and following adjustment the mean checkpatch elevation difference became -0.00 ± 2.28 m. The newer aerial photographs (1966 - 2001) were the most accurate as the elevation differences for the checkpatches were roughly ± 5 m. In comparison, older aerial photographs (i.e., 1947 - 1955) produced less accurate corrected models where the elevation difference for the checkpatches often exceeded ± 5 m (Figure 4.1).

The mean horizontal RMSE*xy* for the 1917 IBCS map was 15.8 m. There were no vertical adjustments to the planar map. The mean checkpatch elevation difference before bias removal was 29.01 ± 37.67 m. The Northing coordinate was the only significant bias that was present in the IBCS map. After bias removal, the mean checkpatch elevation difference was 0.01 ± 35.03 m (Q_{25} = -29.81 m, Q_{50} = -7.44 m, Q_{75} = 12.25 m).

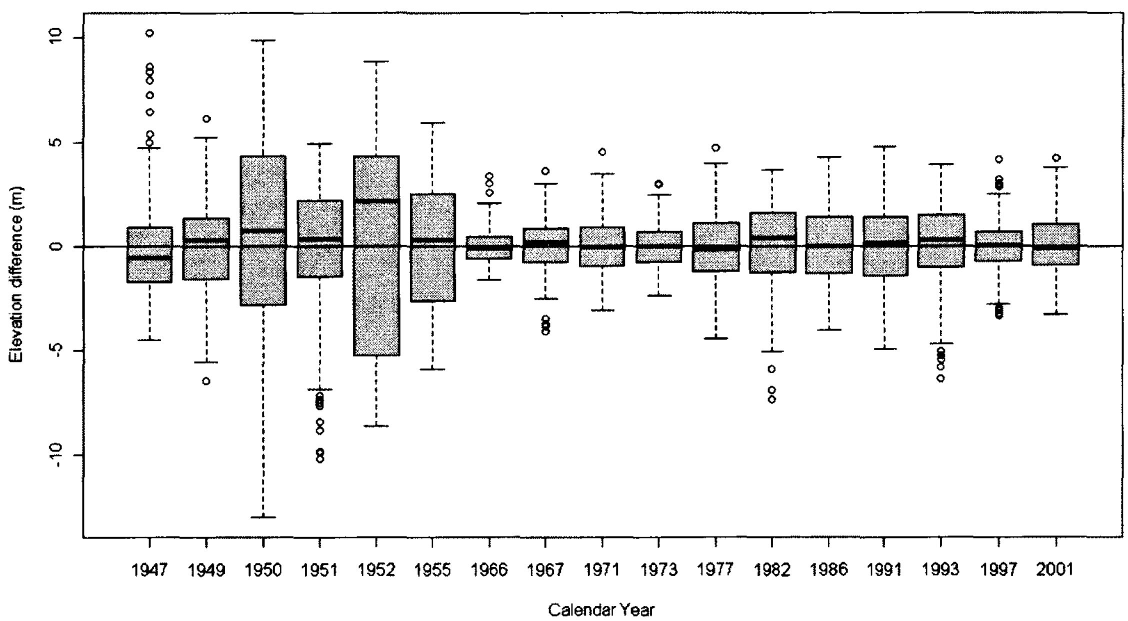

Figure 4.1 Box plot showing the absolute elevation difference of check points after bias removal. Differences are between individual years and the 2005 reference data.

4.1.2 Data completeness

The amount of glacier surface from which elevation could be extracted varied due to photographic coverage, poor contrast in the accumulation zone, cloud cover or a combination of these factors (Figure 3.3). Unknown surface elevations were estimated; however, the accuracy of infilled values was not independently confirmed. The quality of the stereo models was independently assessed by checkpatches (see section 4.1.1.), but the assessment did not consider the percent of the glacier's surface that was available to be measured. Here, the calculated changes to glacier volume are categorized by 'completeness' that reflect the amount of glacier surface measured and my confidence in the quality of the data. Defined periods were specified by years containing: > 99 % of the surface measured; > 70 % of the surface measured; > 50 % of the surface measured; and > 20 % of the surface measured (Table 4.3). The measured glacier surface from the 1947 stereo models resulted in erroneous results, so they are omitted from the remaining results.

Table 4.1 Study periods categorized by the percent of glacier surface measured in the stereo models.

> 99 %	> 70 %	> 50 %	> 20 %
1977-2005	2001-2005	2001-2005	2001-2005
1952-1977	1993-2001	1997-2001	1997-2001
1917-1952	1991-1993	1993-1997	1993-1997
-	1986-1991	1991-1993	1991-1993
-	1977-1986	1986-1991	1986-1991
-	1967-1977	1982-1986	1982-1986
-	1966-1967	1977-1982	1977-1982
-	1952-1966	1971-1977	1973-1977
-	1950-1952	1967-1971	1971-1973
-	1949-1950	1966-1967	1971-1967
-	1917-1949	1952-1966	1967-1966
-	-	1950-1952	1955-1966
-	-	1949-1950	1955-1952
-	-	1917-1949	1952-1951
-	-	-	1950-1951
-	-	-	1949-1950
-	-	-	1917-1949

Categorizing the data by 'completeness' does two things simultaneously: it breaks the data into smaller periods and smaller volume changes. For instance, the average periods are 29.3, 8.0, 6.3, and 5.2 years for each category (> 99, > 70, > 50, and > 20 %, respectively). As the completeness of the data decreases (i.e., > 99 to >20 %), trends in the data emerge (Figure 4.2). That is, as the completeness of the data decreases, the total volume change of glacial ice and total ice (glacier and ice-cored moraines) increases respectively by 9 % and 5 %. The volume change of the lateral ice-cored moraines, in contrast, decreases by 22 % as the completeness decreases. The most complete data have fewer values (n=3) available to compare to sediment yield which is not ideal for finding a correlation. The least complete data have more values (n=17) to compare to sediment yield, but limits the utility of these data to compare to the sediment yield record.

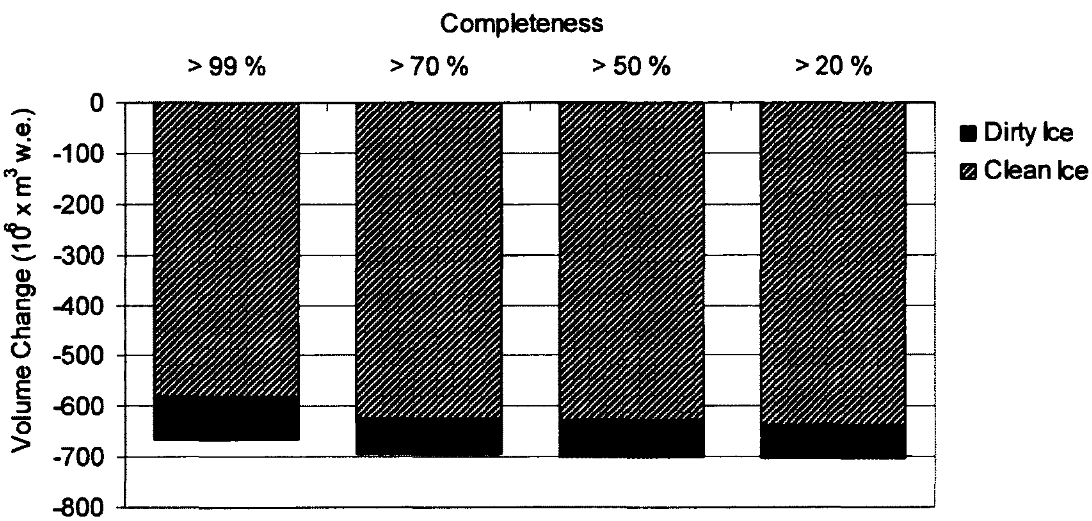

Figure 4.2 Changes in ice volume for Peyto Glacier categorized by the completeness of surface points measured.

4.1.3 Changes to glacier length and area

For the period 1917 - 2005, Peyto Glacier experienced a net retreat (Figure 4.3). During this period, Peyto Glacier retreated a total distance of -2198 ± 18 m along its flow line which yields an average recession rate of -25 ± 0 m yr^{-1} (Table 4.1). Periods with an above average retreat rate include: 1947 - 1949, 1950 - 1951, 1955 - 1966, 1967 - 1971, and 1973 - 1982.

In 1917, the area covered by Peyto Glacier was 15.2 ± 0.5 km^2. By 2005, the glacier shrank to -11.2 ± 0.02 km^2 which corresponds to a retreat rate of -0.046 ± 0.005 km^2 yr^{-1}. Peyto Glacier grew during the periods: 1949 - 1950, 1951 - 1952, and 1971 - 1973 (Table

4.1). These periods of positive growth are likely spurious and attributed to: (1) patches of snow along the perimeter of the glacier that were measured in the more recent set of aerial photographs, but not in the older set; and (2) differences in the time of year when the aerial photographs were acquired (Table 3.1). Generally, the majority of glacier ice melted in regions below the ELA; however, glacier ice was also observed to have melted in peripheral areas of the accumulation zone and in a central location where a rock island began to emerge (*ca.* 1966). Periods with the largest change in glacier coverage include: 1947 - 1949, 1950 - 1951, 1966 - 1971, 1973 - 1977, and 1997 - 2001.

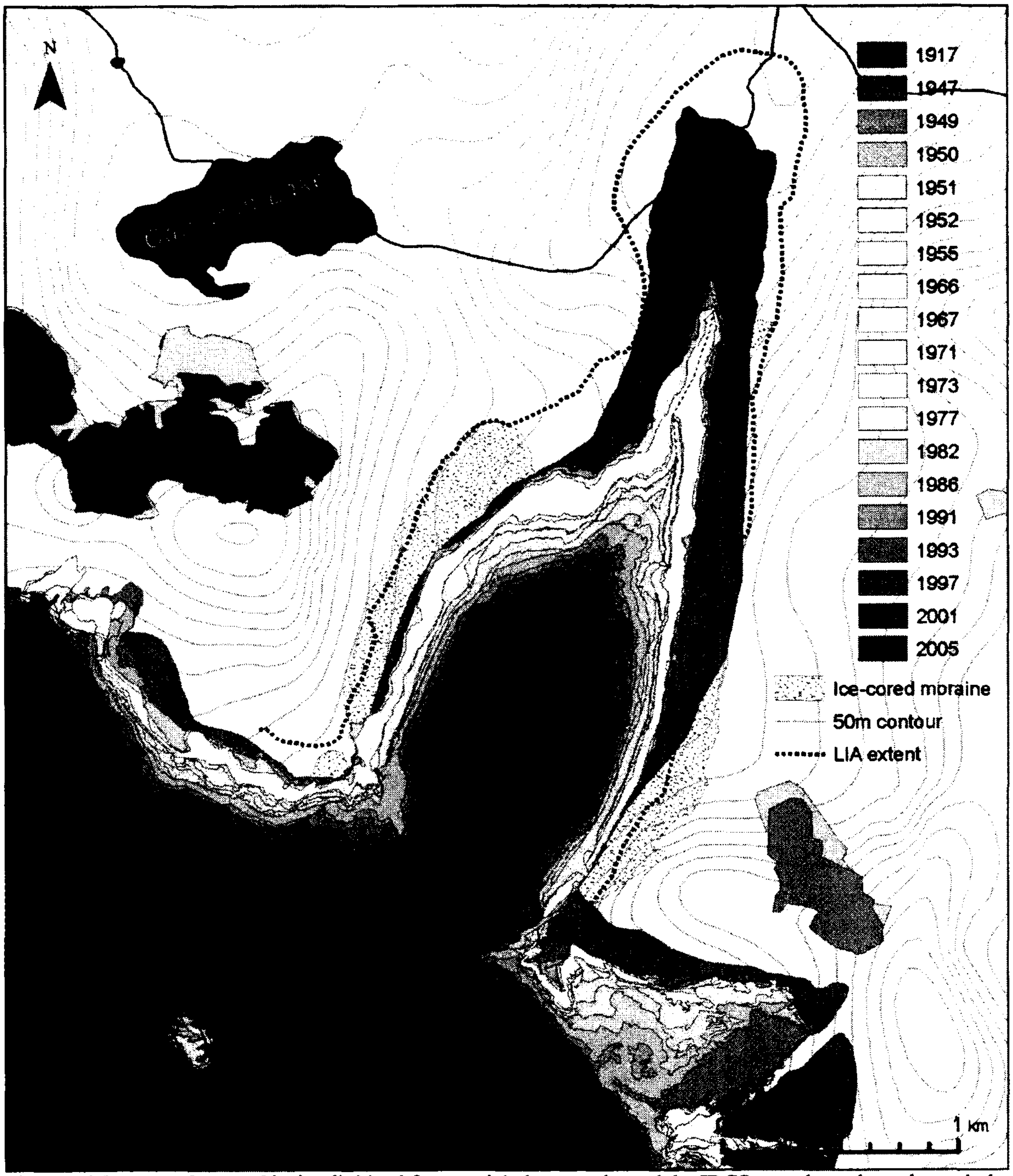

Figure 4.3 Extents of Peyto Glacier digitized from aerial photographs and the IBCS map throughout the period 1917 - 2005.

Table 4.2 Mean rate of length and area changes for Peyto Glacier.

Period	Δ Length (m yr^{-1})	Δ Area (× 10^4 m^2 yr^{-1})
2001 - 2005	-21.5 ± 0.2	-3.83 ± 0.72
1997 - 2001	-18.9 ± 0.2	-12.50 ± 0.64
1993 - 1997	-15.2 ± 0.2	-2.15 ± 0.70
1991 - 1993	-21.4 ± 0.4	-6.52 ± 1.23
1986 - 1991	-14.3 ± 0.2	-6.12 ± 0.58
1982 - 1986	-18.5 ± 0.3	-4.19 ± 0.88
1977 - 1982	-31.8 ± 0.2	-4.80 ± 0.68
1973 - 1977	-28.5 ± 0.2	-7.84 ± 0.71
1971 - 1973	-18.1 ± 0.4	10.65 ± 1.49
1967 - 1971	-41.7 ± 0.2	-7.05 ± 0.89
1966 - 1967	-16.5 ± 0.8	-12.85 ± 3.07
1955 - 1966	-42.3 ± 0.1	-4.33 ± 0.26
1952 - 1955	-7.5 ± 0.4	-3.18 ± 1.41
1951 - 1952	-10.3 ± 1.4	8.66 ± 4.76
1950 - 1951	-119.5 ± 1.5	-11.55 ± 5.52
1949 - 1950	-10.0 ± 1.5	15.71 ± 5.36
1947 - 1949	-26.0 ± 0.5	-13.71 ± 1.66
1917 - 1947	-20.5 ± 0.6	-3.98 ± 1.60
1917 - 2005	-25.0 ± 0.2	-4.55 ± 0.55

4.1.4 Observed volume change

4.1.4.1 Peyto Glacier

Changes to glacier volume were measured and converted to water equivalent (w.e.). I then applied the temperature index model to adjust the volumetric changes of Peyto Glacier attributed to when aerial photographs were acquired (Figure 4.4). The importance of applying a temperature index model to volume change was particularly important for the periods 1949 - 1950, 1966 - 1967, and 1971 - 1973. For these periods, the volume changes for Peyto Glacier were positive before the temperature index model was applied, but became negative after applying the temperature index model.

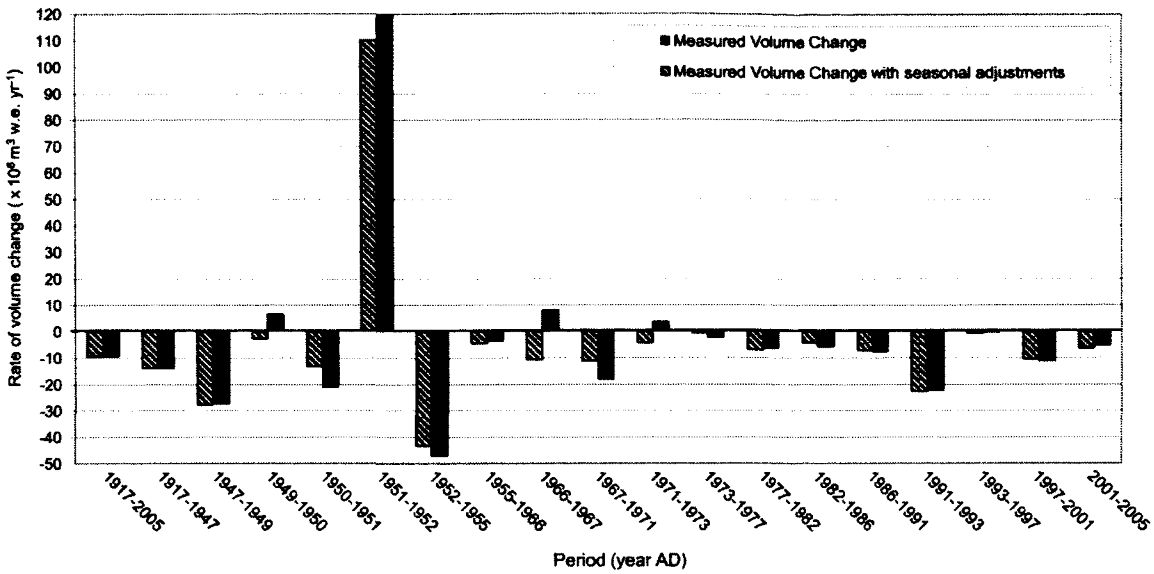

Figure 4.4 Comparison of measured volume changes of w.e. (solid black bars) and measured volume changes of w.e. with seasonal melt adjustments (stripped bars).

Changes to glacier volume were categorized by data completeness ranging from most complete to least complete: > 99 %, > 70 %, > 50 %, and > 20 %. The error terms for the least complete data (> 20 % and > 50%) generally made interpretation inconclusive (Appendix C), so the remaining results focus on the most complete data sets (>70% and >99%).

The most complete data show that Peyto Glacier and the ice-cored moraines lost -666 $\pm$ 406 $\times$ 10^6 m^3 w.e. over the past 88 years (Figure 4.5). Eighty seven percent of this volume change (-581 $\pm$ 404 $\times$ 10^6 m^3 w.e.) originated from the clean ice of Peyto Glacier. If I divide the latter volume by the average area of the glacier (13.2 km^2), the glacier thinned a total of -44.0 $\pm$ 30.6 m w.e. which corresponds to a rate of -0.50 $\pm$ 0.35 m w.e. yr^{-1}. The large error term arises from the low accuracy of the 1917 IBCS map. For the period 1917 - 1952, errors in the 1917 IBCS map is evident when compared to the periods 1952 - 1977 and 1977 - 2005 (Figure 4.6). The eastern portion of the ablation zone, for example, gained volume and regions in the accumulation zone lost unlikely amounts of volume. The highest rate of volume loss for the glacier ($-10.9 \pm 2.1 \times 10^6$ m^3 w.e. yr^{-1}) occurred during the period 1952 - 1977.

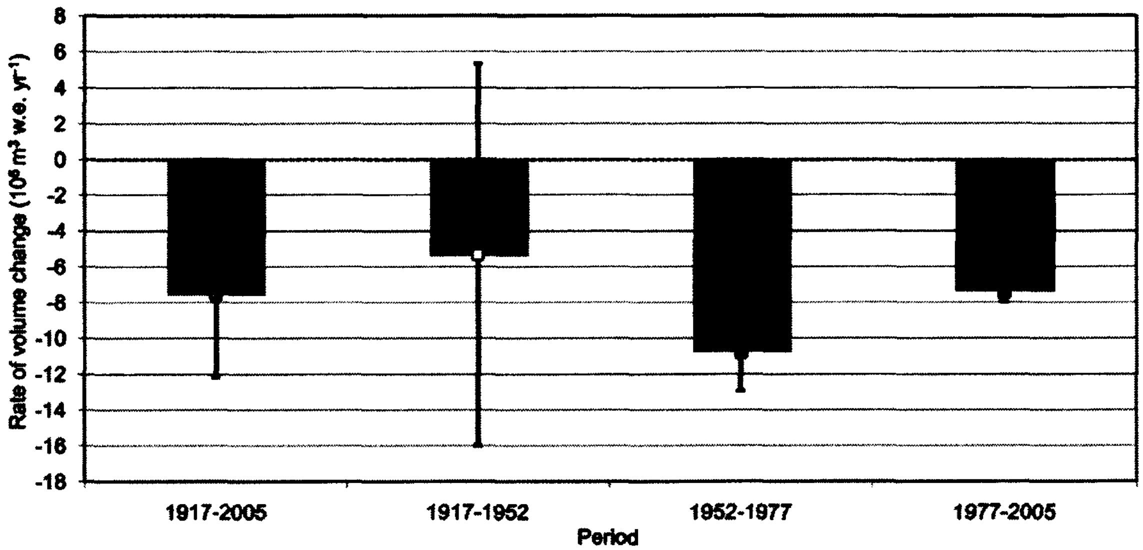

Figure 4.5 Rates of volume change for Peyto Glacier for periods with the most complete data.

The > 70% dataset has similar results; however, the total volume change ($695 \pm 406 \times 10^6$ m^3 w.e.) increased by 4 % when compared to the most complete data set (Figure 4.7). The periods with the highest rates of volume loss include 1952 - 1966 and 1991 - 1993. The period 1950 - 1952 was the only epoch in which the glacier gained volume ($95 \pm 78 \times 10^6$ m^3 w.e. yr^{-1}).

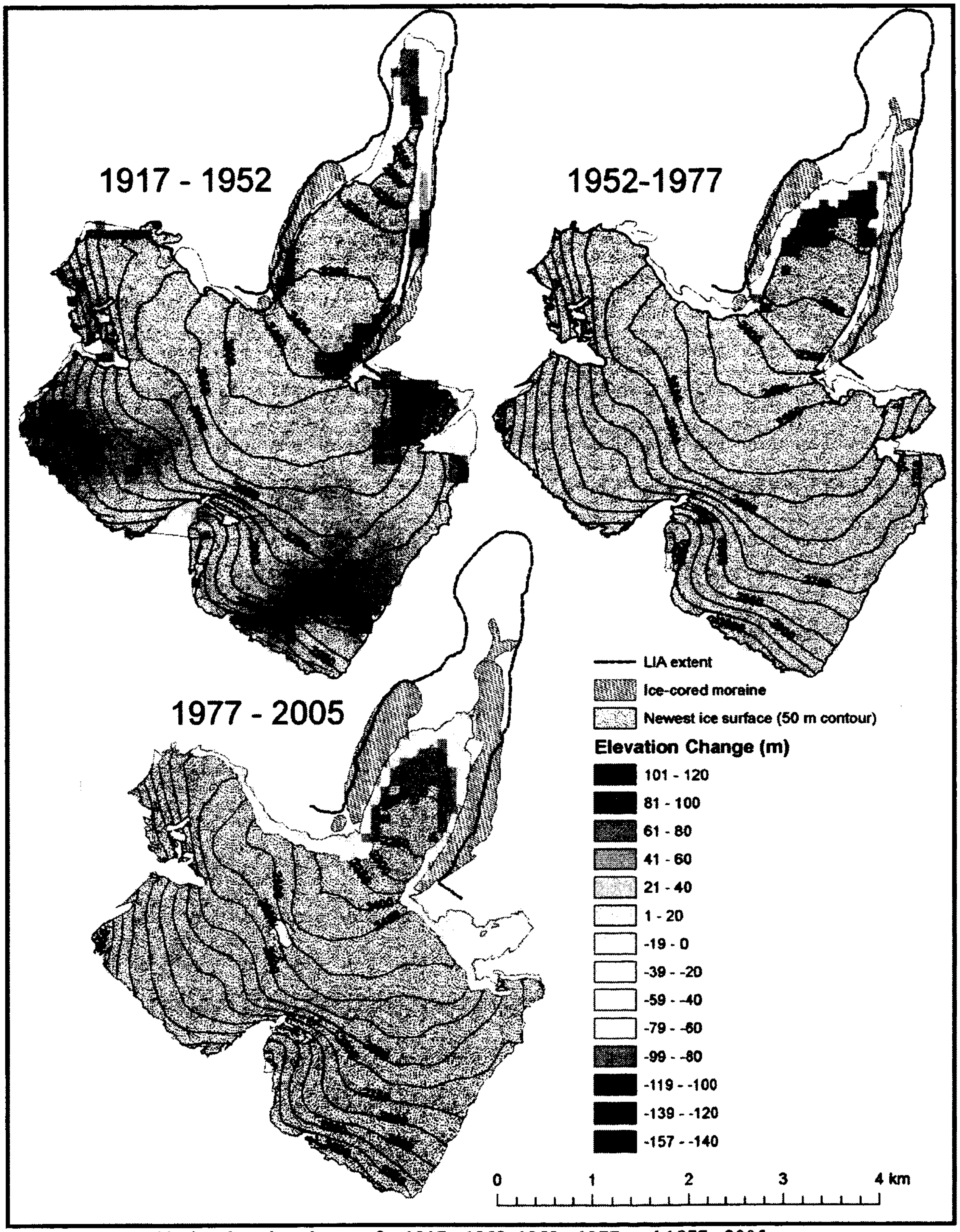

Figure 4.6 Peyto Glacier elevation changes for 1917 - 1952, 1952 - 1977, and 1977 - 2005.

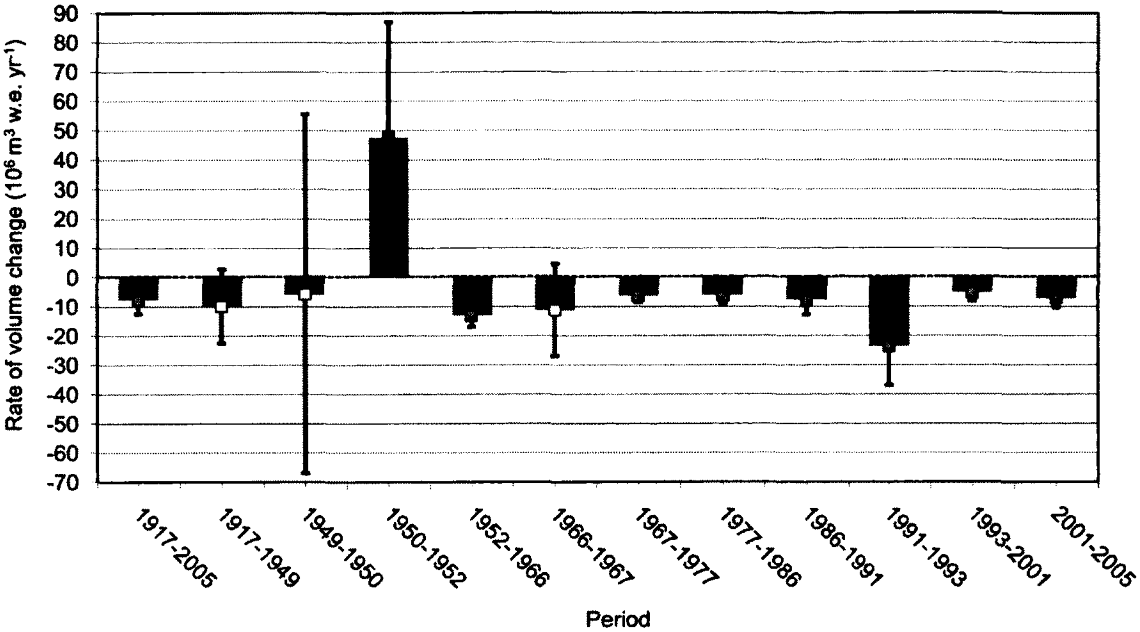

Figure 4.7 Rate of volume change for Peyto Glacier for periods with the second-most complete data.

4.1.2.2 Lateral moraines

Approximately 13% (-85 ± 4 × 10^6 m^3 w.e.) of the total glacier volume change originates from thinning of the ice-cored moraine (Figure 4.8). For the periods 1955 - 1966, 1966 - 1967, and 1973 - 1977 deflation of the ice-cored moraine respectively accounted for 18, 18, and 67 % of the observed ice loss. These elevated contributions could be attributed to the remobilization of freely available sediment on the ice-cored moraine (e.g., Bennett et al., 2000). For unknown reasons the ice-cored moraines experienced volume growth for the periods 1951 - 1952 and 1993 - 1997. Although localized increase in sediment storage could explain this growth, it is more likely explained from differences between the stereo models rather than an increase in ice volume.

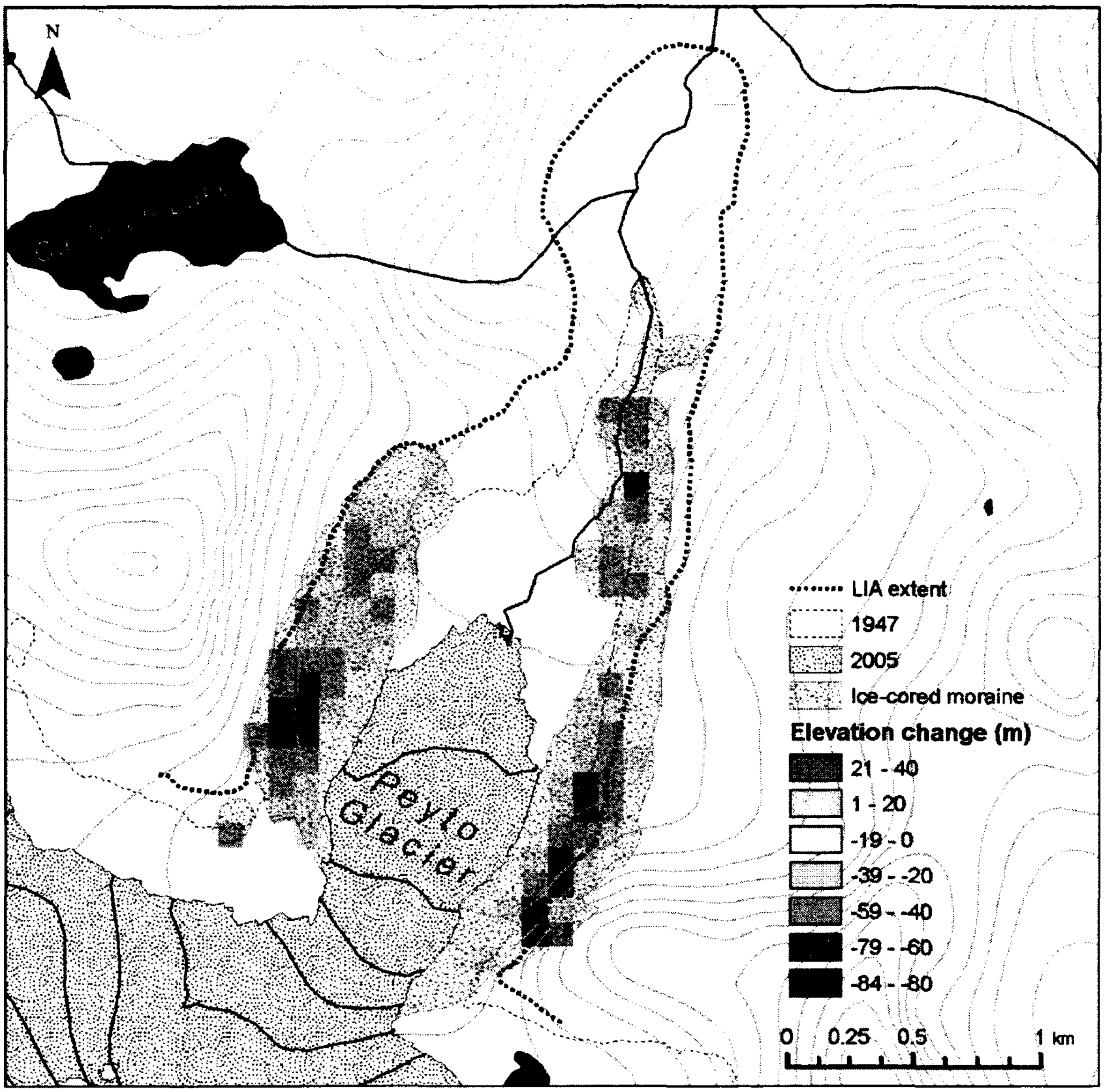

Figure 4.8 Elevation change for the ice-cored moraines adjacent to Peyto Glacier from 1947 to 2005.

4.2 Sediment Analyses

4.2.1 Description of sediments

Of 27 sediment core samples collected, I processed 18 percussion cores and one Ekman-box core. The remaining nine cores were not processed because the laminations were disturbed, unidentifiable, or too thin to measure. In most cores, clear sediment laminations were not visible until the sediments were allowed to partially dry which caused cracks to develop. For the length of the cores (0.2 - 2.9 m), cracks accounted for an average of 4.5 ± 1.8 % of their length. Additionally, sediment cores either had missing laminations near the water-sediment interface, disturbed laminations from barrel distortion, or indistinct laminations from too low of sedimentation.

The annual nature of the laminated silt-clay couplets was independently confirmed by ^{137}Cs radionuclide dating as varves (see section 4.2.3). A 'varve' was originally described by De Geer (1912) as a complete annual cycle consisting of a coarse-grained, pale summer layer below a fine-grained, dark winter layer. Varves in Peyto Lake are relatively thick (> 1 cm) as a result of the sediment laden underflows in the summer months, and low sediment input in the winter months. Visually, the varves typically consist of a thick, light-coloured silt layer and a very thin, dark-coloured clay cap (Figure 3.6). According to Ashley (1975), the varves in Peyto Lake belong to Type III classification where the clay cap is less than half the total varve thickness. In water depths deeper than 30 m, recovered varves are thick with sharp boundaries. Some of the thicker varves (> 2 cm) contain multiple graded beds which are interpreted to arise from intra-annual variation in sedimentation rates (e.g., Figure 4.14; Gilbert, 2003). Closer to the inflow of Peyto Creek, recovered cores contain indistinctly-laminated sands, gravels, and occasionally cobbles. Varves in this region could not be distinguished as a result of the high sedimentation and the dewatering structures present (Zolitschka, 2007).

4.2.2 Bulk-physical properties

4.2.2.1 Horizontal trends

Bulk-physical properties of the Peyto Lake sediments are spatially variable (Figure 4.9). The mean water content within the sediments is 37.5 ± 7.2 %. The lowest water content

(~29%) occurs for sediments in proximity to the delta and water content progressively increases to 52% in the distal and shallower regions. The water content of Peyto Lake sediments is inversely related to dry density ($r^2 = 0.97$, $p < 0.01$, $n = 17$). Water content is inversely related to density (Menounos, 1997; Håkanson and Jansson, 2002). The coarser sediments near the Peyto delta are denser (~1.5 g cm^{-3}) than the silts and clays found in distal settings (< 1.0 g cm^{-3}). The mean dry and wet densities of lake sediments were 1.27 ± 0.24 g cm^{-3} and 2.01 ± 0.18 g cm^{-3}, respectively. The mean organic content was relatively low at 1.9 ± 0.5 %. The spatial distribution of organic content is moderately correlated ($r^2 = 0.45$, $p < 0.01$, $n = 17$) to water content and moderately correlated ($r^2 = 0.35$, $p < 0.01$, $n = 17$) to dry density.

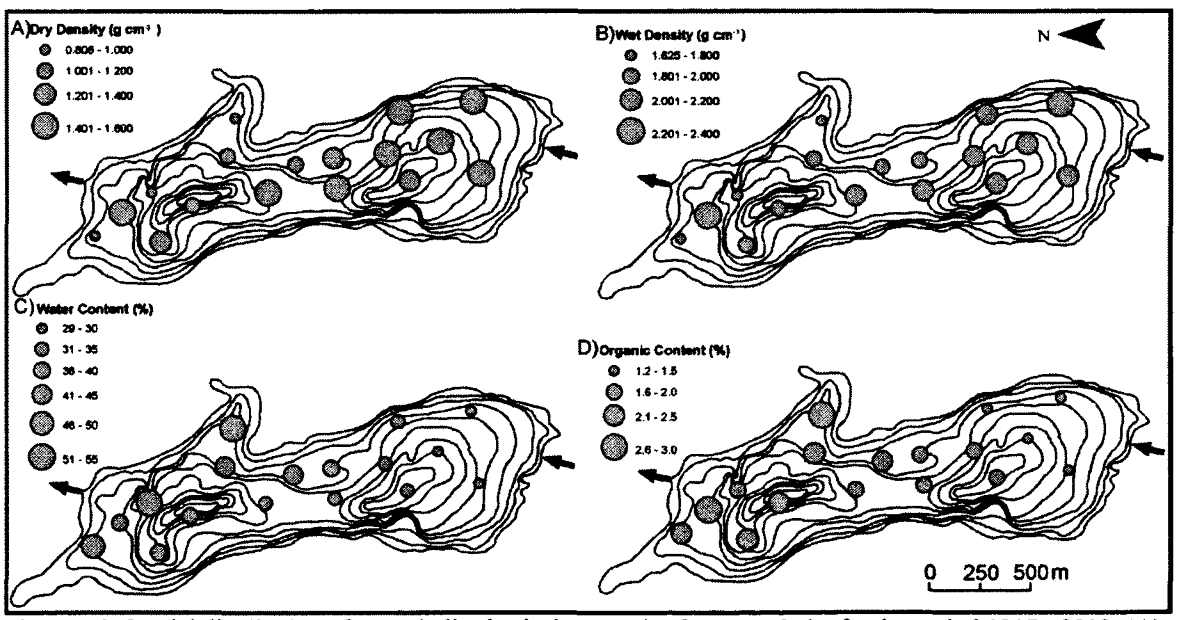

Figure 4.9 Spatial distribution of mean bulk-physical properties for Peyto Lake for the period 1917 - 2010: (A) dry density, (B) wet density, (C) water content, and (D) organic content. Mean values were calculated from the interpolated values between sub-sampled locations down the core for every varve. The small arrows indicate the primary inflow and outflow of Peyto Creek.

4.2.2.2 Vertical trends

Variation of physical properties also changes with depth (Figure 4.10). Water content in the proximal portion of Peyto Lake, for instance, tends to decrease with depth. Core 11-Peyto (N), sampled from the proximal basin, has the highest water content (36.3 %) near the water-sediment interface and progressively decreases at a rate of 2.9 % m^{-1}. Such variation can arise from variable sedimentation rates, quality and character of the deposits, degree of compaction, and bioturbation (Håkanson and Jansson, 2002). For the same core, dry density is the lowest near the water-sediment interface at 1.22 g cm^{-3} and increases to 1.39 g cm^{-3} at 152.5 cm of depth. The general trend of organic content remains relatively low and constant at 1.56 ± 0.27 %.

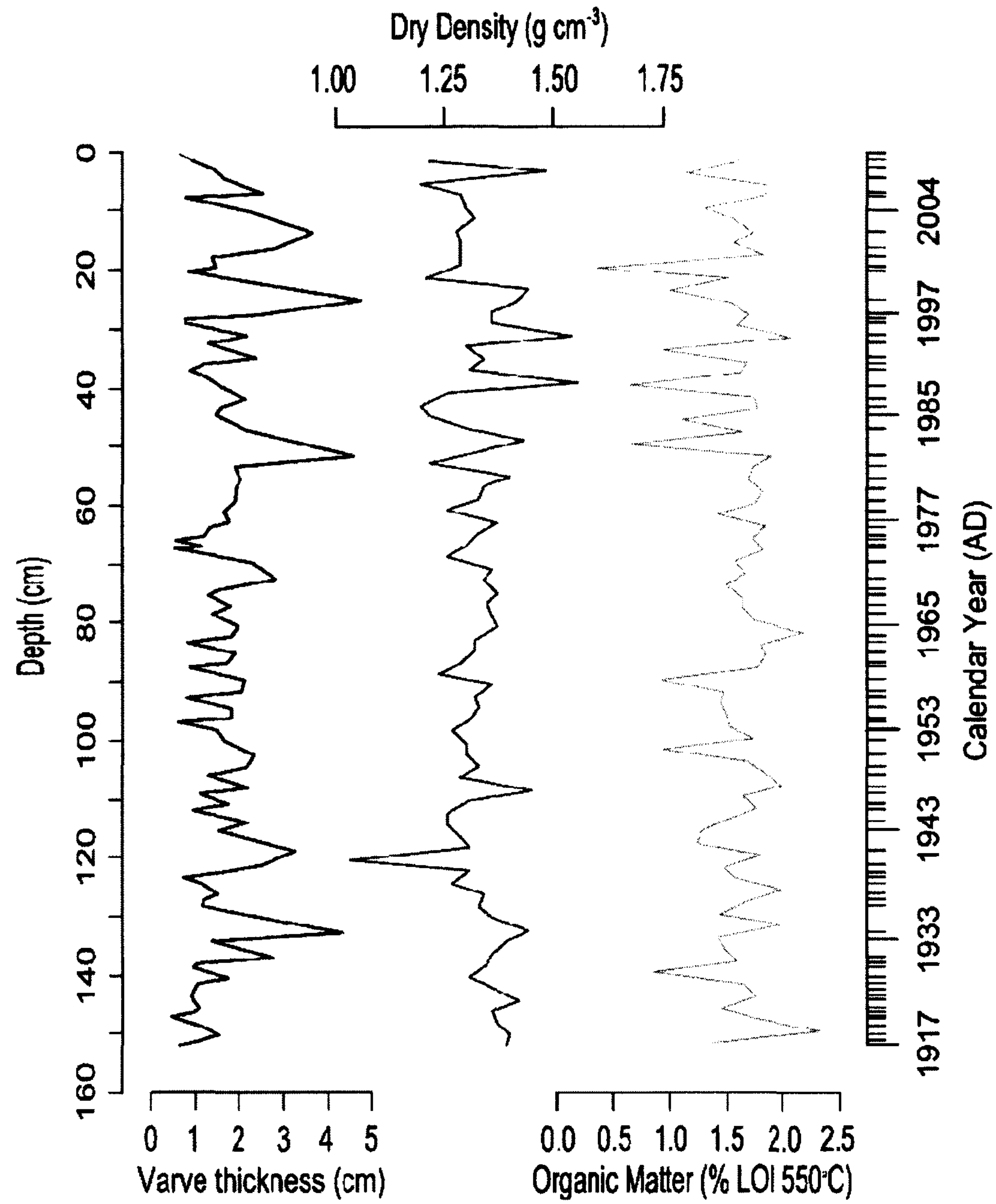

Figure 4.10 Bulk-physical properties for core 11-Peyto(N). Dry density (dark grey line) and organic matter (light grey line) were sub-sampled at 2 cm intervals. Varve thickness was interpolated (red line) near the top and measured (black line) downwards.

4.2.3 Cesium - 137 (^{137}Cs)

The maximum ^{137}Cs activity level occurs at 45.5 cm of depth in core 10-Peyto(02) and independently confirms the varved nature of the sediment record (Figure 4.11).

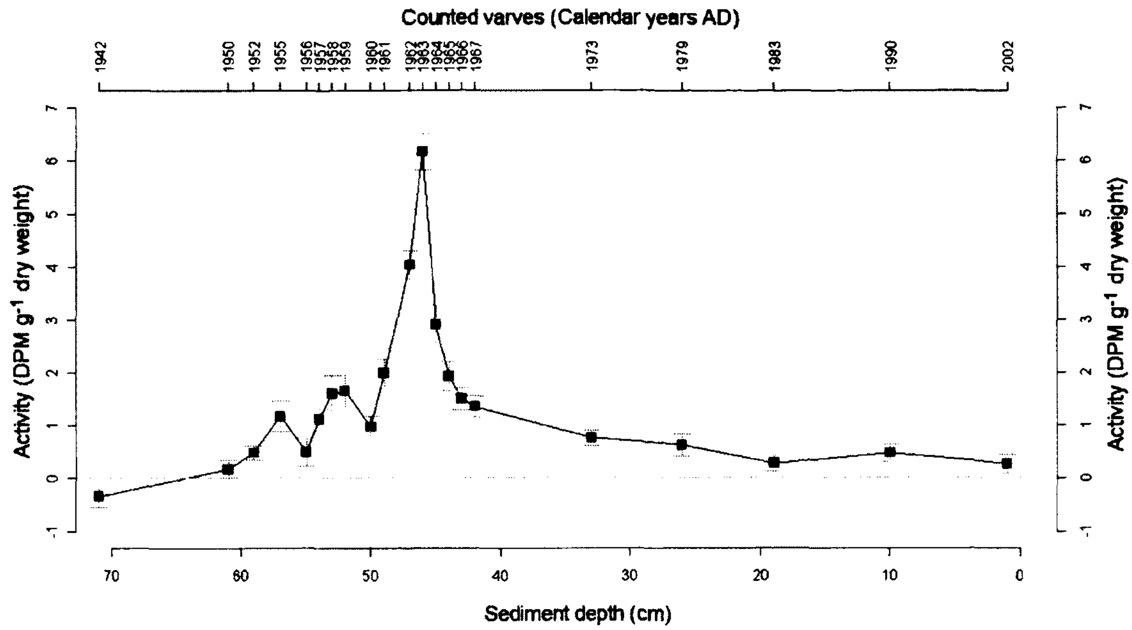

Figure 4.11 Activity levels of Cesium-137 (^{137}Cs) in lake sediments retrieved from core 10-Peyto(02). Vertical error bars indicate counting errors ($\pm$ 1 σ) in ^{137}Cs activity determination. Sediment samples were taken from the centre of identified varves and converted to calendar years (AD).

4.2.4 Varve thickness

Varve thickness generally decreases with distance from the inflow of Peyto Creek, a common pattern found in proglacial lakes (Figure 4.12; Smith and Ashley, 1985; Menounos et al., 2005). The median varve thickness decreases from 2.12 cm (core = I, n=50) near the delta to 0.12 cm in the lake's most distal setting. A multiple linear regression model revealed that 66 % of the variation in mean varve thickness for the period 1917 - 2010 can be explained by distance from the point of inflow and lake depth. For individual years, however, the relation is far more complex and could not be explained by the two variables alone. Other environmental variables such as climate (Zolitschka, 2007), extreme discharge (Sander et al. 2002), change in sediment storage, and/or the complex dynamics of Peyto Lake (Chikita et al., 1996) might reflect the inconsistent patterns of varve thickness from year to year.

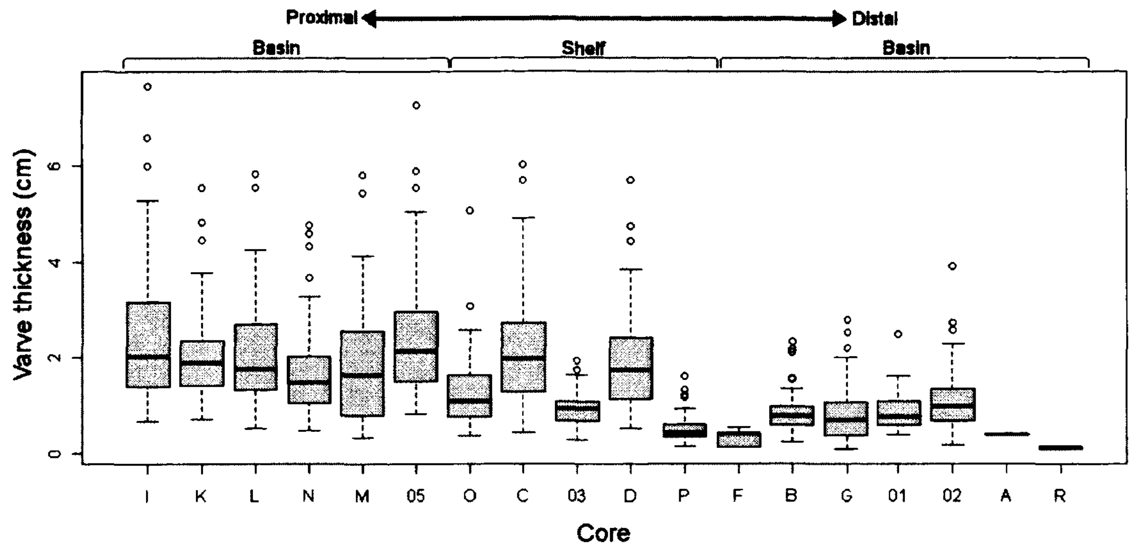

Figure 4.12 Varve thicknesses measured from all collected cores. Proximal cores (left) were collected up to 316 m from the delta and distal cores (right) were collected up to 2215 m from the delta. Note: measurements from cores F, A, and R, were done between marker beds, so varve thicknesses denote average rates.

For the period 1917 - 2010 the median varve thickness for all cores was 1.20 cm (Figure 4.13). The extended varve record measured from two cores (02 and O) revealed that varves deposited during the period 1917 - 2003 are 207 % thicker and more variable (1.14 ± 0.37 cm) and than varves deposited during the previous period 1830 - 1916 (0.55 ± 0.11 cm).

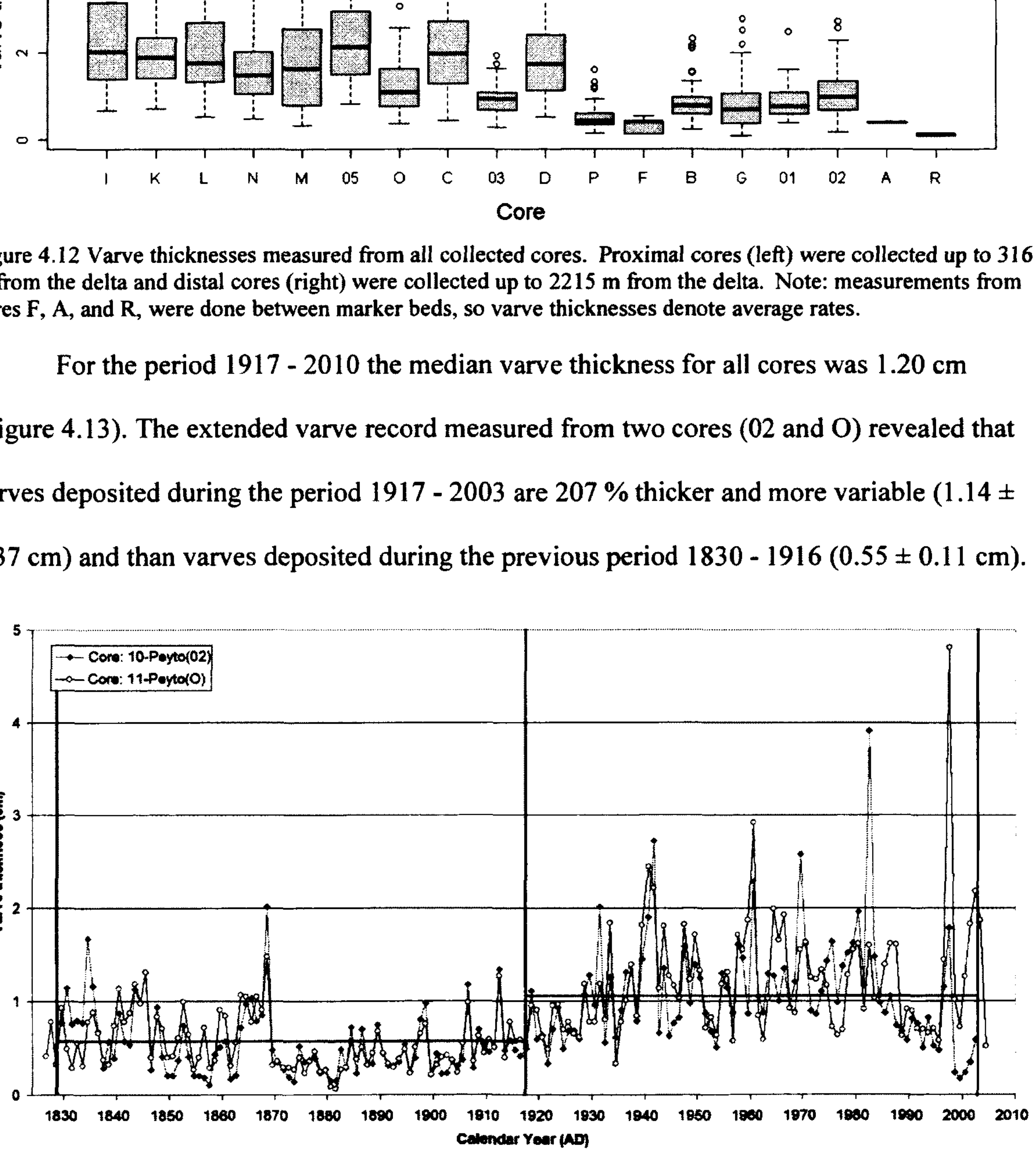

Figure 4.13 Extended varve record from two cores. Vertical black lines delineate periods 1828 - 1916 and 1917 - 2003. Horizontal red lines show the average varve thickness for those periods.

Median varve thickness exeeded 2.0 cm in six years (1941, 1942, 1961, 1970, 1983, and 1998). The thick varve of 1983 likely arose from sediments delivered during an extreme precipitation event which elevated streamflow and caused mass wasting (Johnson and Power, 1985). The thick varves of 1970 and 1998 coincide with years of strong negative mass balance of Peyto Glacier. The nature of the thick varves shown for 1941, 1942, and 1961 cannot be associated with other records; however, the microstratigraphy suggests they formed during conditions similar to that of the 1998 varve (see Figure 4.14).

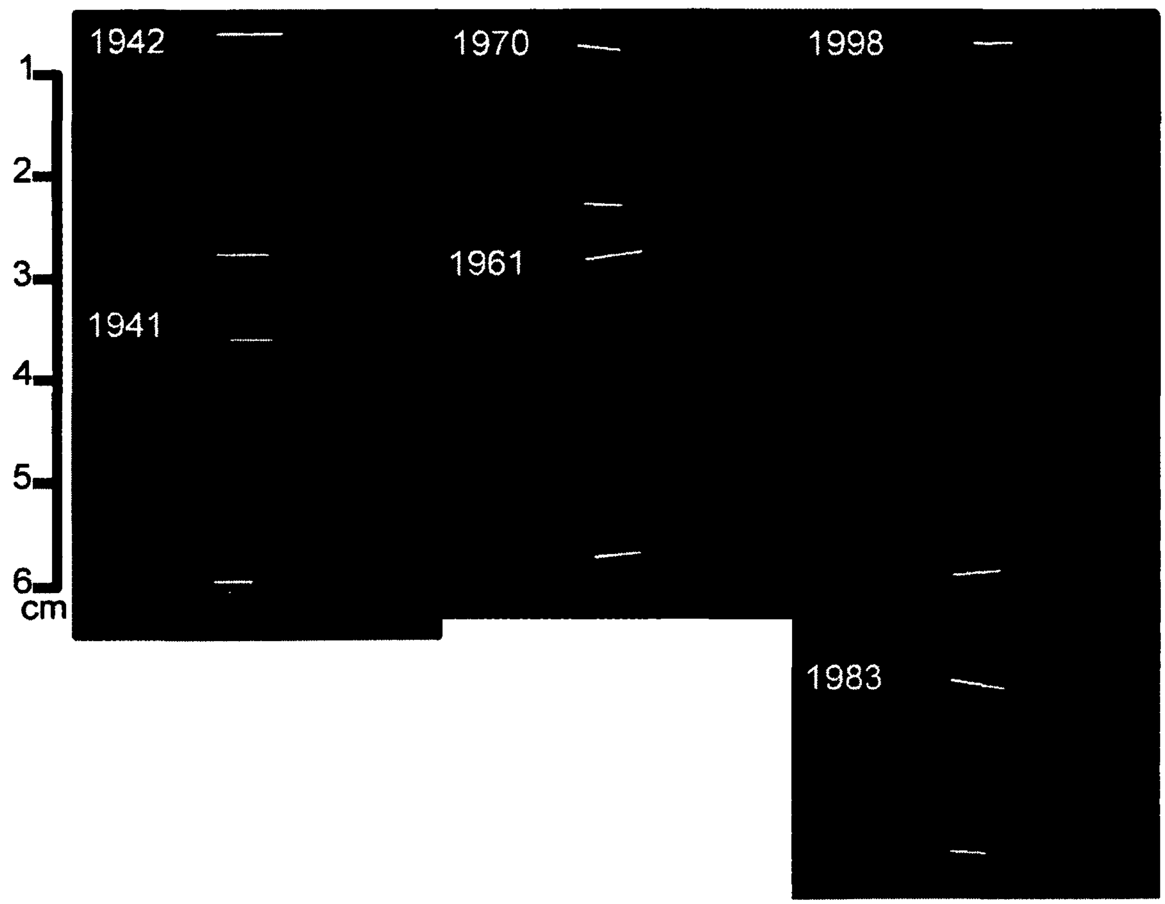

Figure 4.14 Photographs of abnormally thick varves from core 11-Peyto(O).

The inter-annual variation of varve thickness shows a distinct temporal trend (Figure 4.15). The extended varve record shows there was a distinct shift in sedimentation in 1870 (Figure 4.13). From 1870, varves slowly and progressively became thicker to a maximum thickness in 1942. Between 1943 and 1954, varves thinned but thickened again during the period 1954 - 1957. After 1958, varves slowly and progressively became thinner for the following 42 years. Over the period 2000 - 2010, varves thickened from 2000 until 2004 and thinned thereafter.

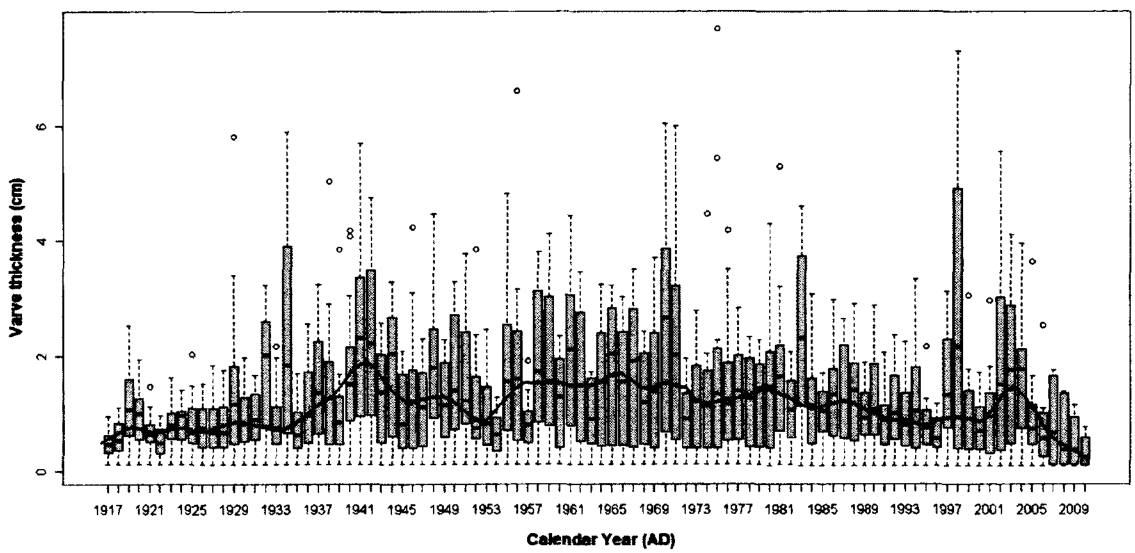

Figure 4.15 Boxplots of measured varve thicknesses for the study period (1917 - 2010). Red line denotes an 8 year running mean. The period 2000-2010 contains less than 14 contributing cores.

4.2.5 Sediment yield calculations

I used two interpolation methods to estimate the areal extent of varve thickness. The spatial distribution of sediment thickness for both interpolation methods substantially differ, but estimates of regularized spline interpolation are more realistic than those using the Thiessen polygon method (Figure 4.16). Not surprisingly, standardized varve thickness (Figure 4.17) is correlated with SSY estimated with Thiessen polygons ($r = 0.94$, $p < 0.001$) and regularized splines ($r = 0.93$, $p < 0.001$; Appendix B).

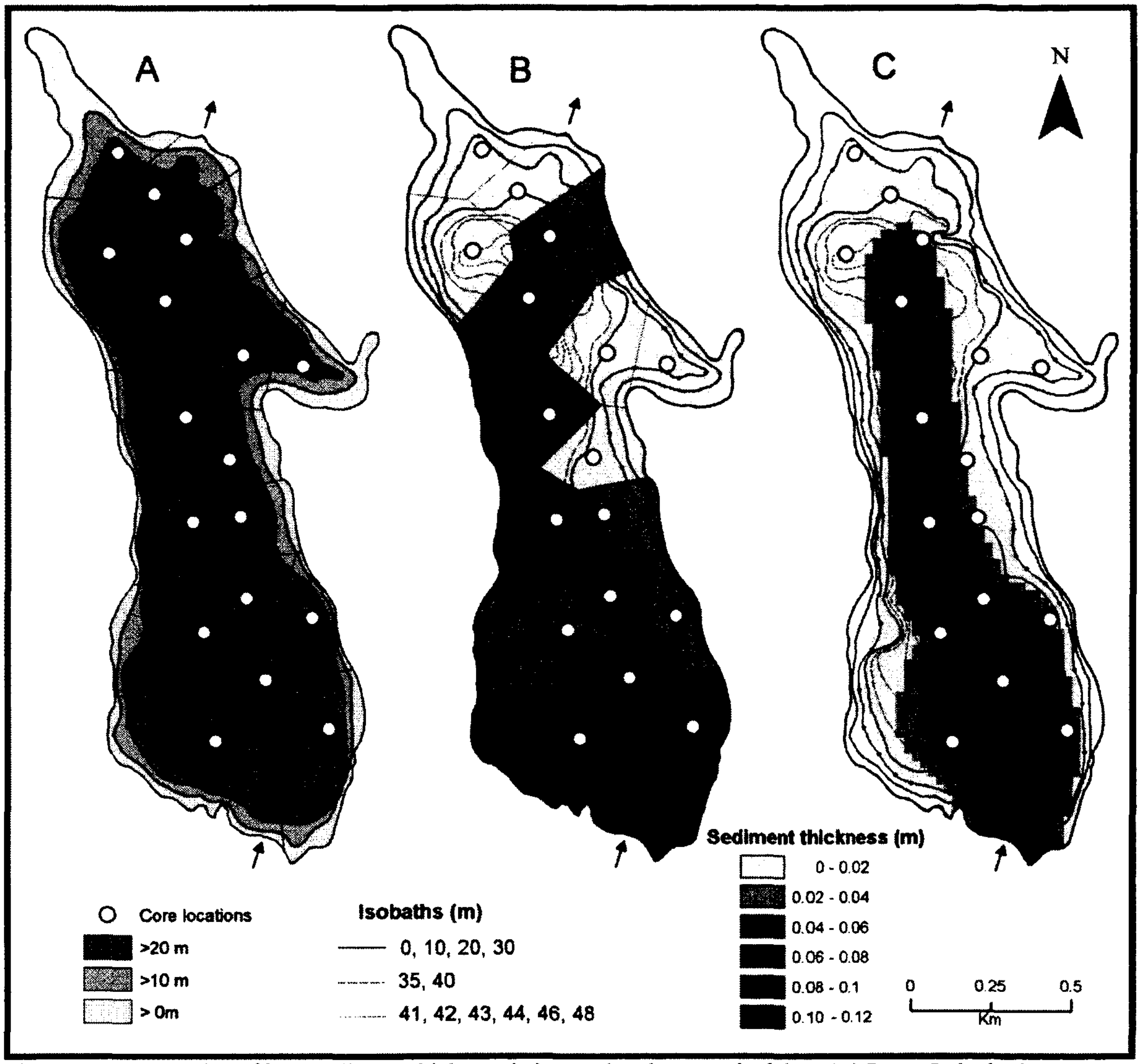

Figure 4.16 Examples of how sediment thickness is interpolated across the lake. (A) Peyto Lake bathymetry highlighting various depths where the rate of sedimentation is assumed to be 0 m yr^{-1}. (B) Sediment thickness in 1970 was uniformly distributed within each Thiessen polygon that surrounds a sediment core. (C) Sediment thickness in 1970 using regularized spline interpolation (25 m × 25 m pixels). Sediment values incorporate areal variation in sediment density and organic content.

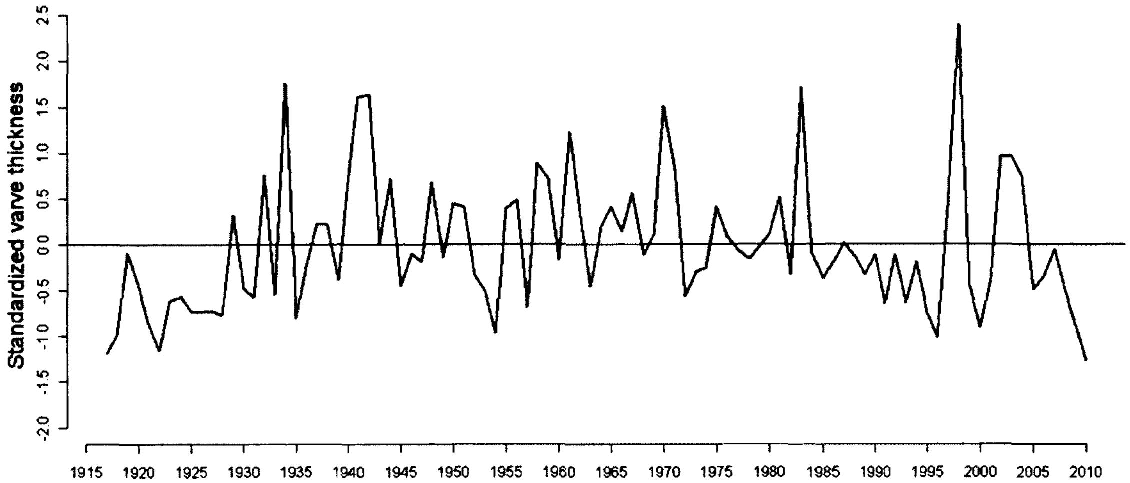

Figure 4.17 Master chronology of varve thickness variation. The y-axis is reported as standardized departures from a mean of zero.

The sensitivity analysis reveals the magnitudes of the observed trends differed among the approaches, but the general trends remained the same (Figure 4.18). Comparably, SSY_{spline}, $SSY_{Thiessen\text{-}20}$, $SSY_{Thiessen\text{-}10}$ were respectively calculated as 30 %, 20 %, and 10 % lower than the $SSY_{Thiessen\text{-}0}$ interpolation (Appendix B). Provided all of these approaches yield similar trends in sediment yield, I elected to simplify the following discussion by only considering data from the SSY_{spline} interpolation (Figure 4.19). For the period 1917 - 2010, SSY_{spline} averaged 446 ± 176 (1σ) Mg km^{-2} yr^{-1}.

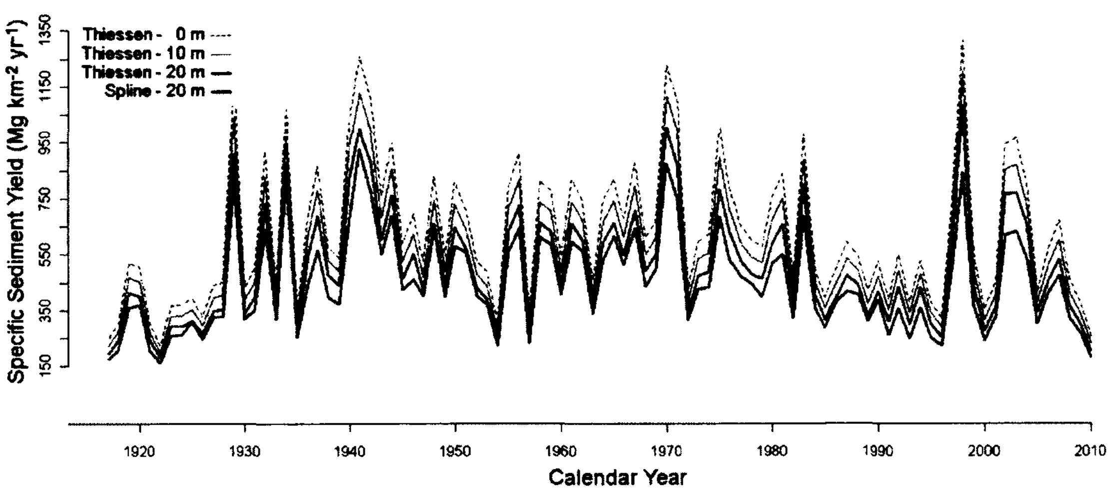

Figure 4.18 Calculated specific sediment yield for the Peyto Lake watershed when sampled sediment thickness was interpolated using Thiessen polygons and spline interpolations. Sedimentation rates were assumed to equal 0 m yr^{-1} when depths were shallower than 0 m, 10 m, and 20 m.

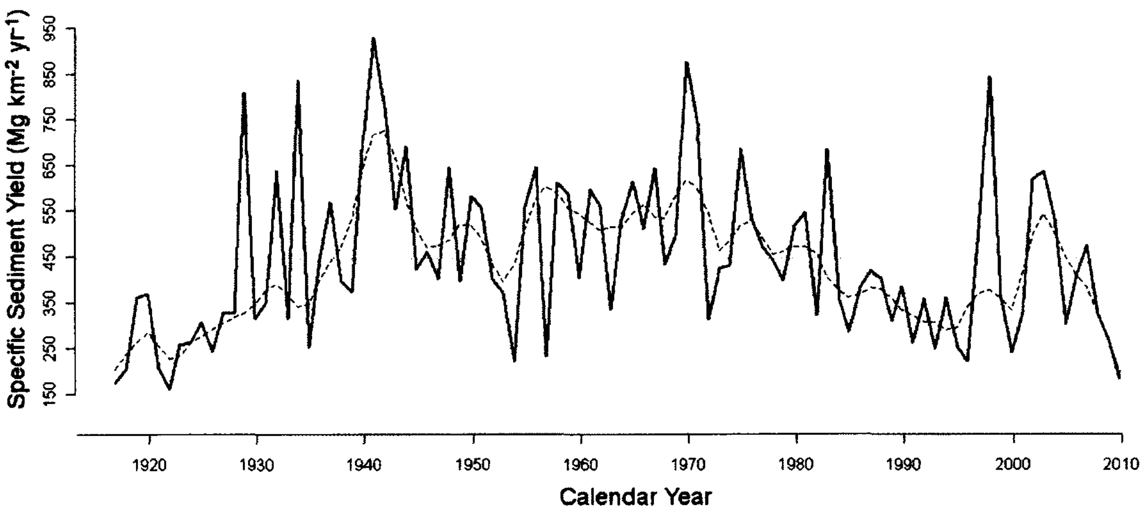

Figure 4.19 Specific sediment yield calculated by using a regularized spline interpolation where sedimentation was assumed to be near 0 m yr^{-1} at 0 - 20 m of depth. The grey horizontal line denotes the mean and the black dashed line denotes an 8 year running mean.

4.3 Environmental controls on sediment yield

There are many interacting and complex environmental processes that can influence the sedimentation in a lake (Hodder et al., 2007). Prior to exploring the cause (i.e., environment) and effect (i.e., sediment yield) relation, the interactions among environmental variables are presented.

Glacier mass balance is closely linked to meteorological conditions that occur at the glacier surface (Rasmussen and Conway, 2004). Generally, the mass balance record for Peyto Glacier was most closely linked to the average temperatures for Jasper. The average maximum summer temperature (June, July, August) from Jasper was significantly correlated with summer mass balance ($r = -0.68$, $p < 0.001$, $n = 27$). Similarly, the average minimum temperatures (May, June, July) were significantly correlated to net mass balance ($r = -0.73$, $p < 0.001$, $n = 43$) and winter mass balance ($r = -0.78$, $p < 0.001$, $n = 27$), respectively.

The hydrometric record of Peyto Creek is relatively short (8 years in length) and obtaining a strong relation to long SSY record (94 years in length) was not ideal. Instead, I used the longer hydrometric records from the nearby stations on the Mistaya and the Sunwapta rivers to reflect regionally representative hydrologic conditions in the area. For the month of August, Peyto Creek discharge is highly correlated to Mistaya River discharge ($r = 0.89$, $p = 0.003$, $n = 8$) and the Sunwapta River discharge ($r = 0.90$, $p = 0.002$, $n = 8$). Mean August discharge for Peyto Creek is also correlated to the mean maximum temperature for August ($r = 0.85$, $p < 0.007$, $n = 8$). Mistaya and Sunwapta rivers are highly correlated for mean August discharge ($r = 0.78$, $p <0.01$, $n = 51$), but this correlation decreases for mean maximum daily discharge ($r = 0.40$, $p <0.01$, $n = 52$). Net, summer, and winter mass balance records are uncorrelated with discharge from all three hydrometric stations.

SSY is not correlated to glacier mass balance or discharge, but is weakly correlated with climate. The mean August maximum temperature for Jasper had a weak correlation with

SSY ($r = 0.37$, $p = 0.001$, $n = 75$) and standardized varve measurements ($r = -0.43$, $p < 0.001$, $n = 75$).

The varve records from several individual cores are correlated with hydro-climatic variables. The varve record from Core N, for example, was weakly correlated to winter mass balance ($r = -0.30$, $p = 0.05$, $n = 28$) and net mass balance ($r = -0.47$, $p = 0.001$, $n = 42$). The standardized variation of varve thickness was also weakly correlated with net mass balance ($r = -0.36$, $p = 0.02$, $n = 44$), ELA ($r = 0.38$, $p = 0.01$, $n = 44$), and AAR ($r = -0.42$, $p = 0.001$, $n = 43$).

Changes in glacier dimensions were calculated for periods when aerial photographs were available. For these periods, SSY has no relation to changes in length, area, volume, and net mass balance of the glacier.

The correlations among glacier mass balances, discharge and climatic variables limited the possible number of variables used in a multiple linear regression. Individually, net mass balance or discharge had no relation to SSY; together the two variables had a weak relation with SSY. SSY had a moderate correlation ($r = 0.45$, $p = 0.009$, $n = 44$) with net mass balance and mean discharge for July and August (Q_{JA}) from the Mistaya River. Similarly, net mass balance and mean Q_{JA} had the strongest correlation ($r = 0.52$, $p = 0.002$, $n = 44$) with the standardized varve record. The relation improved slightly ($r = 0.53$, $p = 0.001$, $n = 44$) when the net mass balance (b_n) was converted to total volume change w.e. (i.e., $b_n \times$ glacier area). There were slightly lower significant correlations when discharge was averaged over different months (Table 4.2). Sediment cores C and 03 were the only cores that had significantly weak correlations with discharge and net mass balance. I also examined the potential for temporal lags among the systems, but no improved relations were found.

Table 4.3 Pearson correlation coefficient (r) for Mistaya River discharge versus net mass balance and standardized varve thickness or SSY_{spline}. $p < 0.05$.

Months of mean discharge*	Standardized Varves (r)	SSY_{spline} (r)
JJA	0.510	0.431
JA	0.520	0.455
A	0.514	0.451
JAS	0.506	0.439
MJJASO	0.512	0.450

*M = May, J = June, J = July, A = August, S = September, O = October

5. Discussion

5.1 Changes to glacier length, area, and volume

5.1.1 Length

Over the period 1917 - 2005 Peyto Glacier receded -2198 ± 18 m which corresponds to a recession rate of -24.98 ± 0.20 m yr^{-1}. Previously, changes to the length of Peyto Glacier were also reported and calculated from photographs (Thorington, 1934; Kingman, 1938), botanical dating of the moraines (Field and Heusser, 1954), annual field surveys (Ommanney, 1972) or employing a combination of these methods (Meek, 1948; Brunger et al., 1967; Henoch, 1971). Ommanney (1972) reported that between 1917 and 1962, Peyto Glacier receded -1141 m which is similar to my estimate (1125 ± 18 m) for the same period.

In comparison to regional glaciers, termini on the Columbia Icefield receded at a slower rate of -12.8 ± 0.4 m yr^{-1} for nearly the same period (1919 - 2009; Tennant and Menounos, 2013). Similarly, Castle Creek Glacier in the Cariboo Mountains receded at the lower rate of -14.3 m yr^{-1} between 1959 and 2009 (Beedle et al., 2009). For the periods 1917 - 1949 and 1919 - 1948, Peyto and Athabasca glaciers receded at similar rates of -20.5 ± 0.6 m yr^{-1} and -20 m yr^{-1} (Kite and Reid, 1977), respectively. Also, Denton (1975) reported Saskatchewan Glacier to have receded -25 m yr^{-1} (1953 - 1963), whereas Peyto retreated -42.3 ± 0.1 m yr^{-1} from 1955 to 1966. Ommanney (1972) recorded the highest rate of retreat (-74.7 m yr^{-1}) from 1956 - 1960 when the glacier receded into a deep, narrow gorge. Due to topographic conditions near the snout, government surveys of terminus change were suspended after 1962 (Ommanney, 1972).

5.1.2 Area

From 1917 to 2005 Peyto Glacier lost -4.0 ± 0.9 km^2 which corresponds to a shrinkage rate of -0.045 ± 0.010 $km^2\ yr^{-1}$. Previous studies calculated shrinkage rates of -0.036 $km^2\ yr^{-1}$ from 1896 to 1917, -0.066 $km^2\ yr^{-1}$ from 1917 to 1966 (Wallace, 1995), and -0.047 $km^2\ yr^{-1}$ from 1966 to 1989 (Glenday, 1991). From 1917 to 1966, my estimate of shrinkage rate (-0.022 ± 0.018 $km^2\ yr^{-1}$) is 67 % smaller than the estimate of Wallace (1995). Such a large discrepancy may be explained by Wallace's use of the original 1917 glacier boundary map where he did not correct for the substantial topographical error. My results, however, are comparable with Glenday (1991) for the period 1966 - 1989.

When compared to other glaciers in the Canadian Rocky Mountains, Peyto Glacier shrank at a moderate rate. DeBeer and Sharp (2007) report that glaciers lost -15% of their area during the period 1951 - 2001, which was slightly less than what I calculated for Peyto (-17.8 ± 0.3 %) for the same period. The Columbia Icefields lost -33.5 ± 6.1% of its area during the period 1919 - 2009 (Tennant et al., 2012) which is slightly more than what I calculated for Peyto Glacier for the period 1917 - 2005 (-26.4 ± 5.8 %).

5.1.3 Volume

My results generally agree with previous calculations of volumetric changes for Peyto Glacier. They indicate that Peyto Glacier, excluding the ice-cored moraines, lost -515 ± 404 × $10^6\ m^3$ w.e. from 1917 to 1991 with an annual volume change of -5.9 ± 4.6 × $10^6\ m^3$ w.e yr^{-1}. The combined results from Wallace (1995) for 1917 - 1966 and Glenday (1991) for 1966 - 1989 equate to a total loss of -854.9 × $10^6\ m^3$. If I convert their volume change to snow water equivalent using a mean ice density of 760 kg m^{-3}, their volume change equates to -649.8 × $10^6\ m^3$ w.e. which is an average rate of -9.0 × $10^6\ m^3$ w.e yr^{-1}. The large discrepancy between our results is probably from different 1917 extents (15.2 km^2 vs. 16.0 km^2) being used. If I account for different 1917 extents being used by dividing volume by average area, my results show Peyto Glacier thinned an average of -0.51 ± 0.40 m w.e. yr^{-1} (1917 - 1991) which is within error of Wallace and Glenday's calculations (-0.64 m w.e. yr^{-1}: 1917 - 1989). From the mass balance record (1966 - 2007), Peyto Glacier thinned an average rate of -0.63 m w.e. yr^{-1} (Demuth and Keller, 2006), which is comparable to my calculations (-0.55 ± 0.04 m w.e. yr^{-1}: 1966 - 2005). My results indicate that Peyto Glacier thinned -44 ± 31 m w.e. on average from 1917 to 2005 (-0.50 ± 0.35 m w.e. yr^{-1}). Glaciers of the Columbia Icefield (Tennant and Menounos, 2013) for the period 1919 - 2009 thinned by a comparable magnitude (-49 ± 25 m w.e.) and at a similar rate (-0.6 ± 0.3 m w.e. yr^{-1}). For the southern Rocky Mountains (approximate ice cover is 849 km^2) from 1985 to 1999, Schiefer et al. (2007) calculated an average thinning rate of -0.64 ± 0.15 m w.e. yr^{-1}.

In this study, rates of volume change calculated for the periods 1917 - 1949, 1949 - 1950, 1950 - 1952, and 1966 – 1967 have large uncertainties. The error term for the period 1917 - 1949 is relatively large because of the uncertainty of the 1917 IBCS map. I expect periods less than three years to have large errors, but the reason for the extremely large error for 1949 - 1950 is associated with the quality of the stereo models. For the period 1950 - 1952, Peyto Glacier could have gained volume as suggested by an increase in area and the minimal retreat from 1950 to 1951. The primary concern for the period 1950 - 1952 is the abnormally large rate of volume change which is far larger than any other period. Although the error term for the period 1966 - 1967 is large, it is within error of the mass balance record of 1967 (i.e., +10 ± 200 mm w.e.).

Many studies identify the ice-cored moraines adjacent to Peyto Glacier (e.g., Østrem and Arnold, 1970; Ommanney, 1972; Nakawo and Young, 1982; Binda, 1984; Johnson and Power, 1985; Glenday, 1991), but few studies quantify its contribution to meltwater in the basin. Using sequential LiDAR surveys over a 23 month period, Hopkinson and Demuth (2006) calculated that the ice-cored moraines contributed to 6% of the total glacier runoff which is about half of my estimate (11 ± 1 %) for the period 1977 - 2005. Like Hopkinson and Demuth (2006), I found no evidence that the downwasting is due to mass movement events with the exception of the mass wasting events of 1983 (Johnson and Power, 1985).

5.2 Sediment yield

Due to complex dynamics of sediment transport in Peyto Lake, I was unable to interpolate sedimentation using a spatial statistical model (e.g. Schiefer, 2004). Instead, I performed two methods of interpolation and assessed the reliability of these methods using a first-order sensitivity analysis. My results indicate that interpolation methods affect the quantity of estimated sediment accumulation in the lake for a given year, but that inter-annual trends in sediment yield remained insensitive to the type of interpolation methods used.

Additional sediment cores would have been useful to determine: (1) the depth at which annual sedimentation rate was close to zero; and (2) the rate and extent of delta progradation (e.g., Appendix C). In this study, I assumed that negligible sedimentation occurred in water depths shallower than 20 m. The rate and extent of delta progradation was also not determined because few samples were taken in proximity to the Peyto Lake delta, and correlation among these cores was difficult. Sedimentation rates near the delta are highly variable where previous research shows a fivefold reduction in sedimentation within a

100 m distance (Vendl, 1978). In addition, aerial photography used in this study indicates Peyto Creek laterally migrated over the delta's surface which complicates areal sedimentation patterns in the proximal basin.

SSC have been studied in the watershed (e.g., Vendl, 1978; Smith et al., 1982; Binda, 1984; Chikita, 1992, 1993; Chikita et al., 1996); only Vendl (1978) reported annual values. For the summer of 1976, Vendl (1978) calculated the total suspended sediment flowing into Peyto Lake as 38000 Mg (approximately 778 Mg km^{-2} yr^{-1}). For the same year, I calculated sediment yield to be on the same order of magnitude: 529 - 789 Mg km^{-2} yr^{-1} depending on the method of interpolation. My calculations are probably underestimated because they do not consider the coarser particles (e.g., gravel) deposited in the delta region. The rough agreement between our values suggests that my SSY calculations are representative of the Peyto Lake watershed.

For the period 1917 - 2010, SSY averaged 446 ± 176 Mg km^{-2} yr^{-1} which is among the highest SSY values in the Canadian Cordillera when plotted by glacier cover (Figure 5.1). Hodder et al. (2006) calculated average SSY for a number of glacierized watersheds in the Canadian Cordillera and suggested that glacier cover is a good predictor for SSY for a given tectonic belt and climate region. My results, however, show that SSY for Peyto watershed does not fit this relation. SSY for the Peyto Lake basin is among the highest fluvial based estimates of SSY for British Columbia when plotted by drainage area (Figure 5.2). Church and Slaymaker (1989) only report four undisturbed watersheds that were above the inferred pattern for British Columbian rivers; all of these outliers are from glacierized watershed. Although SSY for the Peyto watershed is among the highest documented values in western Canada, it is not particularly high for glaciated watersheds elsewhere (Figure 5.3). Hallet et al. (1996) showed glaciated basins have a higher and distinct SSY when compared to non-glaciated basins around the world. They found yields typically increased with basin size, from cirque glaciers to fast-moving glaciers in Alaska, presumably due to higher effective erosion rates of the latter. In short, SSY for the Peyto watershed are among the highest in western Canada, yet relatively low among other glaciated watersheds around the world.

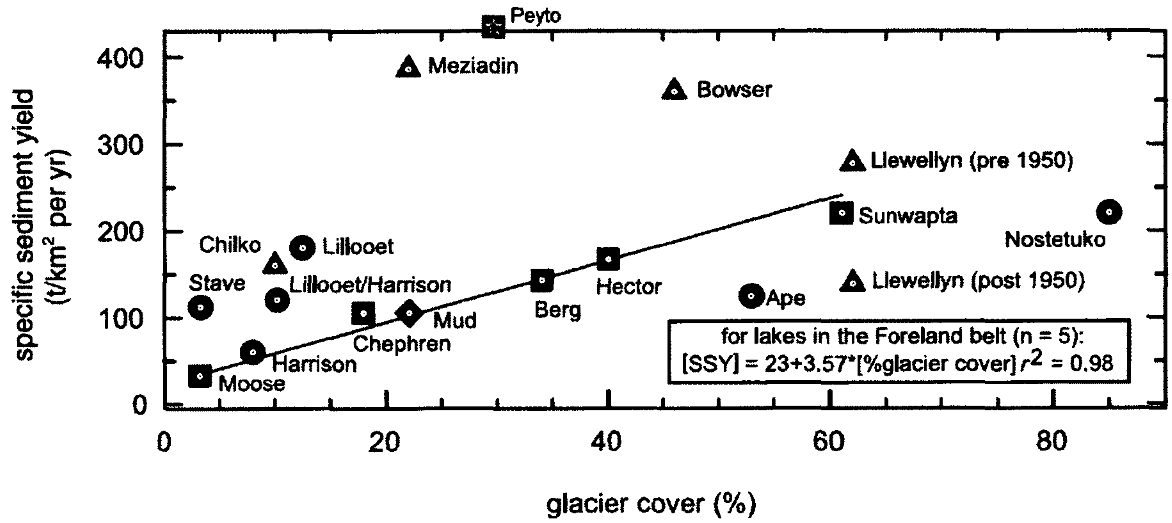

Figure 5.1 Specific sediment yield as a function of percent glacier cover for lakes in British Columbia and Alberta (Graph modified from Hodder et al. (2006)). The various symbols represent different tectonic belts.

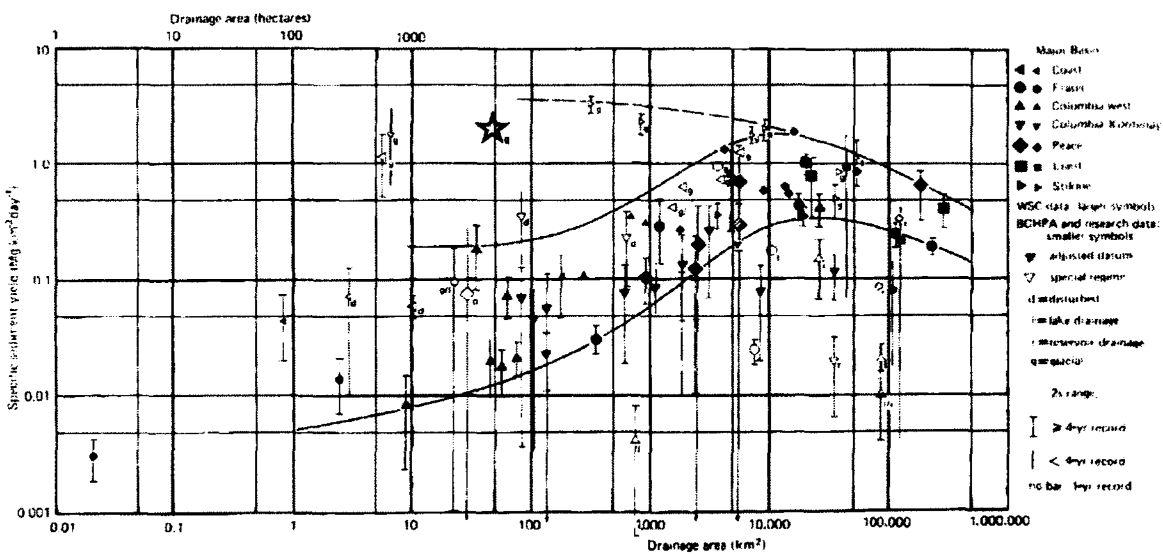

Figure 5.2 Specific sediment yield as a function of drainage area (Graph modified from Church and Slaymaker (1989)). Specific sediment yield for Peyto Lake (star) is shown on the graph.

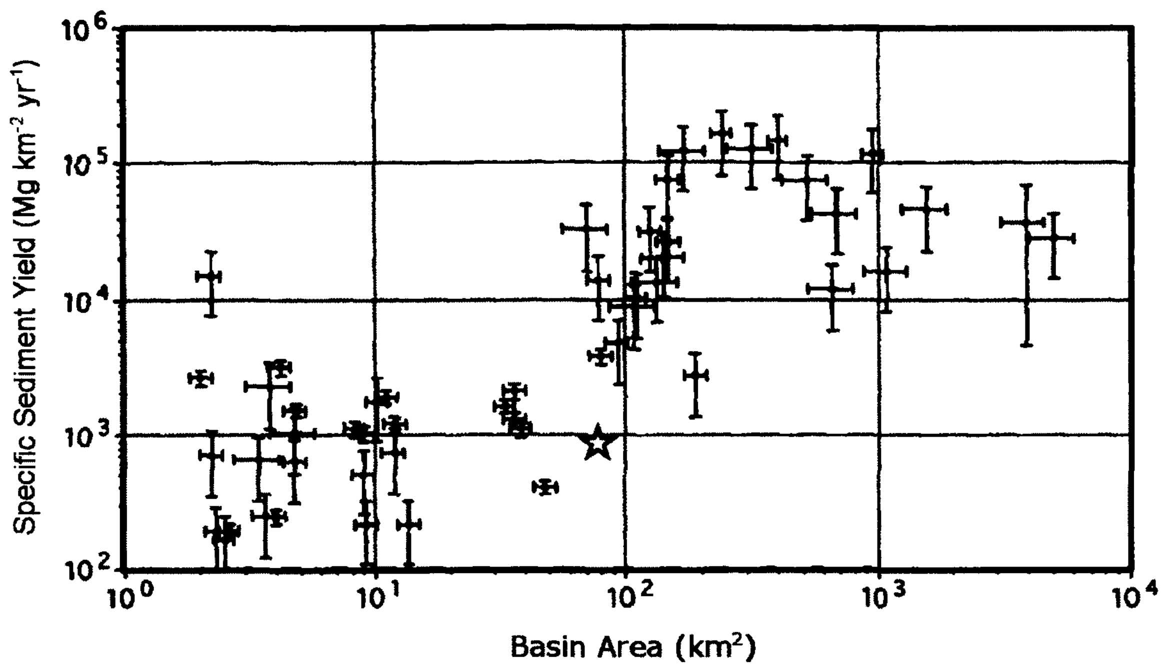

Figure 5.3 The relation of specific sediment yield to basin area. For comparison, the Peyto watershed (star) is plotted among other watersheds with glacier cover (graph modified from Hallet et al., 1996).

5.3 Influence of glacier change on sediment yield

Many environmental variables control lake sedimentation as shown by the conceptual diagram by Hodder et al. (2007; Figure 5.4). The diagram highlights the complex interactions among six basic environmental systems. In this study, I explicitly investigated how the glacier system (i.e., dimensional changes) influenced the lacustrine system (i.e., sediment yield). To account for confounding effects from the climate and fluvial systems, I used available climate and hydrometric records from the region. The results from this study could not clearly link the SSY record to the glacier, climate, or fluvial systems at annual to decadal timescales. It is possible that the combination of all three systems influenced the SSY record to some degree, but the majority of SSY variance remains unexplained.

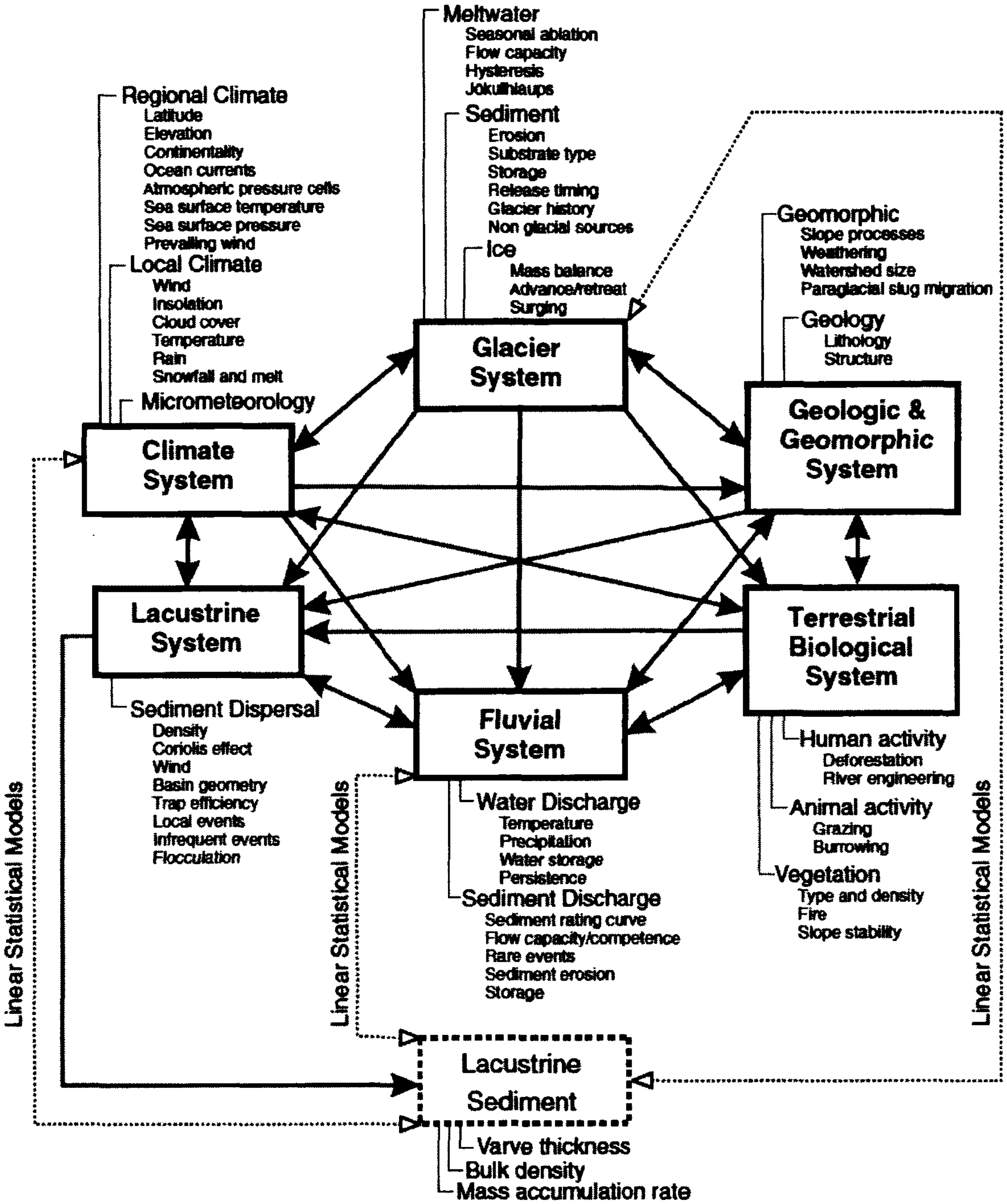

Figure 5.4 Conceptual diagram of the proglacial alpine systems and their linkages to lacustrine sediment (Hodder et al., 2007).

Based on the results presented in chapter 4, I surmise that Peyto Lake SSY is related to the volume of glacial runoff for the following reasons. First, years of high SSY occur during years of strong negative mass balance or high mean temperatures (e.g., 1929, 1934, 1941, 1970, and 1998). The SSY peak of 1970, for example, coincides with a drought year where glacier melt contributed up to 82% of the streamflow (Young, 1991). Second, about 71% of the Peyto Creek discharge originates from Peyto Glacier (Schuster and Young, 2006). Peyto Creek discharge was also shown to be related to related to SSC (r=0.61) and suspended sediment load (r = 0.88; Vendl, 1978). Third, 27 % of the annual variance in SSY was attributed to net mass balance and Mistaya River discharge records. Although the relation is weak, it is significant and suggests that glacier runoff is linked to SSY, but in a complex manner.

The long-term trend in SSY appears to mirror long-term changes in glacier runoff. I hypothesize that discharge contribution from Peyto Glacier reached its peak in mid-20th century and the resulting trend is evident in the SSY record. As a glacier recedes and ice melts, its potential contribution to water supply diminishes over time (Moore et al., 2009; Nolin et al., 2010). Peyto Glacier has continuously retreated since the end of the Little Ice Age; the glacier has lost over 70 % of its volume since 1896 (Demuth and Keller, 1996). As glacier volume declined there was likely a similar decline in glacier runoff. The extended varve record indicates that varves thickened from 1870 to about 1940. If SSY and the magnitude of glacier melt are related, then maximum glacier runoff from Peyto Glacier occurred at about 1940. For the period 1940 - 1980 SSY remained relatively level and high which corresponds to the period (1952 - 1977) with the highest rate of glacier change.

For the proceeding period 1977 - 2005, two additional factors may explain trends in SSY. First, the Pacific Decadal Oscillation (PDO) shift in 1976 caused glaciers throughout western North America, including Peyto Glacier, to lose more mass (Luckman, 1998; Moore et al., 2009). In spite of the strong years of negative net mass balance, the rate of volume change (Figure 4.5) for Peyto Glacier declined confirming that peak flow was likely reached prior to 1976. Second, SSY concurrently declined after 1980, which may be likewise related to the long-term decrease in glacier volume. For the period 1977 - 2005, however, my results indicate the rate of sediment delivery to Peyto Lake was considerably less than the rates for the periods 1917 - 1952 and 1952 - 1977. This decrease in SSY could be explained by several factors including sediment exhaustion from sedimentary stores adjacent to or beneath the glacier (long-term hysteresis), and/or a decrease in the rates of primary erosion. Basal erosion rates, for instance, would be expected to decline as the glacier area in contact with bedrock declines (Hallet et al., 1996).

Declining contribution of glacial meltwater to streamflow has been studied elsewhere in the Canadian Rocky Mountains. Research by Demuth and Pietroniro (2003), for example, found the mean and minimum discharge records of the Mistaya River have been declining since 1950 in spite of a modest increase in precipitation and temperature. They also suggest the ability of glacier cover to regulate streamflow in the Mistaya basin may have been in decline since the mid-1900s. In the neighbouring Bow River watershed, Hopkinson and Young (1998) found the ability of the receding Bow Glacier (*ca.* 1998) to enhance Bow River flow would have been reduced by 2% had the same climate as 1970 occurred. The summer of 1970 was abnormally hot and dry which resulted in an exceptionally high streamflow contribution by glaciers.

This study specifically examined the relation between SSY and dimensional changes of Peyto Glacier, but other factors besides glacier change are known to influence SSY in glaciated catchments. Changes in sediment storage, both beneath the glacier and in the watershed, likely influenced changes in the SSY record. Seasonal hysteresis between discharge and SSY are common beneath glaciers (Riihimaki et al., 2005). Binda (1994), for example, hypothesized that observed hysteresis between SSC and discharge for Peyto Creek was due to the re-organization of sub-glacial channels and sediment availability. As the melt season progresses, sediment exhaustion likewise increases (Gurnell et al., 1994). These temporal changes in sediment availability also occur in proglacial regions and streams. In addition to the sediment supplied by the glacier, sediment could also derive from local channel and hill slope processes. Orwin and Smart (2004) found up to 80 % of the total suspended sediment yield came from the proglacial area below Small Glacier, BC. Stochastic mass movement events within the watershed would also increase the SSY. Based on the photographic record from the basin, I did not find evidence for notable erosive processes within the Peyto watershed. Finally, intermittent storage areas for sediment between Peyto Glacier and Peyto Lake could also induce a time lag that exists at diurnal, seasonal, and annual timescales.

In summary, a number of factors confound the relation between SSY and dimensional changes of Peyto Glacier. I hypothesize that glacier runoff is the primary influence on the SSY trend which climaxed in 1941, but remained high from 1940 to 1980. Elevated runoff would have increased the potential to erode and transport sediments beneath and adjacent to the glacier. My results also suggest the rate of sediment delivery to Peyto Lake, relative to volume change, has declined in recent decades possibly resulting from sediment exhaustion or a decline in primary erosion rates.

5.4 Source of errors and limitations of study

5.4.1 Digital photogrammetry and measurements

Photogrammetric accuracy largely depends on the quality and coverage of existing aerial photographs. In essence, lower coverage or fewer measurements translates to less accurate data, more estimated data, and therefore less reliable data. Incomplete coverage required spatial and temporal interpolation, typically for areas in the accumulation zone of Peyto Glacier. Low photographic contrast in the accumulation zone and in shadows inhibited my ability to perceive depth and hence measure surface elevation change (Vanlooy and Forster, 2011). Determining elevations in areas of steep relief around Peyto Glacier was also difficult and probably led to larger errors in comparison to measurements made in areas of flatter terrain (Fox and Nuttall, 1997; Schiefer and Gilbert, 2007).

Additional sources of error include corrections required for the timing of the aerial photography and the lack of independent estimates of glacier elevations. The surface elevation of the glacier continuously changes as snow accumulates or melts throughout the year, so it is important to compare elevation points collected in the same season (Vanlooy et al., 2006). As the time between consecutive sets of aerial photography increases, the magnitude of this error term decreases (Zemp et al., 2013). For my study, consecutive photos were acquired 14 - 61 days apart for periods less than two years during the melt season. By using a temperature index model, volume adjustments were made to compensate for different acquisition dates; however, this correction does not correct for changes in length or area. Finally I used checkpoints on stable, unvegetated terrain with high photographic contrast to assess possible elevation biases in my stereo models for a given year. This error analysis was conducted in regions of high contrast which allows improved photogrammetric height measurements; however, this is not entirely representative of measurements done on the glacier surface where low contrast is prominent (Fox and Nuttall, 1997). Independent measurements of surface elevation for the glacier would allow me to assess the reliability of my elevation measurements for Peyto Glacier.

5.4.2 Sediment yield

Reliability of sediment yield estimated from varved sediment records depends on the quality of the lake sediment samples and the interpretation of varved sediments by the researcher. Zolitschka (2007) outlines four types of systematic errors associated with varve chronologies: technical problems, depositional events, sedimentation rates, and varve preservation. Incomplete core recovery and core barrel distortion are technical errors inherent in sediment core recovery (Glew et al., 2001). Depositional events (e.g., turbidites) within localized areas of the lake can influence varve thickness. Both low (< 2 mm) and high (> 20 mm) sedimentation rates can make varve identification difficult (Zolitschka, 2007). Changes in lake level or autochthonous productivity can influence the preservation of varves. In addition, interpretive errors from counting extra varves (Type A error) or not counting varves (Type B error) can arise if the chronology cannot be confirmed independently. A relative error (Type C error) can arise if Type A and B errors are consistent among core chronologies (Lamoureux, 2001).

In this study, sediment yield calculations were subject to the quality of sediment samples, depositional events, interpretation of varve boundaries, and interpolation of sediment thickness across Peyto Lake. I was able to distinguish the water-sediment interface on one core; however, other cores either had the upper sediments missing or the upper sediments lacked sharp varve boundaries. All cores had some degree of barrel distortion ranging from minor "U-bending" to severe cracking and bending from pressurized freezing. The lack of water-sediment interface inhibited the measurements of more recent varve formations and the sediment distortion likely altered measurements of varves. Depositional events were widespread in some cores (e.g., H, I, and J) nearest the delta which prevented the measurement of the varves and correlation with other cores. Low sedimentation prevented correlation among cores and measurements within the shallow regions of the lake, but years of high sedimentation increased the likelihood of Type A errors in the varve chronology. For most years, correlation among cores was done with multiple varves reducing the likelihood of Type A and Type B errors. Independent confirmation of the 1983 flood event and identifying 1963 peak associated with ^{137}Cs radionuclide dating suggests that my varve chronology is reliable. However, my chronology is still subject to Type C errors. Interpolations of the varve measurements and chronologies were conducted to calculate a range of sediment yields. Two methods of interpolation were conducted which resulted in a very similar pattern over time suggesting that interpolation methods has a low influence on the temporal pattern but a larger influence on the magnitude of sediment yield.

6. Conclusion and suggestions for further study

The primary goal of this study was to assess the influence of glacier activity on sediment yield within the Peyto Lake watershed. I used photogrammetry to determine dimensional changes (length, area, and volume) of Peyto Glacier. From 1917 to 2005 Peyto Glacier retreated -2198 ± 18 m, shrank -4.0 ± 0.9 km^2, thinned -44 ± 31 m, and lost a volume of -581 ± 404 × 10^6 m^3 w.e. From 1917 to 2010, SSY averaged 446 ± 176 Mg km^2 yr^{-1} which is among the highest in the Canadian Cordillera, but relatively low for glaciated basins. Measured dimensional changes to Peyto Glacier, along with supplemental mass balance, climate, and hydrometric records, were compared to the SSY record. Dimensional changes to Peyto Glacier were uncorrelated to SSY. About 27% of the SSY variance could be explained by net mass balance and Mistaya River discharge. Glacier change likely influenced SSY at the inter-annual to inter-decadal scales, but the majority of the variance remains unexplained.

The work presented in this thesis provides a SSY record for the Peyto Lake watershed and expands the known record of length, area, and volume changes for Peyto Glacier. The Peyto Lake watershed was an ideal site to examine the influence of glacier activity on SSY for a number of reasons: (1) there exists 18 sets of air photos and a historical map that dates to 1917; (2) Peyto Glacier has been the focus of many types of studies; (3) the history of Peyto glacier has been well-preserved on the landscape; (4) sediment transport from the glacier is directly coupled to the lake basin; (5) Peyto Glacier has the longest mass balance record in western Canada; (6) there are nearby climate and hydrometric stations; and (7) Peyto Lake sediments are varved. I was, however, not able to identify primary environmental controls of SSY and this outcome highlights the complexity of sediment transfers in glacierized basins. Additional research could build on this study and use sediment budget framework to understand sediment transfers in the Peyto Lake catchment. A sediment budget study could identify the rate that sediments can be produced and evacuated from the sub-glacial environment of Peyto Glacier. Additional work should also quantify long-term changes in sediment storage between the glacier's snout and Peyto Lake.

Literature cited

Andreassen, L.M., Elvehøy, H. and Kjøllmen, B. 2002. Using aerial photography to study glacier changes in Norway. *Annals of Glaciology,* 34: 343-348.

Appleby, P.G. 2001. Chronostratigraphy techniques in recent sediments. In: Last, W.M. and Smol, J.P. (eds). *Tracking Environmental Change Using Lake Sediments Volume 1: basin analysis, coring, and chronological techniques.* Kluwer Academic Publishers, Dordrecht, The Netherlands. p. 171-203.

Ashley, G.M. 1975. Rhythmic sedimentation in glacial lake Hitchcock, Massachusetts-Connecticut. In: Jopling, A.V. and McDonald, B.C. (eds). *Glaciofluvial and Glaciolacustrine sedimentation.* Society of Economic Palaeontologist and Mineralogists. Special Publication, 23: 304-320.

Ballantyne, C.K. 2002. Paraglacial geomorphology. *Quaternary Science Reviews,* 21: 1935-2017.

Bartholomaus, T.C., Anderson, R.S., and Anderson, S.P. 2008. Response of glacier basal motion to transient water storage. *Nature Geoscience,* 1: 33-37. doi:10.1038/ngeo.2007.52

Beedle, M.J., Menounos, B., Luckman, B.H. and Wheate, R., 2009. Annual push moraines as climate proxy. *Geophysical Research Letters*, 36. L20501. DOI:10.1029/2009GL039533.

Bennett, M.R., Huddart, D., Glasser, N.F., and Hambrey, M.J. 2000. Resedimentation of debris on an ice-cored lateral moraine in the high-Arctic (kongsvegen, Svalbard). *Geomorphology,* 35: 21-40.

Binda, G.G. 1984. *Fluvioglacial sediment and hydrochemical dynamics, Peyto Glacier, Alberta.* MA thesis. Ottawa, ON, University of Ottawa. 139 pp.

Bolch, T., Menounos, B. and Wheate, R., 2010. Landsat-based inventory of glaciers in western Canada, 1985-2005. *Remote Sensing of Environment*, 114: 127-137. DOI:10.1016/j.rse.2009.08.015.

Brune, G.M. 1953. Trap efficiency of reservoirs. *Transactions of the American Geophysical Union,* 34: 407-18.

Brunger, A.G., Nelson, J.G., and Ashwell, I.Y. 1967. Recession of the Hector and Peyto Glaciers: further studies in the Drummond glacier, Red Deer Valley area, Alberta. *Canadian Geographer,* XI (1): 35-48.

Chikita, K.A. 1992. The role of Sediment-Laden Underflows in Lake Sedimentation: Glacier-Fed Peyto Lake, Canada. *Journal of the Faculty of Science, Hokkaido University. Series VII (Geophysics)*, 9: 211-224.

Chikita, K.A. 1993. Acomparative study on suspended sediment discharge initiated by snow- or glacier-melting. *IAHS Publ.*, 217: 257-267.

Chikita, K.A., Smith, N.D., Yonemitsu, N., and Perez-Arlucea, M. 1996. Dynamics of sediment-laden underflows passing over a subaqueous sill: glacier-fed Peyto Lake, Alberta, Canada. *Sedimentology,* 43: 865-875.

Church, M. and Slaymaker, O. 1989. Disequilibrium of Holocene sediment yield in glaciated British Columbia. *Nature,* 337: 452-454.

Cogley, J.G., Hock, R., Rasmussen, L.A., Arendt, A.A., Bauder, A., Braithwaite, R.J. Jansson, P., Kaser, G., Möller, M., Nicholson, L. and Zemp, M. 2011. *Glossary of Glacier Mass Balance and Related Terms,* IHP-VII Technical Documents in Hydrology No. 86, IACS Contribution No. 2, UNESCO-IHP, Paris. 114 pp.

DeBeer, C.M. and Sharp, M.J. 2007. Recent changes in glacier area and volume within the sourthern Canadian Cordillera. *Annals of Glaciology,* 46: 215- 221

De Geer, G. 1912. A geochronology of the last 12000 years. *Congr. Géol. Int.* Stockholm 1910, C.R. p. 241-253.

Dedkov, A.P. and Moszherin, V.T. 1992. Erosion and sediment yield in mountain areas of the world. In: Walling, D.E., Davies, T.R. and Hasholt, B.(eds). *Erosion, Debris Flows and Environment in Mountain Regions.* IAHS Publ. 209: 29-36.

Demuth, M.N. and Keller, R. 2006. An assessment of the mass balance of Peyto Glacier (1966-1995) and its relation to recent and past century climatic variability. In: Demuth, M.N., Munro, D.S., and Young, G.J. (eds). *Peyto Glacier: One Century of Science.* NHRI Science Report No. 8. p. 82-134.

Demuth, M.N., and Pietroniro, A. 2003. The Impact of Climate Change on the Glaciers of the Canadian Rocky Mountain Eastern Slopes and Implications for Water Resource-related Adaptation in the Canadian prairies, "Phase 1"—Headwaters of the North Saskatchewan River Basin. *Report to the Climate Change Action Fund—Prairie Adaptation Research Collaborative, PARC. Project P55.* Geological Survey of Canada Open File 4322.

Demuth, M.N., Sekerka, J. and Bertollo, S. 2009. Glacier mass balance observations for Peyto Glacier, Alberta, Canada. Spatially Referenced Data Set contribution to the National Glacier-Climate Observing System, State and Evolution of Canada's Glaciers, http://pathways.geosemantica.net/collections/documents_folderview.aspx?coll=0456508e-048a-48d1-965e-b22efe0e79b9, Geological Survey of Canada.

Denton, G.H., 1975. Glaciers of the Canadian Rocky Mountains. In W.O. Field (ed.). *Mountain Glaciers of the Northern Hemisphere.* Hanover, NH: United States Army Cold Regions Research and Engineering Laboratory. p. 603-653.

Denton, G.H. and Karlén, W. 1973. Holocene climatic variations-the pattern and possible cause. *Quaternary Research,* 3: 155-174.

Desloges, J.R. 1994. Varve deposition and the sediment yield record at three small lakes of the southern Canadian cordillera. *Artic and Alpine Research, 25*: 130-140.

Evans, M. 1997. *Holocene sediment yield and geomorphic sensitivity in alpine landscapes, Cathedral Lakes, British Columbia.* Phd Dissertation. UBC, Vancouver, 295 pp.

Field, W.O., and Heusser, C.J. 1954. Glacier and botanical studies in the Canadian Rockies, 1953. *Canadian Alpine Journal,* 37: 127-140.

Foster, I.D. L., Dearing, J.A., Grew, R. and Orend, K. 1990. The sedimentary data base: an appraisal of lake and reservoir sediment based studies of sediment yield. In: Walling, D.E., Yair, A. And Berkowicz, S. (eds). *Erosion, Transport and Deposition Processes.* IAHS Publ., 189: 19-43.

Fox, A.J. and Nuttall, A.M. 1997. Photogrammetry as a research tool for glaciology. *Photogrammatric Record,* 15: 725-737.

Gilbert, R. 2003. Varves. In: Middleton, G.V. (ed.) *Encyclopaedia of Sediments and Sedimentary Rocks*. Springer, Dordrecht, The Netherlands. p.764-765.

Glenday, P.J. 1991. *Determination of morphologic and volumetric change, Peyto Glacier, Alberta, 1966-1989.* MA Thesis. Waterloo, ON, Wilfrid Laurier University. 130 pp.

Glew, J.R., Smol., J.P. and Last, W.M. 2001. In: Last, W.M. and Smol, J.P. (eds). *Tracking Environmental Change Using Lake Sediments Volume 1: basin analysis, coring, and chronological techniques*. Kluwer Academic Publishers, Dordrecht, The Netherlands. p. 73-105.

Granshaw, F.D. and Fountain, A.G. 2006. Glacier change (1958-1998) in the North Cascades National Park Complex, Washington, USA. *Journal of Glaciology,* 52: 251-256.

Gurnell, A. M., Hodson, A., Clark, M.J., Bogen, J., Hagen, J.O., and Tranter, M. 1994. Water and sediment discharge from glacier basins; an arctic and alpine comparison. In: Olive, L.J., Loughran, R.J., and Kesby, J.A. (eds) *Variability in stream erosion and sediment transport.* IAHS Publication, 224: 325-334

Hallet, B., Hunter, L. and Bogen, J. 1996. Rates of erosion and sediment evacuation by glaciers: A review of field data and their implications. *Global and Planetary Change,* 12: 213-235.

Hånkanson, L. 1995. Models to predict organic content of lake sediments. *Ecological Modelling,* 82: 233-245.

Hånkanson, L. and Jansson, M. 2002. *Principles of Lake Sedimentology*. The Blackburn Press, New Jersey, USA. 316 pp.

Harbor, J. and Warburton, J. 1993. Relative rates of glacial and nonglaical erosion in alpine environments. *Arctic and Alpine Research*, 25: 1-7.

Harbor, J., Bhaduri, B., Angelakis, L. and Snyder, J. 1997. *Sediment basins, using modified stormwater management basins and sediment basins to reduce water pollution from construction sites in Ohio*. Kent, OH: Department of Geology, Kent State University.

Heiri, O., Lotter, A.F., and Lemcke, G. 2001. Loss on ignition as a method for estimating organic and carbonate content in sediments: reproducibility and comparability of results. *Journal of Paleolimnology*, 25: 101-110.

Henoch, W.E.S. 1971. Estimate of Glaciers Secular (1948-1966) Volumetric Change and its contribution to the discharge in the Upper North Saskatchewan River basin. *Journal of Hydrology*, 12: 145-160.

Heusser, C.J. 1956. Postglacial environments in the Canadian Rocky Mountains. *Ecological Monographs*, 26: 253-302.

Hicks, D.M., McSaveney, M.J., and Chinn, T.J.H. 1990. Sedimentation in proglacial Ivory Lake, Southern Alps, New Zealand. *Arctic and Alpine Research*, 22: 26-42.

Hickmann, M. and Reasoner, M.A. 1998. Late Quaternary diatom response to vegetation and climate change in a subalpine lake in Banff National Park, Alberta. *Journal of Paleolimnology*, 20: 253-265.

Hobbs, W.O, Vinebrooke, R.D. and Wolfe, A.P. 2011. Biogeochemical responses of two alpine lakes to climate change and atmospheric deposition, Jasper and Banff National Parks, Canadian Rocky Mountains. *Canadian Journal of Fisheries and Aquatic Sciences*, 68: 1480-1494.

Hock, R. 2003. Temperature index melt modelling in mountain areas. *Journal of Hydrology*, 282: 104-115.

Hodder, K.R., Desloges, J.R., and Gilbert, R. 2006. Pattern and timing of sediment infill at glacier-fed Mud Lake: implications for late glacial and Holocene environments in the Monashee Mountain region of British Columbia, Canada. *The Holocene*, 16: 705-716.

Hodder, K.R., Gilbert, R., and Desloges, J.R., 2007. Glaciolacustrine varved sediment as an alpine hydroclimatic proxy. *Journal of Paleolimnology*, 38: 365-394. DOI 10.1007/s10933-006-9083-9

Holdsworth, G., Demuth, M.N., and Beck, T.M.H. 2006. Radar Measurements of Ice Thickness on Peyto Glacier, Alberta- Geophysical and Climatic Implications. In: Demuth, M.N., Munro, D.S., and Young, G.J. (eds). *Peyto Glacier: One Century of Science*. NHRI Science Report No. 8. p. 59-79.

Hopkinson, C. and Demuth, M. N. 2006. Using airbone lidar to assess the influence of glacier downwasting on water resources in the Canadian Rockey Mountains. *Canadian Journal of Remote Sensing,* 32: 212-222.

Hopkinson, C. and Young, G.J. 1998. The effect of glacier wastage on the flow of the Bow River at Banff, Alberta, 1951-1993. *Hydrological Processes,* 12: 1745-1762.

Hovius, N., 1998. Controls on sediment supply by large rivers. In: *Relative Role of Eustasy, Climate, and Tectonism in Continental Rocks*. Society of Sedimentary Geology. Special Publ., 59: 3-16.

Jansson, P., Rosqvist, G. and Schneider, T. 2005. Glacier Fluctuations, Suspended sediment flux and glacio-lacustrine sediments. *Geografiska Annaler, 87A*: 37-50.

Johnson, P.G. and Power, J.M. 1985. Flood and landslide events, Peyto Glacier terminus, Alberta, Canada, 11-14 July 1983. *Journal of Glaciology,* 31: 86-91.

Interprovincial Boundary Commission. 1917. *Report of the Commission Appointed to Delimit the Boundary between the Provinces of Alberta and British Columbia: From 1913-1916, Part I.* Ottawa, Ontario, Office of the Surveyor General.

Kääb, A. and Vollmer, M. 2000. Surface geometry, thickness changes and flow fields on creeping mountain permafrost: automatic extraction by digital image analysis. *Permafrost Periglacial Processes,* 11: 315-326.

Kingman, H.S. 1938. Peyto Glacier, in Glacier Observations, 1936 and 1937 by A.A.McCoubrey. *Canadian Alpine Journal,* 25: 113-116.

Kite, G.W. and Reid, I.A., 1977. Volumetric change of the Athabasca Glacier over the last 100 years. *Journal of Hydrology,* 32: 279-294.

Koppes, M. and Hallet, B. 2006. Erosion rates during rapid deglaciation in Icy Bay, Alaska. *Journal of Geophysical Research* 111: F02023, doi:10.1029/2005JF000349.

Lacourse, T. and Gajewski, K. 2000. Late Quaternary vegetation history of Sulphur Lake, southwestern Yukon territory, Canada. *Arctic,* 53: 27-35.

Lamoureux, S. 2001. Varve Chronology Techniques. In: Last, W.M. and Smol, J.P. (eds). *Tracking Environmental Change Using Lake Sediments Volume 1: basin analysis, coring, and chronological techniques*. Kluwer Academic Publishers, Dordrecht, The Netherlands. p. 247-260.

Leonard, E.M. 1986. Varve studies at Hector Lake, Alberta, Canada, and the relationship between glacial activity and sedimentation. *Quaternary Research,* 25: 199-214.

Leonard, E.M. 1997. The relationship between glacial activity and sediment production: evidence from a 4450-year varve record of neoglacial sedimentation in Hector Lake, Alberta, Canada. *Journal of Paleolimnology,* 17: 319-330.

Letreguilly, A. 1988. Relation between the mass balance of western Canadian mountain glaciers and meteorological data. *Journal of Glaciology,* 34: 11-18.

Loso, M.G., Anderson, R.S. And Anderson, S.P. 2004. Post-Little Ice Age record of Coarse and fine clastic sedimentation in an Alaskan proglacial lake. *Geology,* 32: 1065-1068. doi:10.1130/G20839.1

Luckman, B.H., 1996. Dendroglaciology at Peyto Glacier, Alberta. In *Tree, Rings, Environment, and Humanity,* Dean, J.S., Meko, D.S., and Swetnam, T.W. (eds). Radiocarbon, Tucson, Arizona. p.679-688.

Luckman, B.H., 1998. Landscape and climate change in the central Canadian Rockies during the 20th century. *The Canadian Geographer*, 42: 319-336.

Luckman, B.H. 2006. The neoglacial history of Peyto Glacier. In: Demuth, M.N., Munro, D.S., and Young, G.J. (eds). *Peyto Glacier: One Century of Science.* NHRI Science Report No. 8. p. 25-58.

Luckman, B.H. and Osborn, G.D. 1979. Holocene glacier fluctuations in the middle Canadian Rocky Mountains. *Quaternary Research,* 11: 52-77.

Luckman, B.H., Holdsworth, G. and Osborn, G. 1993. Neoglacial Glacier Fluctuations in the Canadian Rockies. *Quaternary Research,* 39: 144-153.

McGlone, J. (ed). .2004. *Manual of Photogrammetry,* 5th ed. American Society for Photogrammetry and Remote Sensing, Bethesda, MD, USA. 1151 pp.

Meek. V. 1948. Glacier Observations in the Canadian Cordillera. *Canadian Geographical Journal,* 37: 190-209.

Mekis, É. and Vincent, L.A. 2011. An overview of the second generation adjusted daily precipitation dataset for trend analysis in Canada. *Atmosphere-Ocean,* 49: 163-177.

Menounos, B. 1997. The water content of lake sediments and its relationship to other physical parameters: an alpine case study. *The Holocene,* 7: 207-212.

Menounos, B. 2006. Anomalous early 20th century sedimentation in proglacial Green Lake, British Columbia, Canada. *Canadian Journal of Earth Science,* 43: 671-678.

Menounos, B., Clague, J. Gilbert, R., and Slaymaker, O., 2005. Environmental reconstruction from a varve network in the southern Coast Mountains, British Columbia, Canada. *The Holocene*, 15: 1163-1171.

Moore, R.D., Fleming, S.W., Menounos, B., Wheate, R., Fountain, A., Stahl, K., Holm, K., and Jakob, M. 2009. Glacier change in western North America: influences on hydrology, geomorphic hazards and water quality. *Hydrological Processes*, 23: 42-61.

Munro, D.S. 2006. Linking the weather to glacier hydrology and mass balance at Peyto Glacier. In: Demuth, M.N., Munro, D.S., and Young, G.J. (eds). *Peyto Glacier: One Century of Science*. NHRI Science Report No. 8. p. 134-176.

Nakawo, M., and Young, G.J. 1982. Estimate of glacier ablation under a debris layer from surface temperature and meteorological variables. *Journal of Glaciology,* 28: 29-34.

Nolin, A.W., Phillippe, J., Jefferson, A., and Lewis, S.L. 2010. Present-day and future contributions of glacier runoff to summertime flows in a Pacific Northwest watershed: Implications for water resources. *Water Resources Research* 46, W12509, doi:10.1029/2009WR008968.

Ommanney, C.S.L. 1972. *Glacier Surveys by District Personnel of the water survey of Canada: 2.Peyto Glacier.* Department of environment, Inland waters Branch, Glacier Inventory Note No. 7. 20 pp.

Ommanney, C.S.L. 2002. Glaciers of the Canadian Rockies. In *Glaciers of North America - Glaciers of Canada - Glaciers of the Canadian Rockies.* U.S. Geological Survey Professional Paper 1386-J-1.

Orwin, J. F. and Smart, C. C. 2004. Short-term spatial and temporal patterns of suspended sediment transfer in proglacial channels Small River Glacier, Canada. *Hydrological Processes*, 18: 1521-1542.

Østrem, G., and Arnold, K. 1970. Ice-cored moraines in southern British Columbia and Alberta.*Geografiska Annaler* 52A: 120-128. doi:10.2307/520605.

Owens, P. and Slaymaker, O. 1993. Lacustrine Sediment Budgets in the Coast Mountains of British Columbia, Canada. In: McManus, J. and Duck, R.W. (eds). *Geomorphology and Sedimentology of Lakes and Reservoirs*. John Wiley and Sons Publishers, Toronto, Canada. p. 105-123.

Rasmussen, L.A., and Conway, H. 2004. Climate and Glacier Variability in Western North America. *Journal of Climate,* 17: 1804 - 1815.

Reasoner, M.A. 1993. Equipment and procedure improvements for a lightweight, inexpensive, percussion core sampling system. *Journal of Paleolimnology,* 8: 273-281.

Restrepo, J.D., Kjerfve, B., Hermelin, M. and Restrepo, J.C. 2006. Factors controlling sediment yield in a major South American drainage basin: the Magdalena River, Columbia. *Journal of Hydrology,* 316: 213-232.

Riihimaki, C.A., MacGregor, K.R., Anderson, R.S., Anderson, S.P., and Loso, M.G. 2005. Sediment evacuation and glacial erosion rates at a small alpine glacier. *Journal of Geophysical Research* 110: F03003, doi:10.1029/2004JF000189.

Sander, M., Bengtsson, L., Holmquist, B., Wohlfarth, B. and Cato, I. 2002: The relationship between annual varve thickness and maximum annual discharge (1909-1971). *Journal of Hydrology, 263*: 23-25.

Schiefer, E.K. 2004. *Contemporary Sedimentation Patterns within Green Lake, Southern Coast Moutains, British Columbia.* Phd dissertation. UBC, Vancouver, 206 pp.

Schiefer, E. and Gilbert, R. 2007. Reconstructing long-term morphometric change in a proglacial landscape using historical aerial photography and automated DEM Generation. *Geomorphology,* 88: 167-178.

Schiefer, E., Menounos, B. and Wheate, R. 2007. Recent volume loss of British Columbia glaciers, Canada. *Geophysical Research Letters,* L16503, loi:10.1029/2007GL030780.

Schuster, C.J. and Young, G.J. 2006. The derivation of runoff from the Peyto Glacier catchment. In: Demuth, M.N., Munro, D.S., and Young, G.J. (eds). *Peyto Glacier: One Century of Science*. NHRI Science Report No. 8. p. 226-254.

Shea, J.M., Moore, R.D., and Stahl, K. 2009. Derivation of melt factors from glacier mass-balance records in western Canada. *Journal of Glaciology* 55: 123-130.

Slaymaker, O. 1977. *Estimation of sediment yield in temperate alpine environments*. IAHS Publ., 122: 109-117.

Smith, N.D. and Ashley, G.M. 1985. Proglacial Lacustrine Environment. In: G.M. Ashley, J.Shaw and N.D. Smith (eds.) *Glacial Sedimentary Environments*. Society of Economic Paleontologists and Mineralogists, Short Course 16, Tulsa, OK, p. 135-216.

Smith, D.G., and Jol, H.M. 1997. Radar structure of a Gilbert-type delta, Peyto Lake, Banff National Park, Canada. *Sedimentary Geology,* 113: 195-209.

Smith, N.D., Vendl, M.A. and Kennedy, S.K. 1982. Comparison of sedimentation regimes in four glacier-fed lakes of western Alberta. In: Davidson-Arnott, R., Nickling, W. and Fahey, B.D. (eds.) *Research in Glacio, Glacio-Fluvial and Glacio-Lacustrine Systems*, Proceedings of the 6th Guelph Symposium on Geomorphology, 1980. Geobooks, Norwich, p. 203-238.

Tennant, C., and Menounos, B. 2013. Glacier change of the Columbia Icefield, Canadian Rocky Mountains, 1919-2009. *Journal of Glaciology, 59*: 671-686.

Tennant, C. Menounos, B., Wheate, R., and Clague, J. 2012. Glacier Change in the Canadian Rocky Mountains, 1919 to 2006. *The Cryosphere,* 6: 1541-1552.

Thorington, J.M. 1934. Peyto Glacier, in Glacial Observations in the Canadian Cordillera 1933-1934 by A.O. Wheeler. *Canadian Alpine Journal,* 22: 172-198.

Vanlooy, J.A. and Forster, R.R. 2011. Use of historical elevation data to calculate surface-elevation and volume changes of Ha-iltzuk Icefield, southwest British Columbia, Canada, 1970 to mid-1980s. *Annals of Glaciology,* 52: 109-115.

VanLooy, J.A., Forster, R.R. and Ford, A. 2006. Accelerating thinning of Kenai Peninsula glaciers, Alaska. *Geophysical Research Letters* 33, L21307, dio:10.1029/2006GL028060

Vanoni, V. A. 2006. *Sedimentation Engineering.* American Society of Civil Engineers, New York, USA, 418 pp.

Vendl, M.A. 1978. *Sedimentation in Glacier-fed Peyto Lake, Alberta.* MSc. thesis. Chicago, Illinois, University of Illinois at Chicago Circle. 71 pp.

Verstraeten, G. and Poesen, J. 2000. Estimating trap efficiency of small reservoirs and ponds: methods and implications for the assessment of sediment yield. *Progress in Physical Geography,* 24: 219-251.

Vincent, L.A., Wang, X.L., Milewska, E.J., Wan, H., Yang, F. and Swail, V. 2012. A Second Generation of Homogenized Canadian Monthly Surface Air Temperature for Climate Trend Analysis. *Journal of Geophysical Research* 117, D18110, doi:10.1029/2012JD017859.

Wallace, A.L. 1995. *The volumetric change of the Peyto Glacier, Alberta, Canada 1896-1966.* MA Thesis. Waterloo, ON, Wilfred Laurier University, 140 pp.

Walling, D.E. 1983. The sediment delivery problem. *Journal of Hydrology,* 65: 209-237.

Walling, D.E. 1994. Measuring sediment yield from river basin. In: *Lal, R. (ed.), Soil Erosion Research Methods.* Soil and Water Conservation Society, Ankeny, IA, p. 39-80.

Wang, T., Hamann, A., Spittlehouse, D.L. and Murdock, T.Q. 2012. ClimateWNA - High-resolution spatial climate data for western North America. *Journal of Applied Meteorology and Climatology,* 51: 16-29.

Watson, E. and Luckman, B.H. 2004. Tree-ring-based mass-balance estimates for the past 300 years at Peyto Glacier, Alberta, Canada. *Quaternary Research,* 62: 9-18.

Wheeler, A.O. 1920. The application of photography to the mapping of the Canadian Rocky Mountains. *Canadian Alpine Journal*, 2: 76-87.

Wilcox, C.D., Dove, S.B., McDavid, W.D., and Greer, D.B. 2002. *UTHSCSA Image Tool Version 2.01:* Freeware software available from the Department of Dental Diagnostic Science at the University of Texas Health Science Center at San Antonio: http://compdent.uthscsa.edu/dig/itdesc.html or search for "Image Tool 3.0"

Young, G.J. 1981. The mass balance of Peyto Glacier, Alberta. Canada, 1965 to 1978. *Arctic and Alpine Research,* 13: 307-318.

Young, G.J. 1991. Hydrological interactions in the Mistaya basin, Alberta, Canada. Snow, Hydrology and Forests in High Alpine Areas. Proceedings of the Vienna Symposium, August 1991, IAHS Publications. No. 2005: p. 237-244.

Zemp, M., Thibert, E., Huss, M., Stumm, D., Rolstad Denby, C., Nuth, C., Nussbaumer, S.U., Moholdt, G., Mercer, A., Mayer, C., Joerg, P.C., Jansson, P. Hynek, B., Fischer, A., Escher-Vetter, H., Elvehøy, H., and Andreassen, L.M. 2013. Uncertainties and re-analysis of glacier mass balance measurements. *The Cryosphere Discussions*, 7: 789-839.

Zolitschka, B. 2007. Varved lake sediments, In: S.A. Elias (ed.), *Encyclopaedia of Quaternary Science*. Elsevier, Amsterdam, The Netherlands. p. 3105-3114.

Appendices

Appendix A: Ancillary core information

Table A.1 Measured (white), interpolated (light grey) and averaged (dark grey) varve thicknesses (cm) for the period 1917 - 2010.

	Core Sample																	
2010													0.76					
2009													1.15		0.94			
2008													1.36		1.38			
2007	0.96												1.76		1.66			
2006	1.09		0.60										0.93	0.55	2.53			
2005	0.81		0.67	3.63								1.65	1.51	0.73	0.77	0.54		
2004	1.44		1.09	3.94								1.82	3.70	1.76	2.26	1.97		
2003	1.61	0.59	1.30	4.10								1.89	2.69	3.06	3.67	2.29		
2002	1.55	0.35	1.30	5.55								1.44	3.92	3.22	2.81	1.92		
2001	0.65	0.24	0.84	1.06								1.81	2.96	1.16	1.38	1.33		
2000	0.38	0.17	0.44	1.28			0.69					1.08	1.71	1.12	1.47	0.76		
1999	0.52	0.24	0.99	1.62			1.39					1.06	1.77	3.05	0.81	1.07	0.46	
1998	2.49	1.79	1.62	7.28			4.90					1.81	5.54	3.11	4.76	5.05	0.40	
1997	1.32	1.16	0.71	1.28			2.99	2.68				2.15	3.11	2.03	2.43	1.53	0.80	
1996	0.42	0.48	0.44	1.16			0.90	0.57				1.04	1.11	0.92	0.76	0.61	0.33	
1995	0.52	0.52	1.11	1.07			1.01	0.98			2.16	0.98	1.26	0.56	0.76	0.75	0.38	
1994	0.82	0.83	1.25	3.33			1.94	1.65			1.40	1.61	2.28	0.41	2.16	0.69	0.31	
1993	0.49	0.50	0.94	2.24			0.43	0.92			1.99	0.85	1.42	1.48	1.29	0.74	0.44	
1992	0.68	0.76	0.42	0.98			1.70	1.61			2.32	1.36	2.05	1.01	2.36	0.75	1.60	
1991	0.75	0.81	0.64	1.09			1.10	2.05			1.64	1.19	1.06	0.51	1.19	0.94	0.40	
1990	0.75	0.58	0.65	1.69			2.20	1.63			2.87	2.16	1.55	2.01	0.87	0.97	1.16	
1989	0.59	0.67	0.80	0.98			1.70	1.31			1.40	1.89	0.87	1.59	1.21	0.66	1.32	
1988	0.75	0.74	0.51	1.49			2.34	1.66			1.29	2.20	2.90	2.06	1.59	1.69	0.53	
1987	0.59	1.06	1.09	2.40			2.23	0.96			2.65	1.97	2.41	1.31	2.12	1.70	0.53	
1986		0.88	1.08	1.72			1.93	0.83			1.80	2.18	1.33	2.97	1.57	1.46	0.29	
1985		0.99	0.92	1.57			1.69	1.00		1.08	0.80	1.42	1.35	1.32	1.47	1.11	0.55	
1984		1.48	1.18	3.07			1.46	1.28		0.58	0.86	1.74	2.62	1.10	2.12	1.09	0.37	
1983		3.91	1.64	3.00			3.75	3.72		2.80	1.41	3.26	4.26	1.83	4.59	1.68	0.83	
1982		1.17	0.94	1.77			1.27	2.06		0.73	1.99	1.31	1.37	0.70	1.87	0.96	0.46	

1981	[redacted]	1.96	1.57	2.36	[redacted]	[redacted]	2.84	3.19	[redacted]	0.69	5.29	1.93	0.95	0.79	2.02	1.70	0.70	[redacted]
1980	[redacted]	1.62	1.30	2.16	[redacted]	[redacted]	1.99	2.39	[redacted]	0.09	4.29	2.41	0.87	1.32	1.91	1.64	0.40	[redacted]
1979	[redacted]	1.52	1.42	1.98	[redacted]	[redacted]	2.29	2.22	[redacted]	0.41	1.83	1.57	1.31	1.45	1.89	1.34	0.42	[redacted]
1978	[redacted]	1.38	1.16	2.00	[redacted]	[redacted]	2.31	1.91	[redacted]	0.24	2.07	2.33	1.12	1.62	1.64	0.73	0.42	[redacted]
1977	[redacted]	0.99	1.02	2.33	[redacted]	[redacted]	2.83	2.28	[redacted]	0.75	2.05	1.95	1.76	1.96	1.76	0.67	0.35	[redacted]
1976	[redacted]	1.64	0.99	2.08	[redacted]	[redacted]	3.50	2.85	[redacted]	0.37	4.18	1.69	1.48	0.74	1.34	0.76	0.64	[redacted]
1975	[redacted]	1.44	1.06	2.17	[redacted]	[redacted]	2.09	2.04	[redacted]	0.28	7.67	2.26	1.62	5.44	1.21	1.23	0.35	[redacted]
1974	[redacted]	1.11	0.97	1.60	[redacted]	[redacted]	1.85	2.04	[redacted]	0.15	4.46	1.63	1.17	1.85	0.57	1.41	0.35	[redacted]
1973	[redacted]	0.86	0.88	1.51	[redacted]	[redacted]	2.11	2.02	[redacted]	0.22	2.78	1.63	1.45	2.64	1.13	1.30	0.22	[redacted]
1972	[redacted]	0.90	0.88	1.34	[redacted]	[redacted]	1.96	1.91	[redacted]	0.37	1.29	1.44	0.91	1.36	0.53	1.32	0.22	[redacted]
1971	[redacted]	1.62	1.01	3.30	[redacted]	[redacted]	3.15	3.22	[redacted]	0.45	6.00	2.36	3.21	3.30	2.29	1.72	0.64	[redacted]
1970	[redacted]	2.58	1.59	4.24	[redacted]	[redacted]	6.03	5.69	[redacted]	0.93	3.70	3.22	4.02	2.73	2.83	1.63	0.30	[redacted]
1969	[redacted]	1.21	0.80	2.58	[redacted]	[redacted]	2.87	2.22	[redacted]	0.41	1.60	1.99	3.70	3.21	1.55	0.92	0.29	[redacted]
1968	[redacted]	0.94	1.08	1.88	[redacted]	[redacted]	2.31	1.98	[redacted]	0.45	2.09	1.54	2.35	2.42	1.32	0.97	0.48	[redacted]
1967	[redacted]	1.35	1.26	2.41	[redacted]	[redacted]	3.37	2.68	[redacted]	0.41	3.50	2.75	3.20	2.89	1.79	2.02	0.43	[redacted]
1966	[redacted]	1.00	0.85	2.38	[redacted]	[redacted]	2.14	2.46	[redacted]	0.24	2.44	2.34	3.03	2.82	1.38	1.74	0.48	[redacted]
1965	[redacted]	1.28	1.05	2.83	[redacted]	[redacted]	3.23	3.12	[redacted]	0.47	2.36	2.90	2.35	2.84	1.98	2.09	0.21	[redacted]
1964	[redacted]	1.30	1.02	2.68	[redacted]	[redacted]	2.50	2.64	[redacted]	0.34	3.24	2.31	2.31	2.22	1.80	1.08	0.46	[redacted]
1963	[redacted]	0.89	0.94	1.56	[redacted]	[redacted]	1.52	1.39	[redacted]	0.26	1.72	1.69	1.69	1.65	0.83	0.62	0.57	[redacted]
1962	[redacted]	1.05	1.11	2.29	[redacted]	[redacted]	2.61	3.46	[redacted]	0.39	2.17	3.03	2.90	2.91	1.89	0.88	0.66	[redacted]
1961	[redacted]	2.28	1.95	2.55	[redacted]	[redacted]	3.49	4.44	[redacted]	0.34	1.25	3.05	3.20	2.95	1.70	3.07	1.21	[redacted]
1960	[redacted]	0.86	0.89	2.12	[redacted]	[redacted]	1.72	1.74	[redacted]	0.24	1.90	2.33	2.35	1.67	0.87	1.97	0.42	[redacted]
1959	[redacted]	1.46	1.04	3.46	[redacted]	[redacted]	2.44	3.53	[redacted]	1.30	1.27	3.17	2.87	4.12	2.10	1.64	0.55	[redacted]
1958	[redacted]	1.61	1.64	3.48	[redacted]	[redacted]	3.80	3.13	[redacted]	1.54	1.09	3.58	3.13	1.84	2.06	1.80	0.62	[redacted]
1957	[redacted]	0.88	0.82	0.90	[redacted]	[redacted]	1.17	1.41	[redacted]	0.65	0.86	0.78	1.33	1.90	0.81	0.60	0.37	[redacted]
1956	[redacted]	1.15	1.34	2.30	[redacted]	[redacted]	2.78	2.42	[redacted]	0.67	6.59	3.15	2.43	1.99	1.80	1.38	0.37	[redacted]
1955	[redacted]	1.31	1.00	2.52	[redacted]	[redacted]	2.57	2.59	[redacted]	1.21	4.82	2.64	2.21	2.19	1.80	1.24	0.42	[redacted]
1954	[redacted]	0.51	0.59	1.05	[redacted]	[redacted]	1.09	1.00	[redacted]	0.78	0.88	1.28	0.82	0.31	0.61	0.67	0.18	[redacted]
1953	[redacted]	0.68	0.78	1.45	[redacted]	0.79	1.39	1.26	[redacted]	0.78	1.54	2.45	1.77	0.52	1.48	0.87	0.22	[redacted]
1952	[redacted]	0.88	0.72	1.38	[redacted]	0.57	1.98	3.85	[redacted]	0.74	0.68	2.36	1.75	0.84	1.63	0.76	0.20	[redacted]
1951	[redacted]	1.25	1.08	2.41	[redacted]	1.16	3.47	1.22	[redacted]	0.82	1.21	3.77	3.01	3.05	2.33	1.40	0.42	[redacted]
1950	[redacted]	1.39	1.36	3.28	[redacted]	0.72	2.92	1.02	[redacted]	0.95	3.16	3.02	2.72	2.53	2.16	1.80	0.42	[redacted]

1949	[redacted]	0.98	0.89	2.28	[redacted]	0.53	1.89	1.15	[redacted]	1.06	2.01	2.15	2.05	1.54	1.32	1.29	0.59	[redacted]
1948	[redacted]	1.59	1.45	3.17	[redacted]	0.92	2.68	2.28	[redacted]	1.60	2.47	4.45	2.74	1.79	2.21	1.92	0.31	[redacted]
1947	[redacted]	0.83	1.24	1.97	[redacted]	0.44	2.18	1.72	[redacted]	1.07	1.19	2.29	1.86	1.63	1.10	1.09	0.40	[redacted]
1946	[redacted]	0.76	0.86	3.10	[redacted]	0.24	2.08	1.65	[redacted]	0.21	4.23	1.36	2.61	1.75	1.74	1.23	0.59	[redacted]
1945	[redacted]	0.63	0.70	1.88	[redacted]	0.53	1.77	1.59	[redacted]	0.21	[redacted]	1.99	1.41	2.09	0.93	1.34	0.37	[redacted]
1944	[redacted]	1.35	1.04	2.70	[redacted]	2.19	2.63	3.26	[redacted]	0.80	[redacted]	3.29	2.71	2.59	2.19	1.90	0.37	[redacted]
1943	[redacted]	0.66	0.87	1.97	[redacted]	1.55	2.08	2.22	[redacted]	0.56	[redacted]	2.57	1.70	2.40	1.53	1.20	0.42	[redacted]
1942	[redacted]	2.73	1.74	4.13	[redacted]	0.74	3.54	4.75	[redacted]	1.63	[redacted]	3.60	3.43	2.09	3.27	2.33	1.19	[redacted]
1941	[redacted]	1.90	0.97	3.35	[redacted]	2.11	5.70	2.92	[redacted]	1.65	[redacted]	4.83	3.38	3.39	2.51	2.57	0.92	[redacted]
1940	[redacted]	1.45	1.04	4.18	[redacted]	1.57	3.04	2.31	[redacted]	1.17	[redacted]	1.65	2.00	4.08	1.40	1.91	0.73	[redacted]
1939	[redacted]	0.79	0.52	3.85	[redacted]	1.35	1.68	1.15	[redacted]	0.80	[redacted]	1.24	1.21	1.40	0.72	0.89	0.31	[redacted]
1938	[redacted]	1.40	0.76	5.03	[redacted]	0.83	2.89	1.96	[redacted]	2.19	[redacted]	1.44	1.84	0.46	1.15	1.46	0.46	[redacted]
1937	[redacted]	1.32	0.77	2.59	[redacted]	0.72	2.65	2.15	[redacted]	1.63	[redacted]	1.42	2.35	3.24	1.51	1.06	0.59	[redacted]
1936	[redacted]	0.91	0.58	2.13	[redacted]	0.85	1.95	1.59	[redacted]	1.38	[redacted]	1.01	1.85	2.55	1.19	0.82	0.42	[redacted]
1935	[redacted]	0.62	0.47	1.06	[redacted]	0.83	0.70	0.65	[redacted]	0.99	[redacted]	1.36	1.70	0.52	1.15	0.36	0.26	[redacted]
1934	[redacted]	1.26	1.47	5.89	[redacted]	2.33	3.47	2.76	[redacted]	1.75	[redacted]	5.55	5.83	0.65	4.32	1.93	0.68	[redacted]
1933	[redacted]	0.56	0.72	2.18	[redacted]	0.85	0.78	0.89	[redacted]	0.71	[redacted]	1.80	1.98	0.71	1.36	0.84	0.29	[redacted]
1932	[redacted]	2.02	1.09	3.23	[redacted]	1.05	2.43	2.15	[redacted]	2.01	[redacted]	3.02	3.14	2.38	2.77	1.24	0.53	[redacted]
1931	[redacted]	0.97	0.70	1.59	[redacted]	0.76	1.42	1.07	[redacted]	0.69	[redacted]	1.67	1.27	1.50	1.04	0.82	0.15	[redacted]
1930	[redacted]	1.28	0.77	1.68	[redacted]	0.61	1.29	1.28	[redacted]	0.82	[redacted]	1.97	1.14	0.77	0.95	0.82	0.44	[redacted]
1929	[redacted]	1.07	0.92	2.97	[redacted]	0.28	1.71	1.83	[redacted]	0.54	[redacted]	3.40	1.81	5.81	1.74	1.24	0.70	[redacted]
1928	[redacted]	0.60	0.46	1.55	[redacted]	0.74	0.72	0.72	[redacted]	0.17	[redacted]	1.75	1.19	1.50	1.04	0.64	0.42	[redacted]
1927	[redacted]	0.68	0.48	1.73	[redacted]	0.41	0.99	0.87	[redacted]	0.22	[redacted]	1.84	1.65	1.19	0.95	0.69	0.44	[redacted]
1926	[redacted]	0.68	0.48	1.49	[redacted]	0.89	1.27	0.90	[redacted]	0.32	[redacted]	1.35	1.53	0.31	0.91	0.82	0.44	[redacted]
1925	[redacted]	0.50	0.51	1.49	[redacted]	0.63	0.91	1.25	[redacted]	0.19	[redacted]	2.03	1.36	0.77	0.93	0.73	0.49	[redacted]
1924	[redacted]	0.93	0.53	1.35	[redacted]	1.00	1.04	1.05	[redacted]	0.61	[redacted]	1.41	1.01	0.56	1.08	1.02	0.66	[redacted]
1923	[redacted]	0.70	0.45	1.44	[redacted]	0.79	0.93	1.02	[redacted]	0.84	[redacted]	1.19	1.63	0.59	0.93	1.00	0.60	[redacted]
1922	[redacted]	0.33	0.29	0.82	[redacted]	0.94	0.71	0.55	[redacted]	0.22	[redacted]	0.75	0.97	0.33	0.47	0.51	0.26	[redacted]
1921	[redacted]	0.64	0.37	1.46	[redacted]	0.63	0.81	0.80	[redacted]	1.12	[redacted]	0.70	1.01	0.63	0.59	0.65	0.46	[redacted]
1920	[redacted]	0.60	0.53	1.91	[redacted]	0.66	1.08	1.13	[redacted]	1.04	[redacted]	1.94	1.48	1.36	1.16	0.96	0.55	[redacted]

1919	[illegible]	1.12	0.75	1.91	[illegible]	0.46	1.33	1.35	[illegible]	2.53	[illegible]	1.66	1.77	0.90	1.52	1.00	0.71	[illegible]
1918	[illegible]	0.50	0.33	1.11	[illegible]	0.87	0.78	0.52	[illegible]	0.49	[illegible]	0.79	0.98	0.71	1.06	0.56	0.29	[illegible]
1917	[illegible]	0.41	0.28	0.95	[illegible]	0.37	0.59	0.61	[illegible]	0.42	[illegible]	0.81	0.52	0.61	0.66	0.62	0.26	[illegible]
Mean	0.98	1.07	0.92	2.31	0.38	1.14	2.13	1.94	0.31	0.83	2.60	2.04	2.05	1.79	1.62	1.26	0.55	0.11

Table A.2 Mean bulk-physical properties for samples cores for the period 1917 - 2010.

Core Sample	Type[$] (E,P)	Length* (cm)	Cracks[¥] (%)	Dry density (g cm^{-3})	Organic content (%)	Wet density (g cm^{-3})	Water content (%)
01	E	19	6.8	0.81	1.8	1.63	50.1
02	P	232	0.0	0.81	1.8	1.63	50.3
03	P	235	6.8	1.12	2.2	1.91	41.5
05	P	221	5.9	1.43	1.6	2.11	32.3
A	P	133	3.7	1.42	2.8	2.23	36.2
B	P	292	4.6	1.20	2.4	1.95	38.7
C	P	218	1.5	1.43	1.7	2.07	30.9
D	P	191	5.8	1.41	1.9	2.15	34.5
F	P	210	4.5	1.15	2.1	1.93	40.1
G	P	208	3.1	1.24	2.0	2.00	38.0
I	P	153	0.0	1.55	1.4	2.20	29.9
K	P	225	3.3	1.56	1.2	2.20	29.4
L	P	234	1.6	1.53	1.3	2.18	29.8
M	P	216	3.4	1.42	1.4	2.11	32.7
N	P	205	3.6	1.33	1.6	2.01	34.0
O	P	205	4.8	1.22	1.6	1.96	37.9
P	P	144	6.4	0.81	2.9	1.69	52.2
R	P	82	6.7	0.92	2.4	1.79	49.0
Mean		200	3.9	1.27	1.9	2.01	37.5
SD		48	2.2	0.24	0.5	0.18	7.2

*Length of wet sediment within each core

¥ Measured in the sharpest photos and refers to the amount of crack space that developed along the entire length of the sediment.

$ E = Ekman core, P = Percussion core

Appendix B: Specific sediment yield results and sediment core correlation.

Table B.1 Specific Sediment Yield interpolated by Thiessen polygons and regularized spline.

Year	2010	2009	2008	2007	2006	2005	2004	2003	2002	2001	2000	1999	1998	1997	1996	1995	1994
Thiessen - 0 m	257	380	466	674	570	418	798	966	943	453	352	552	1314	745	320	382	525
Thiessen - 10 m	230	341	417	603	511	380	725	871	856	408	315	494	1202	672	287	342	478
Thiessen - 20 m	202	300	367	532	454	343	652	773	765	363	277	432	1080	597	252	300	430
Spline - 20 m	181	268	324	474	412	302	531	634	618	326	239	365	843	508	220	252	360
Year	**1993**	**1992**	**1991**	**1990**	**1989**	**1988**	**1987**	**1986**	**1985**	**1984**	**1983**	**1982**	**1981**	**1980**	**1979**	**1978**	**1977**
Thiessen - 0 m	377	548	387	526	419	542	593	502	394	489	980	470	835	748	575	600	652
Thiessen - 10 m	339	489	348	470	372	490	534	450	355	445	888	423	748	669	518	538	589
Thiessen - 20 m	298	431	307	415	326	439	474	397	315	401	796	375	657	587	461	476	526
Spline - 20 m	248	357	261	383	308	404	417	382	285	353	684	321	547	517	396	441	470
Year	**1976**	**1975**	**1974**	**1973**	**1972**	**1971**	**1970**	**1969**	**1968**	**1967**	**1966**	**1965**	**1964**	**1963**	**1962**	**1961**	**1960**
Thiessen - 0 m	789	1004	620	593	423	1092	1226	667	606	878	679	819	736	457	743	815	542
Thiessen - 10 m	709	895	554	532	380	982	1115	609	548	793	613	741	664	410	671	736	488
Thiessen - 20 m	629	780	486	470	337	868	1003	549	489	707	547	663	592	363	600	659	435
Spline - 20 m	529	685	431	424	313	742	874	497	433	643	511	614	530	335	561	596	404
Year	**1959**	**1958**	**1957**	**1956**	**1955**	**1954**	**1953**	**1952**	**1951**	**1950**	**1949**	**1948**	**1947**	**1946**	**1945**	**1944**	**1943**
Thiessen - 0 m	779	812	338	912	788	301	491	525	709	811	546	829	526	694	588	952	762
Thiessen - 10 m	706	736	305	818	710	270	440	476	639	729	490	743	472	626	525	858	683
Thiessen - 20 m	632	663	271	724	631	240	390	428	572	646	434	659	420	554	462	761	604
Spline - 20 m	587	611	232	645	558	220	370	401	558	581	397	646	400	461	423	690	552
Year	**1942**	**1941**	**1940**	**1939**	**1938**	**1937**	**1936**	**1935**	**1934**	**1933**	**1932**	**1931**	**1930**	**1929**	**1928**	**1927**	**1926**
Thiessen - 0 m	1099	1259	1041	539	576	869	682	344	1068	427	919	499	431	1175	450	439	327
Thiessen - 10 m	989	1128	937	490	527	782	614	310	973	386	827	447	386	1044	402	393	295
Thiessen - 20 m	879	999	826	439	476	690	542	276	881	344	732	394	340	906	352	347	265
Spline - 20 m	776	928	682	372	396	568	443	252	837	316	639	350	316	808	326	325	243
Year	**1925**	**1924**	**1923**	**1922**	**1921**	**1920**	**1919**	**1918**	**1917**	**Mean**	**SD**						
Thiessen - 0 m	394	369	364	222	308	507	522	302	247	630	251						
Thiessen - 10 m	352	330	327	200	277	453	467	271	221	567	227						
Thiessen - 20 m	311	291	290	178	244	398	412	240	193	503	203						
Spline - 20 m	307	264	257	161	205	368	359	206	173	446	176						

Table B.2 Core sample and SSY correlation table. **Bolded** values are significant ($p < 0.05$).

	SSY Thiessen 20	SSY spline	01	02	03	05	B	C	D	G	I	K	L	M	N	O	P	Std.
Std.	**0.94**	**0.93**	**0.95**	**0.76**	**0.79**	**0.79**	**0.58**	**0.90**	**0.81**	**0.47**	**0.32**	**0.72**	**0.84**	**0.55**	**0.85**	**0.82**	**0.36**	**1.00**
P	**0.26**	**0.25**	-0.10	**0.30**	0.18	0.09	0.17	**0.25**	**0.28**	**0.36**	-0.01	**0.23**	**0.22**	0.13	**0.29**	0.20	**1.00**	
O	**0.73**	**0.71**	**0.89**	**0.51**	**0.65**	**0.69**	**0.54**	**0.71**	**0.63**	0.23	0.18	**0.48**	**0.69**	**0.46**	**0.67**	**1.00**		
N	**0.75**	**0.73**	**0.88**	**0.63**	**0.65**	**0.70**	**0.52**	**0.70**	**0.62**	**0.53**	0.06	**0.59**	**0.79**	**0.28**	**1.00**			
M	**0.69**	**0.69**	**0.59**	**0.30**	**0.39**	**0.37**	0.16	**0.49**	**0.41**	-0.02	**0.35**	**0.40**	**0.41**	**1.00**				
L	**0.75**	**0.75**	**0.81**	**0.50**	**0.59**	**0.73**	**0.56**	**0.74**	**0.61**	**0.42**	0.01	**0.62**	**1.00**					
K	**0.69**	**0.78**	0.41	**0.57**	**0.59**	**0.45**	**0.53**	**0.68**	**0.59**	**0.33**	0.12	**1.00**						
I	**0.60**	**0.54**	-0.24	0.19	0.16	0.24	-0.36	0.25	0.21	-0.26	1.00							
G	**0.32**	**0.31**	**NA**	**0.48**	**0.24**	**0.49**	0.25	**0.33**	0.20	**1.00**								
D	**0.77**	**0.76**	**0.93**	**0.75**	**0.69**	**0.53**	**0.39**	**0.79**	**1.00**									
C	**0.87**	**0.87**	**0.92**	**0.75**	**0.70**	**0.69**	**0.57**	**1.00**										
B	**0.51**	**0.54**	**NA**	0.32	0.32	**0.48**	**1.00**											
05	**0.75**	**0.72**	**0.85**	**0.47**	**0.59**	**1.00**												
03	**0.70**	**0.70**	**0.65**	**0.70**	**1.00**													
02	**0.68**	**0.68**	**0.65**	**1.00**														
01	**0.96**	**0.95**	**1.00**															
SSY_{spline}	**0.99**	**1.00**																
$SSY_{Thiessen\ 20}$	**1.00**																	

Std. = Standardized varve thickness

Appendix C: Measured delta progradation and ancillary volume change results.

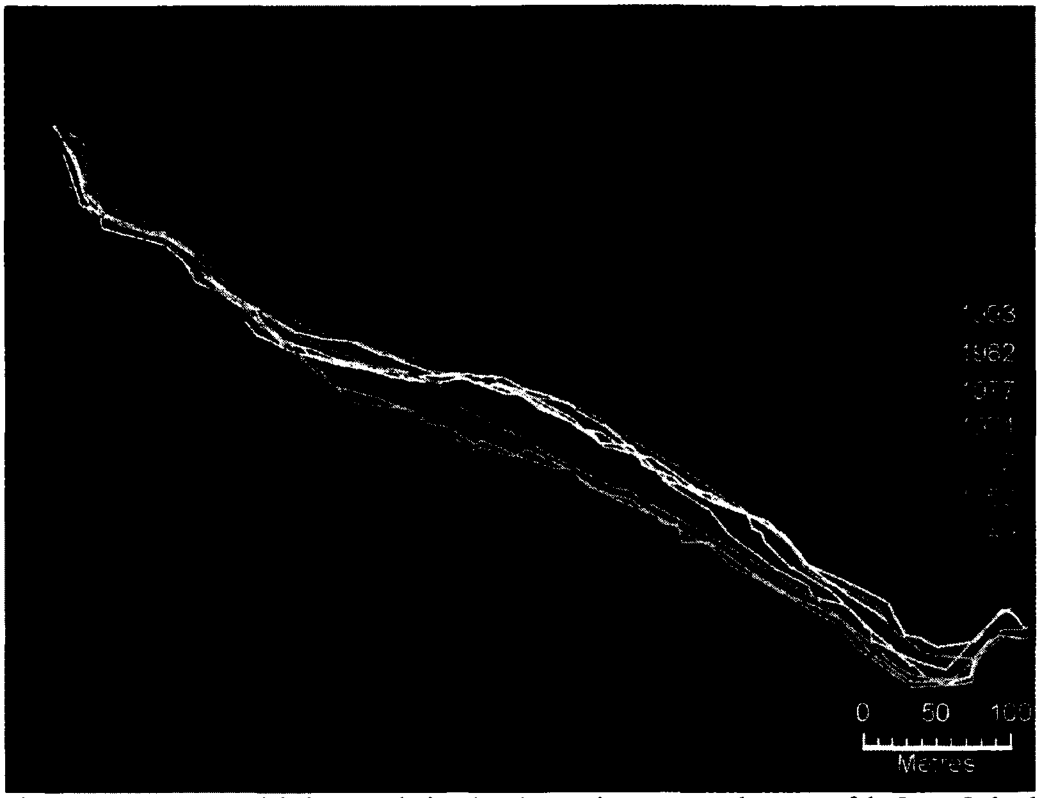

Figure C.1 2005 AT aerial photograph showing the previous measured extents of the Peyto Lake delta.

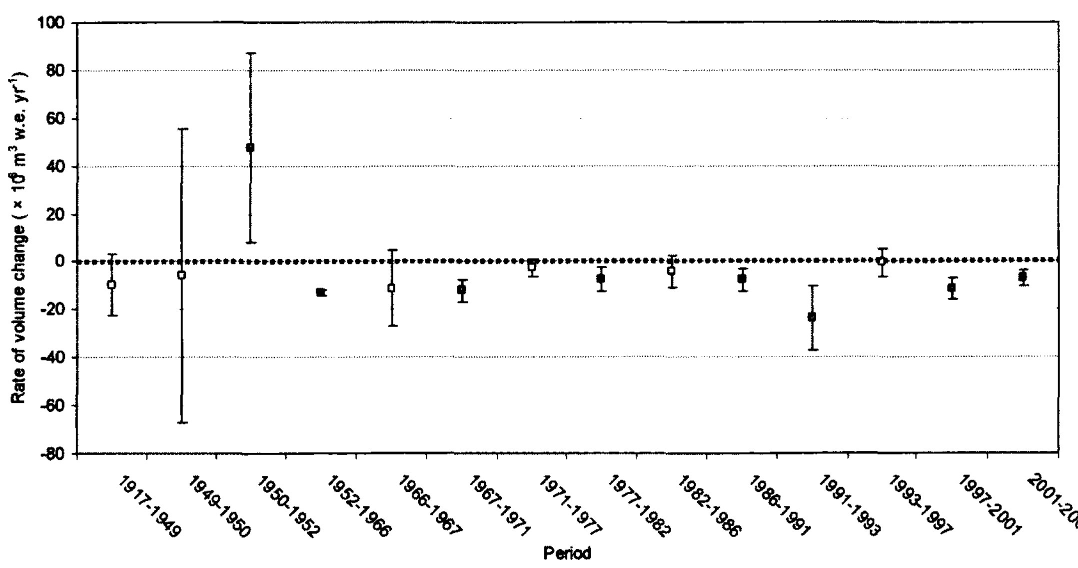

Figure C.2 The rate of volume change that Peyto Glacier has undergone for the period 1917 - 2005 is categorized by data completeness of > 50 %. Glacier changes highlighted in pink are within bounds of the error term.

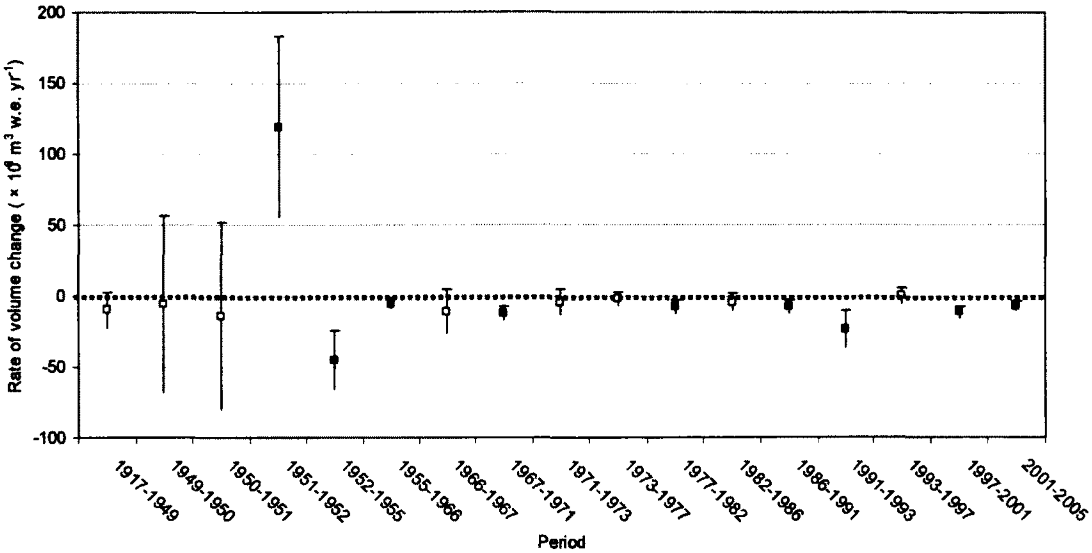

Figure C.3 The rate of volume change that Peyto Glacier has undergone for the period 1917 - 2005 is categorized by data completeness of > 20 %. Glacier changes highlighted in pink are within bounds of the error term.